Cluster Gravitational Lensing with Subaru

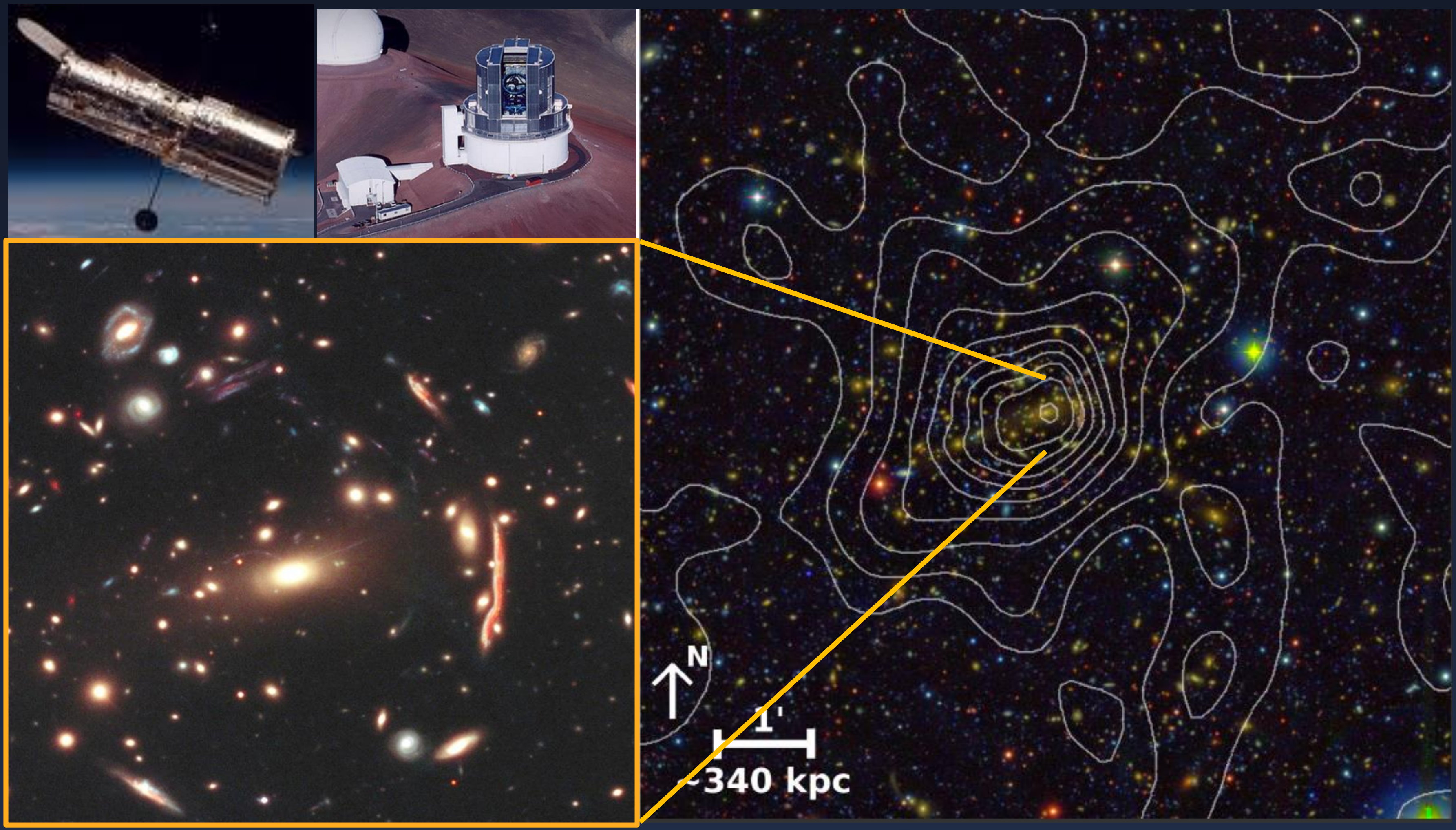

Keiichi Umetsu (ASIAA, since 2001)

My Science Interests

Nature of dark matter and its role in cosmic structure formation

Study galaxy clusters and their surrounding environments using (weak + strong) gravitational lensing as a direct probe

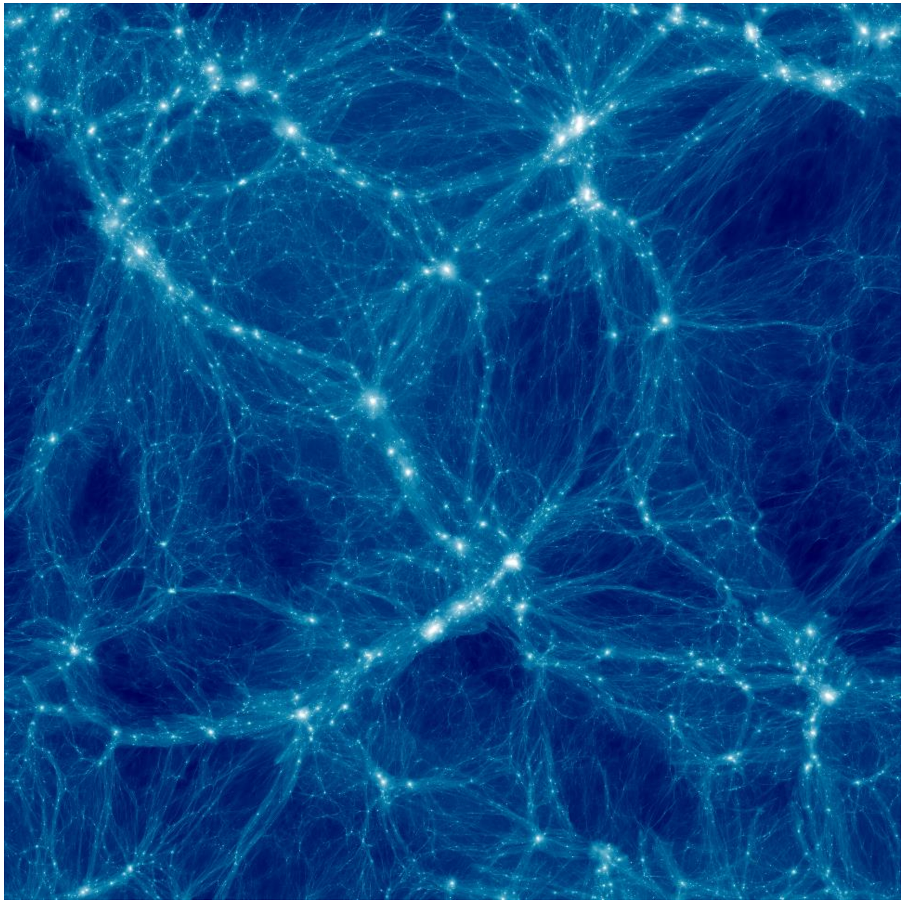

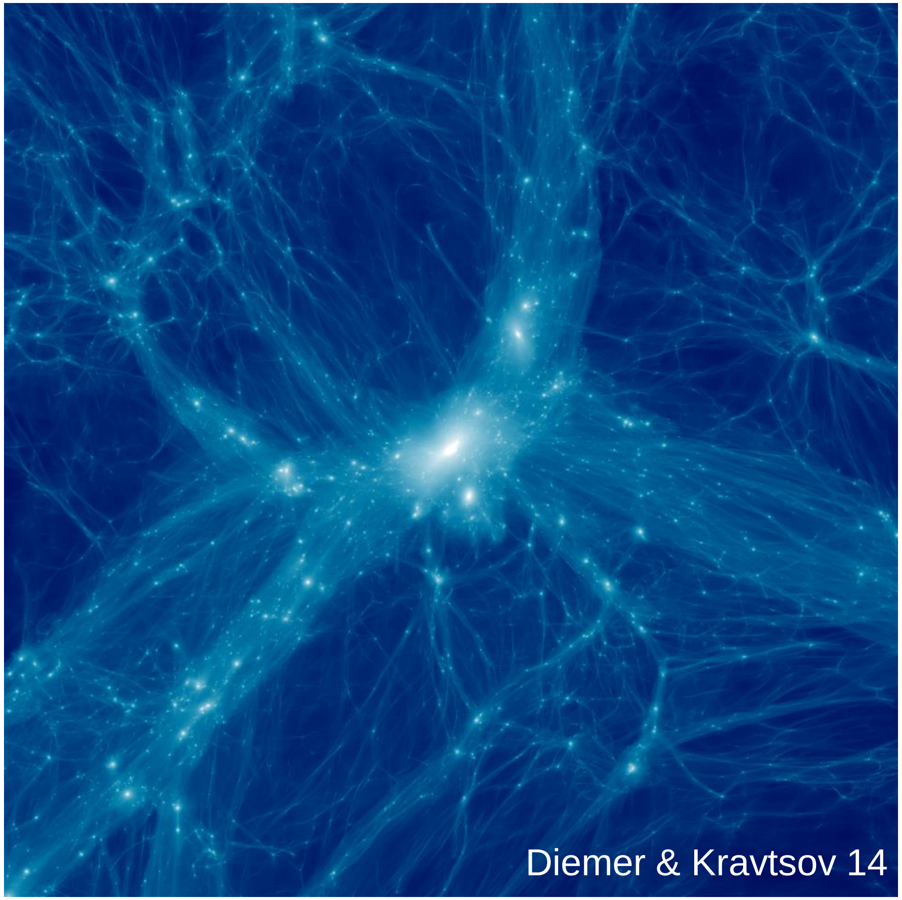

Subaru/Suprime-Cam multi-color imaging for wide-field weak lensing

High-resolution space imaging with *HST* (ACS/WFC3) for strong lensing

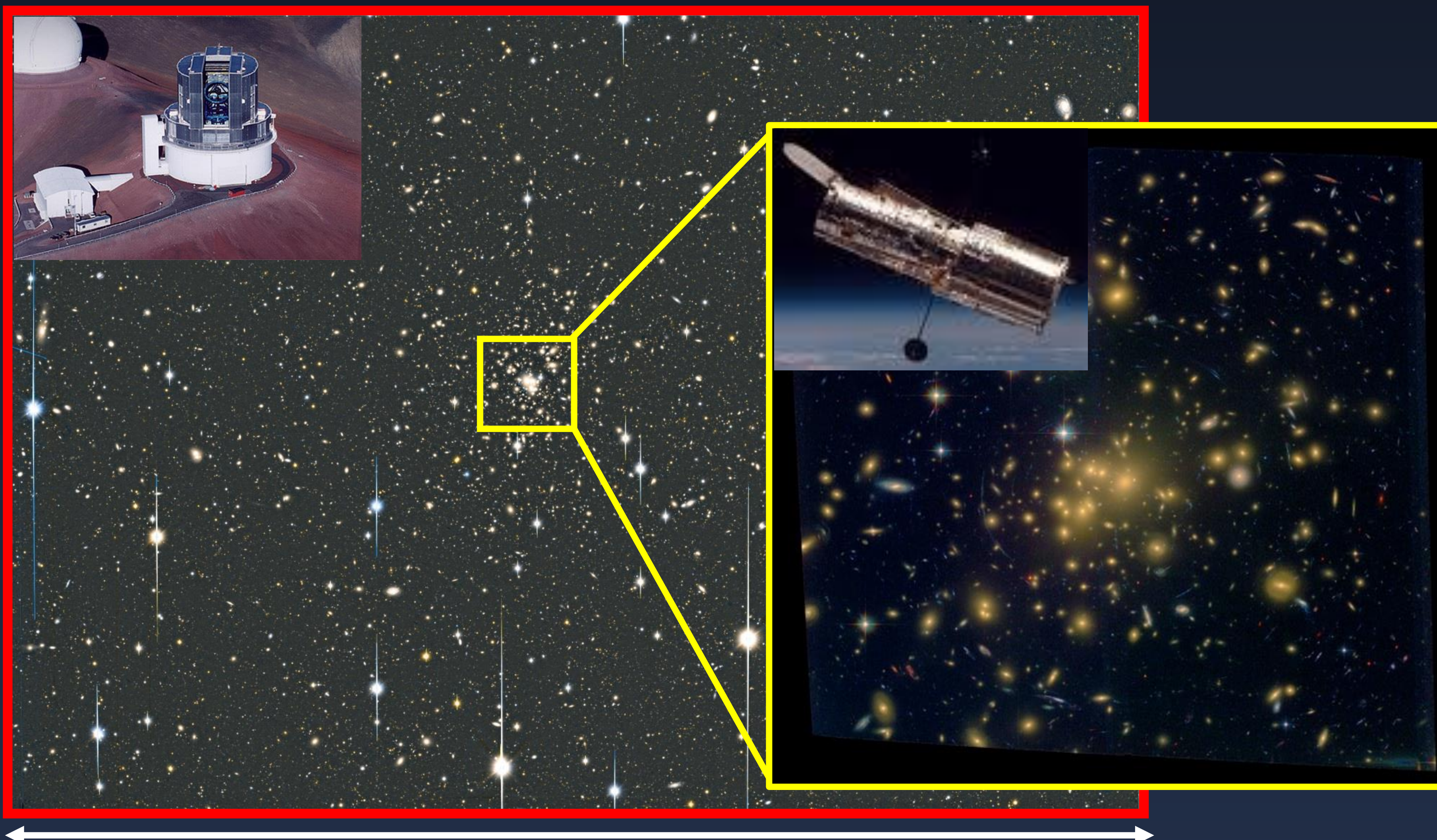

Cluster Lensing And Supernova survey with Hubble

524-orbit *HST* Treasury Program (2010-2013) to deeply observe 25 high-mass clusters in 16 filters (ACS/WFC3)

PI. Marc Postman (STScI)

Major science goals, targeting

1. **20 X-ray-selected relaxed high-mass clusters**
   - Establish the equilibrium cluster density profile
   - Test LCDM predictions of the concentration-mass relation
2. **5 high-magnification clusters**
   - Search for and study magnified high-z (z>8) galaxies

Postman e al. 2012, *ApJS*, 199, 25

CLASH Subaru Weak-lensing Dataset

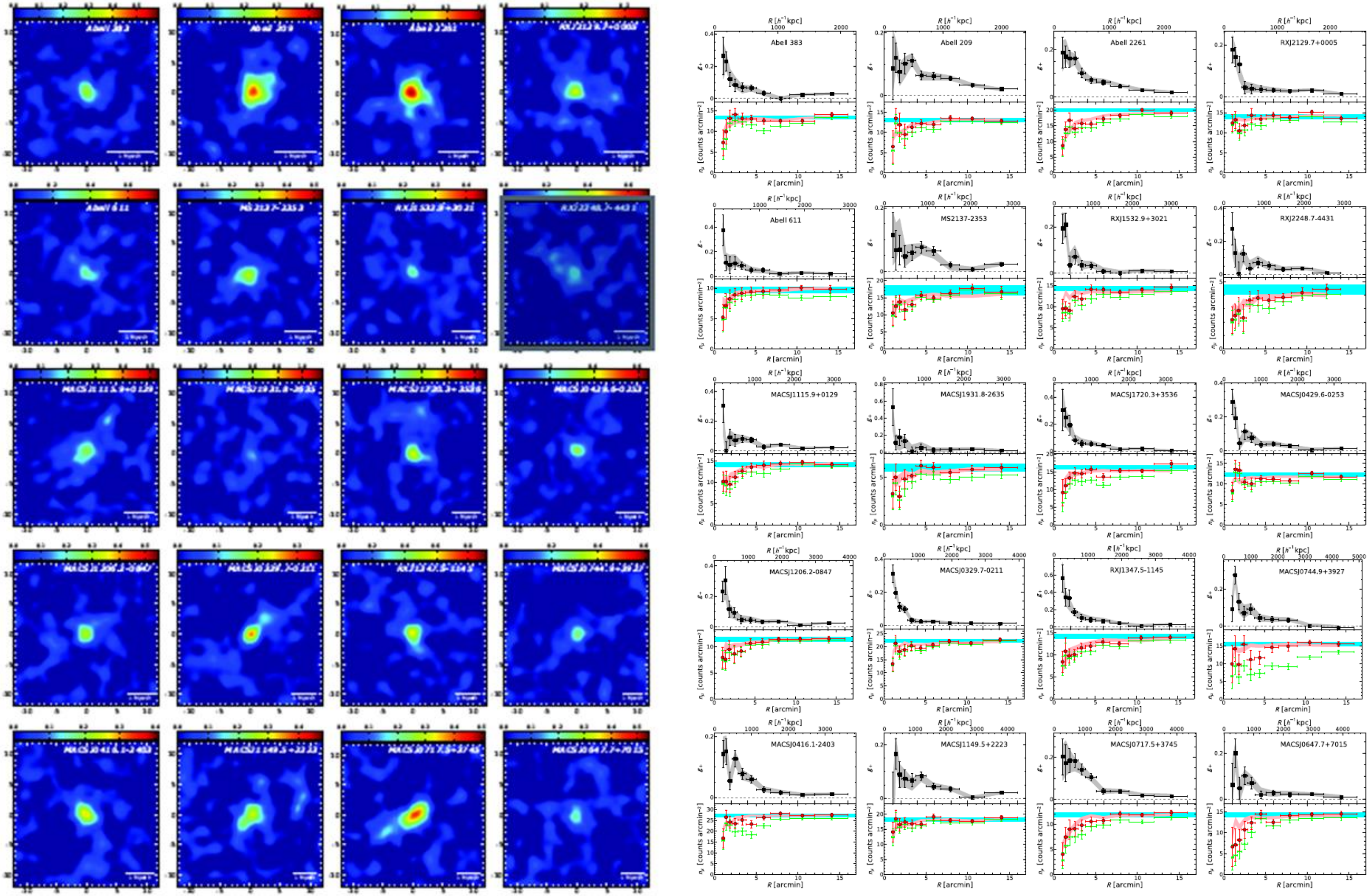

Umetsu, Medezinski, Nonino et al. 2014, *ApJ*, 795, 163

CLASH *HST* Strong-lensing Dataset

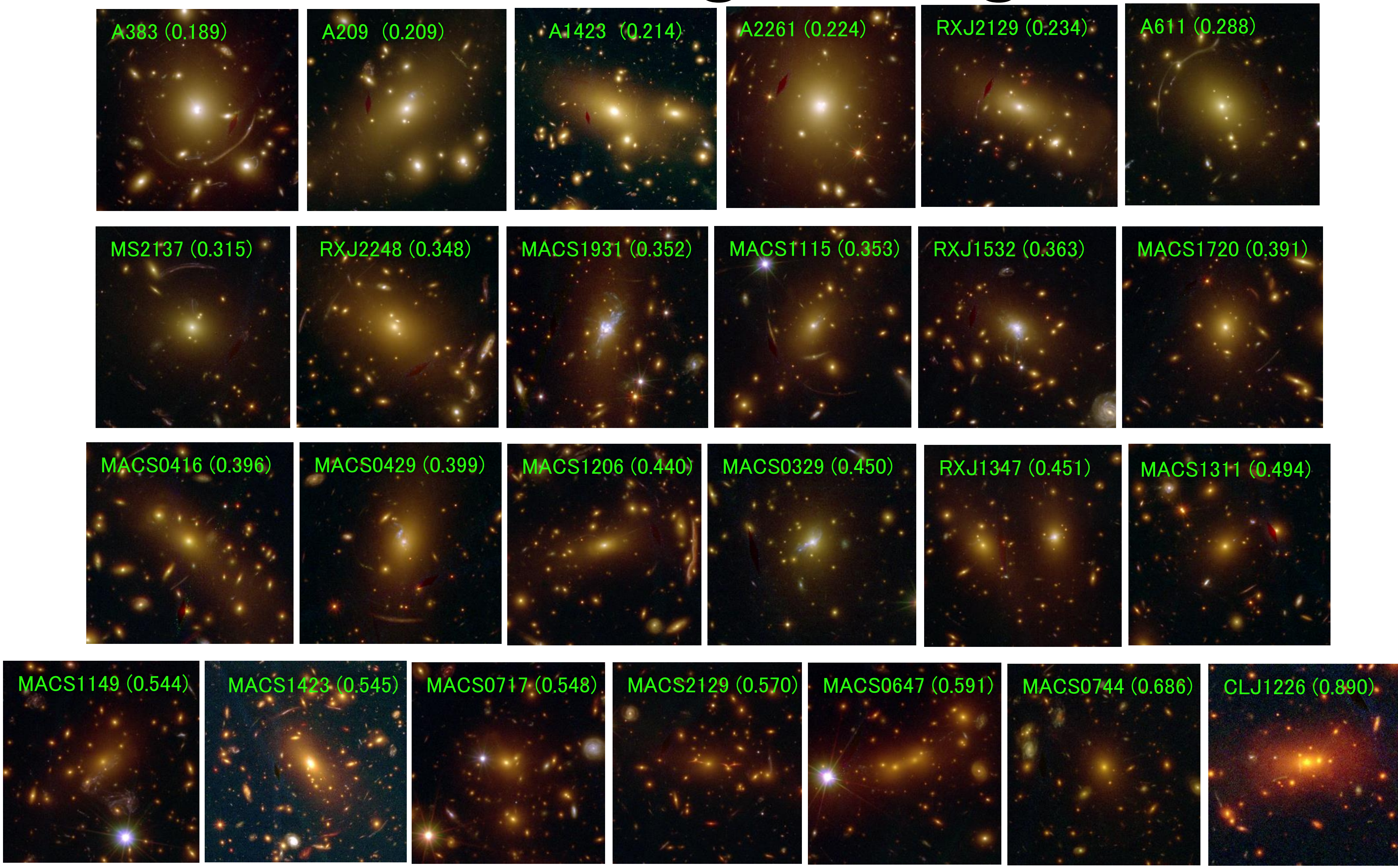

Zitrin et al. 2015, *ApJ*, 801, 44

Results: Ensemble Mass Density Profile

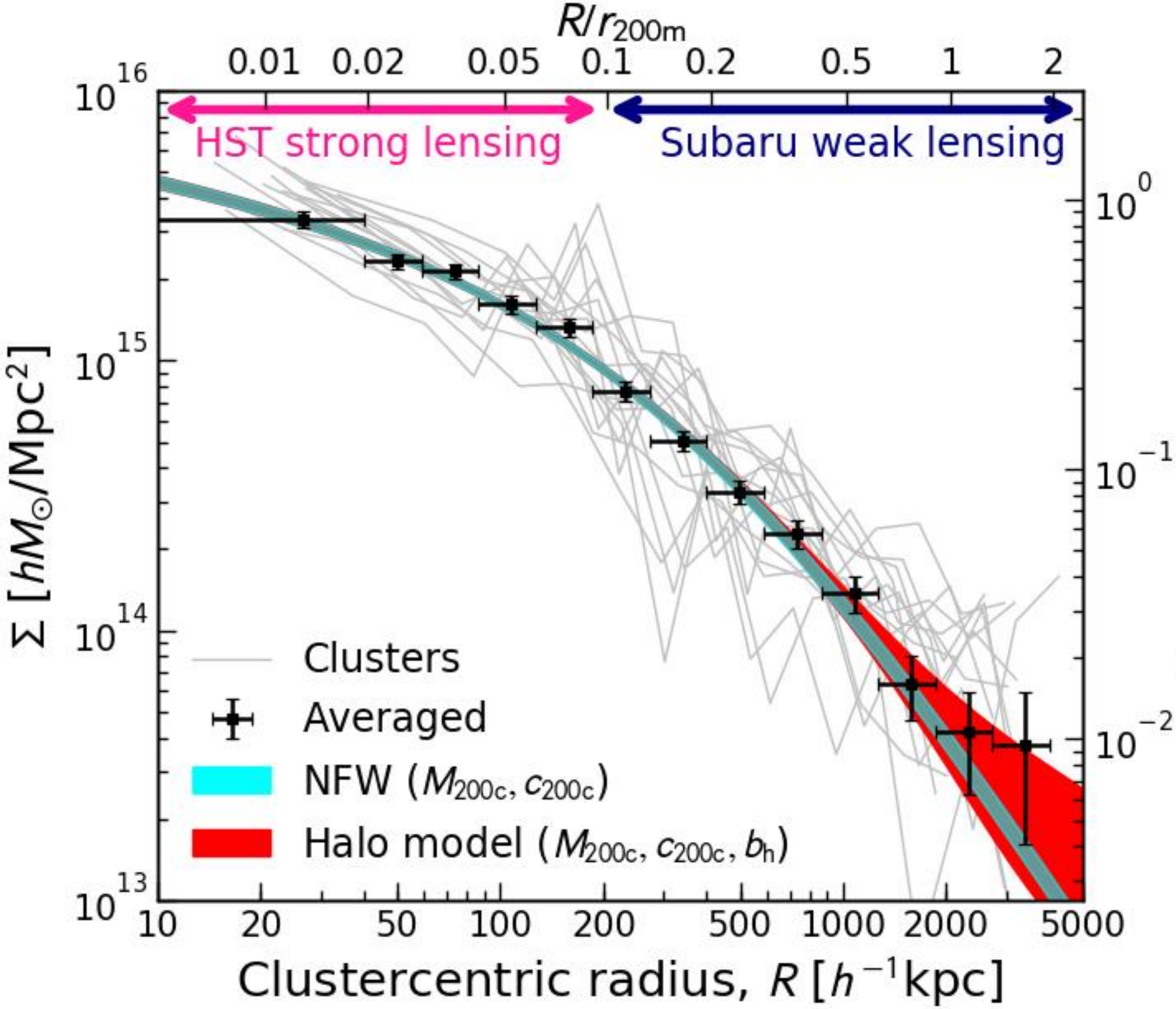

$$c_{200c} := \frac{R_{200c}}{r_s} = 3.79^{+0.30}_{-0.28}$$

$$M_{200c} = 1.4^{+0.1}_{-0.1} \times 10^{15} M_{sun}$$

$$\langle z \rangle \approx 0.34$$

Umetsu et al. 2016

Cuspy outward steepening profiles favored by CLASH lensing data

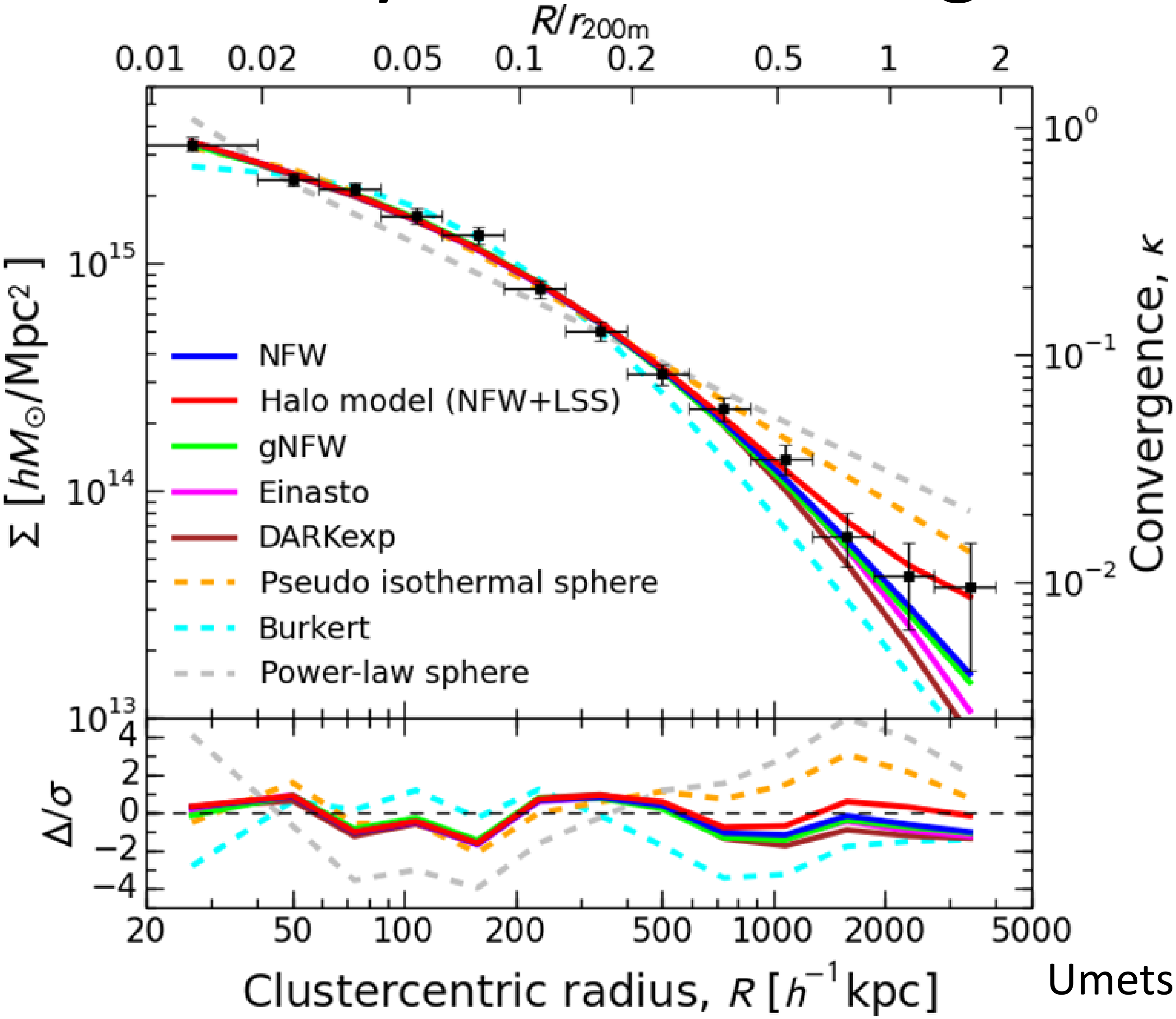

Umetsu et al. 2016

Results: Concentration–Mass Relation

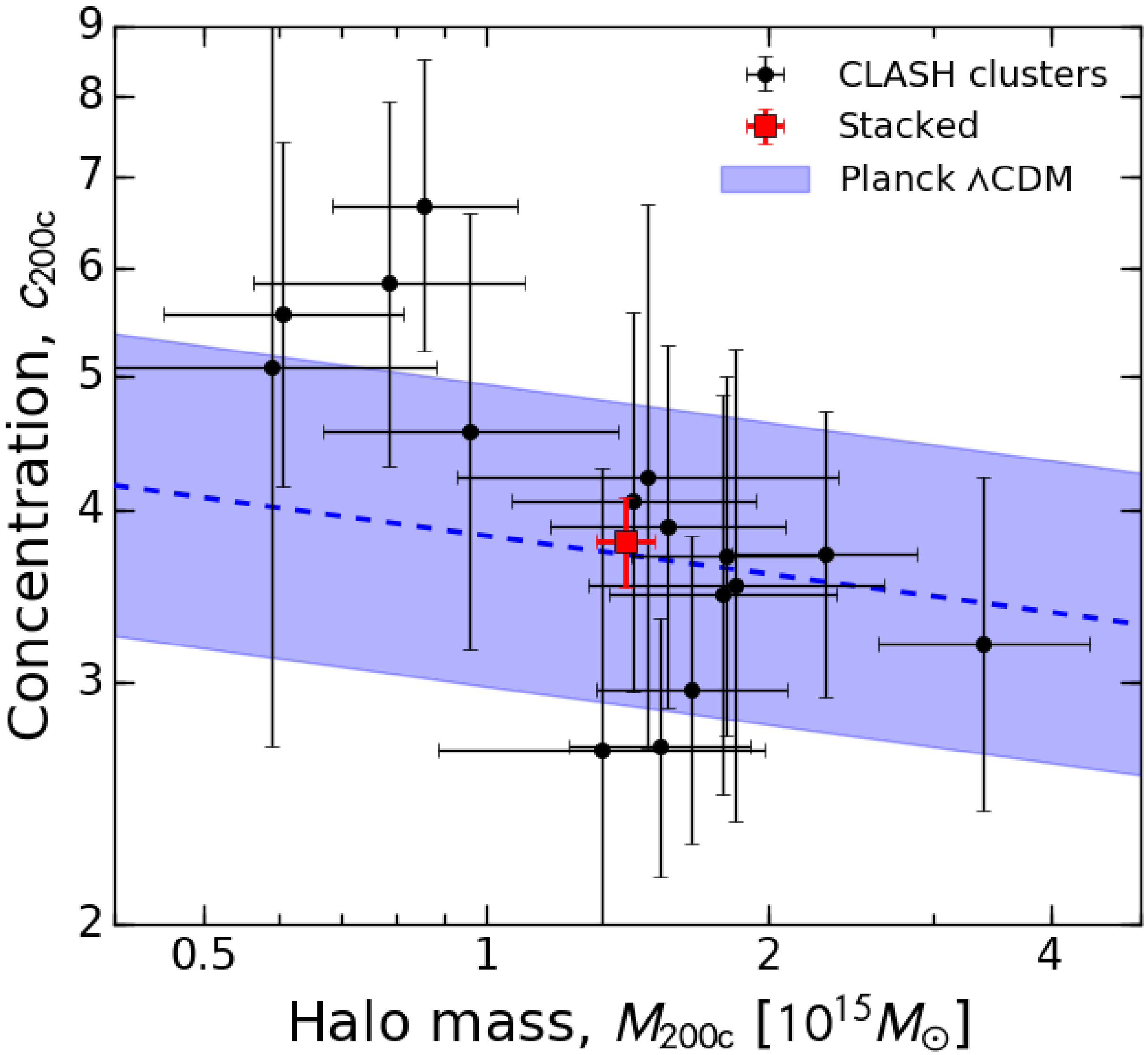

Stacked CLASH lensing

$$c_{200c} = 3.79^{+0.30}_{-0.28}$$

$$\text{at } M_{200c} = 1.4^{+0.1}_{-0.1} \times 10^{15} M_{\text{sun}}$$

Consistent with *c*-*M* relations calibrated for recent cosmologies (WMAP7 and later)

Umetsu et al. 2016

CLASH vs. Superlens Clusters

- 16 **lensing-unbiased** CLASH clusters (Umetsu+16)
- 4 **superlens** clusters with Einstein radius >30” (Umetsu+11b)

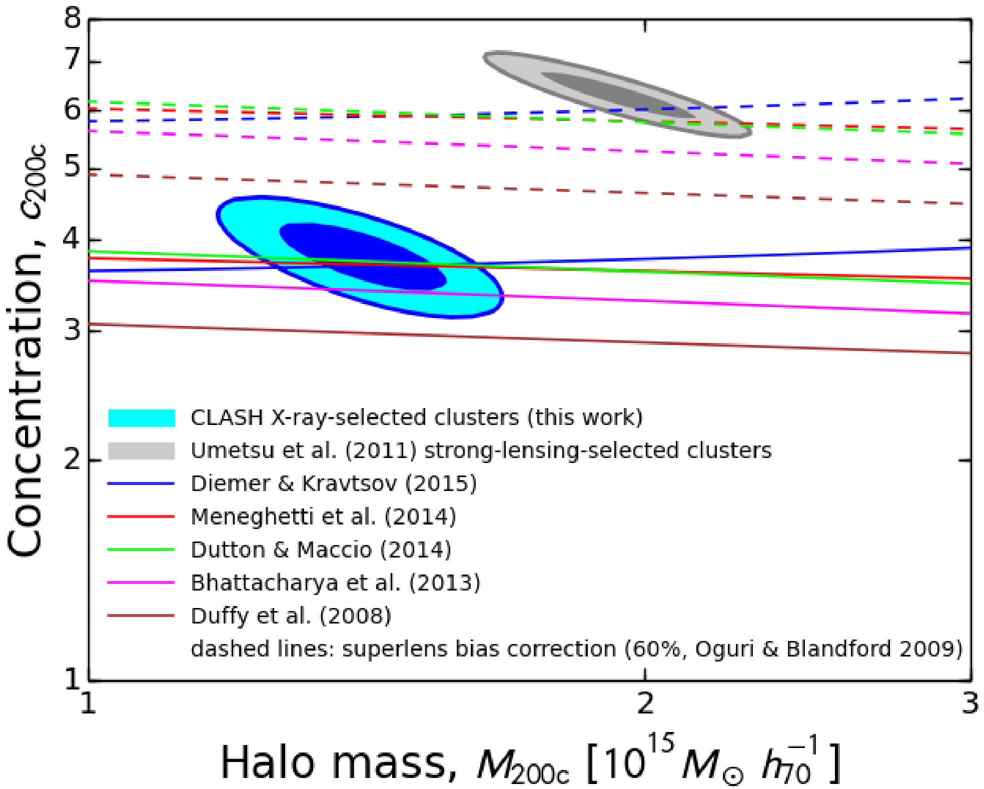

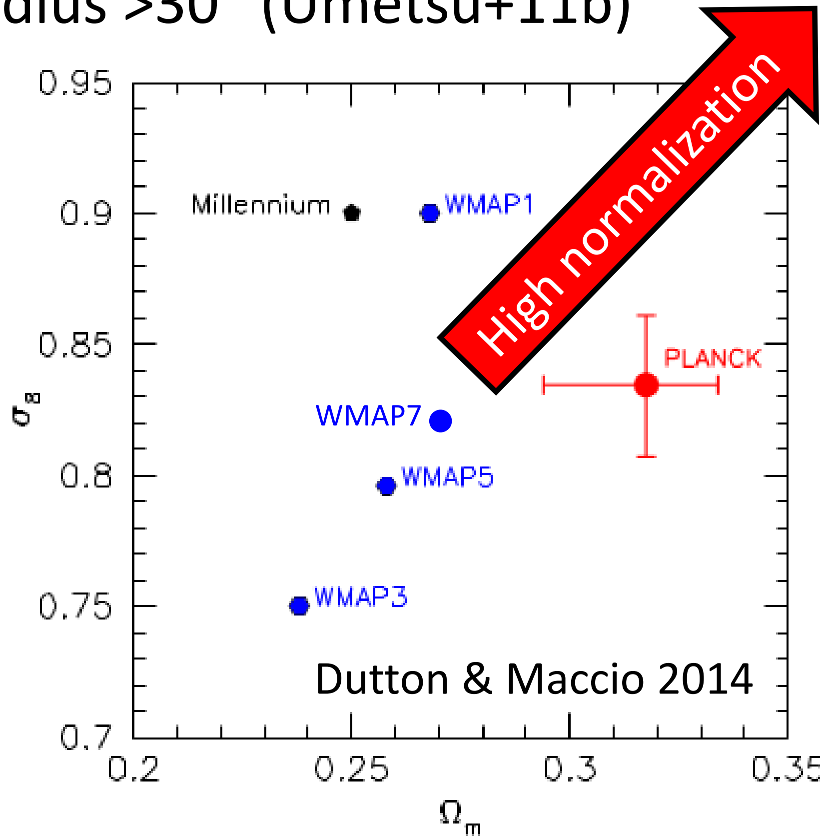

Higher normalization LCDM cosmology (WMAP7 and later) + predicted 60% superlens correction can explain superlens mass profiles!

CLASH Lensing Constraints on the Splashback Radius of Galaxy Clusters

Umetsu & Diemer 2017, *ApJ*, 836, 231

Splashback radius, R_{sp}: Physical halo boundary

Slow accreting halos

$R_{sp} >> R_{200m}$

Fast accreting halos

$R_{sp} \sim R_{200m}$

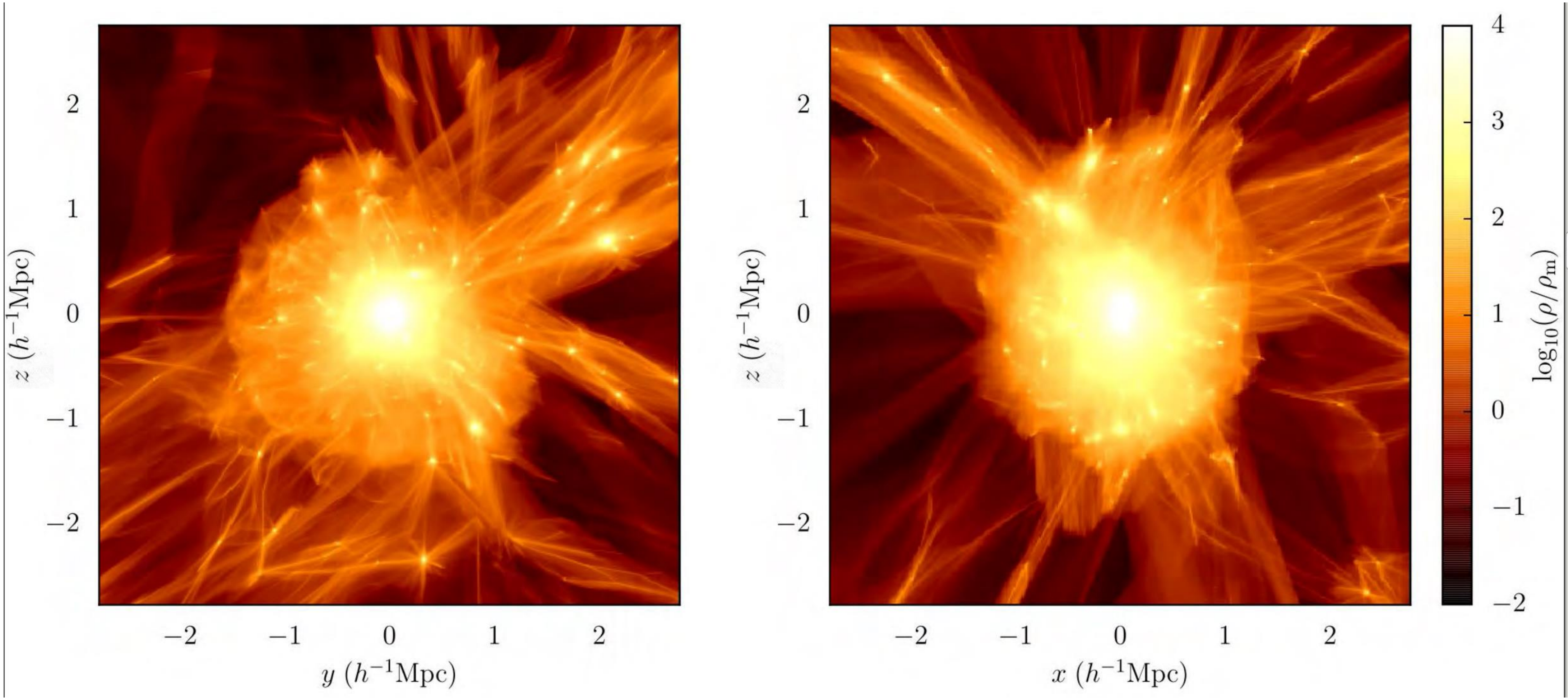

More, Diemer, & Kravtsov 2015

Splashback feature in real space

Steepest "3D" gradient point as splashback radius R_{sp}

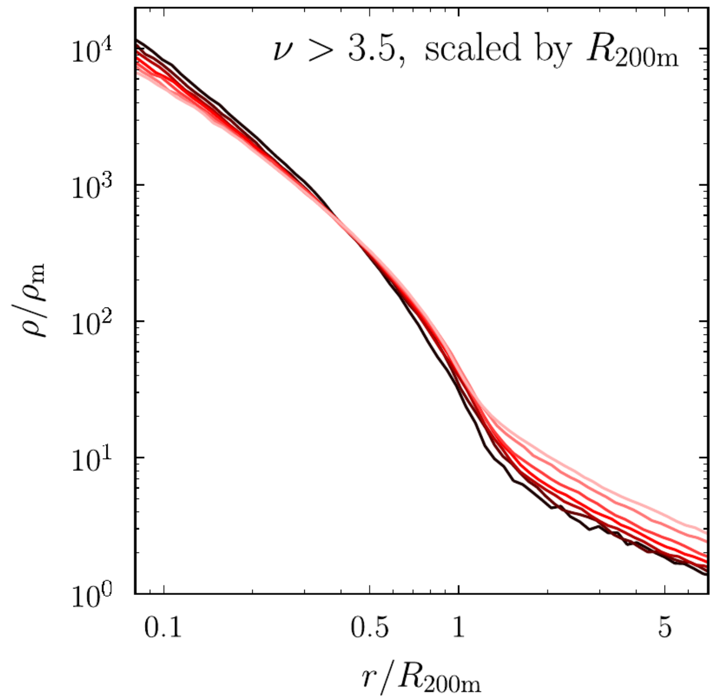

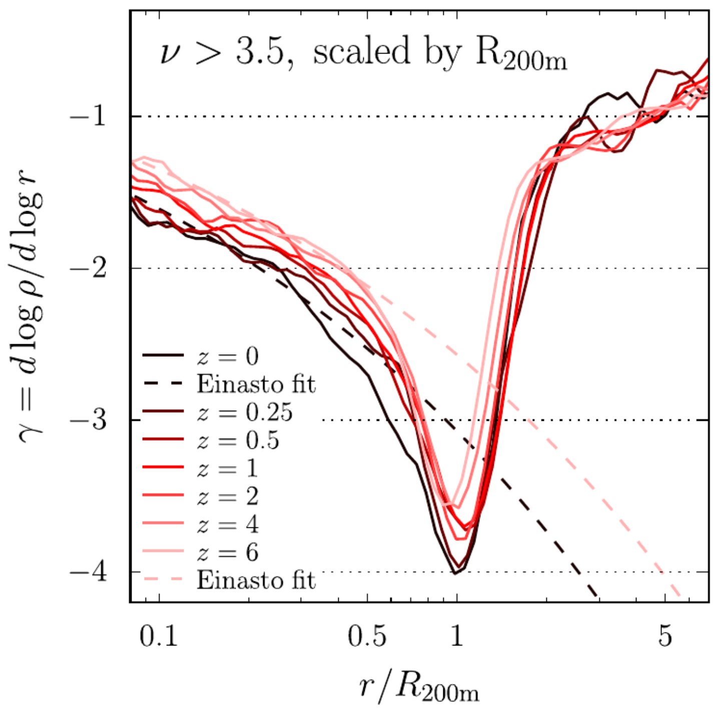

N-body simulations (Diemer & Kravtsov 14, DK14)

Practical issues

- CLASH spans a factor of ~5 (1.7) in mass (radius), so that sharp gradient feature is washed out when stacked in physical length units.
- In 2D, the splashback feature is weakened by projection of shallow 2-halo term

Solution: Parametric forward modeling of "scaled" cluster lensing profiles

Mass distribution around halos in ΛCDM (DK14)

$$\Delta\rho(r) = \rho(r) - \rho_{\rm m} = \rho_{\rm inner} \times f_{\rm trans} + \rho_{\rm outer}$$

A scaled version of DK14 density profile (Umetsu & Diemer 17)

$$\begin{aligned}\Delta\rho(r = r_\Delta x) &= \mathcal{N}\left\{\exp\left[-\frac{2}{\alpha}c_\Delta^\alpha(x^\alpha - 1)\right]\left[1+\left(\frac{x}{\tau_\Delta}\right)^\beta\right]^{-\gamma/\beta} + \frac{B_\Delta}{\epsilon_\Delta + x^{s_{\rm e}}}\right\} \\ &\propto f_{\rm inner}(x) f_{\rm trans}(x) + f_{\rm outer}(x),\end{aligned}$$

$$y(x) := \frac{\Sigma(R = r_\Delta x)}{\Sigma(r_\Delta)}$$

specified by $\boldsymbol{p} = \{c_\Delta, \alpha, \tau_\Delta, B_\Delta, s_{\rm e}, \beta, \gamma\}$

We marginalize over nuisance shape parameters ($s_{\rm e}$, β, γ) using "generic" priors found from *N*-body simulations of DK14

Results: CLASH scaled density profiles

$r_\Delta = r_{200\mathrm{m}}$

$r_\Delta = r_{2500\mathrm{c}} \sim 0.2 r_{200\mathrm{m}}$

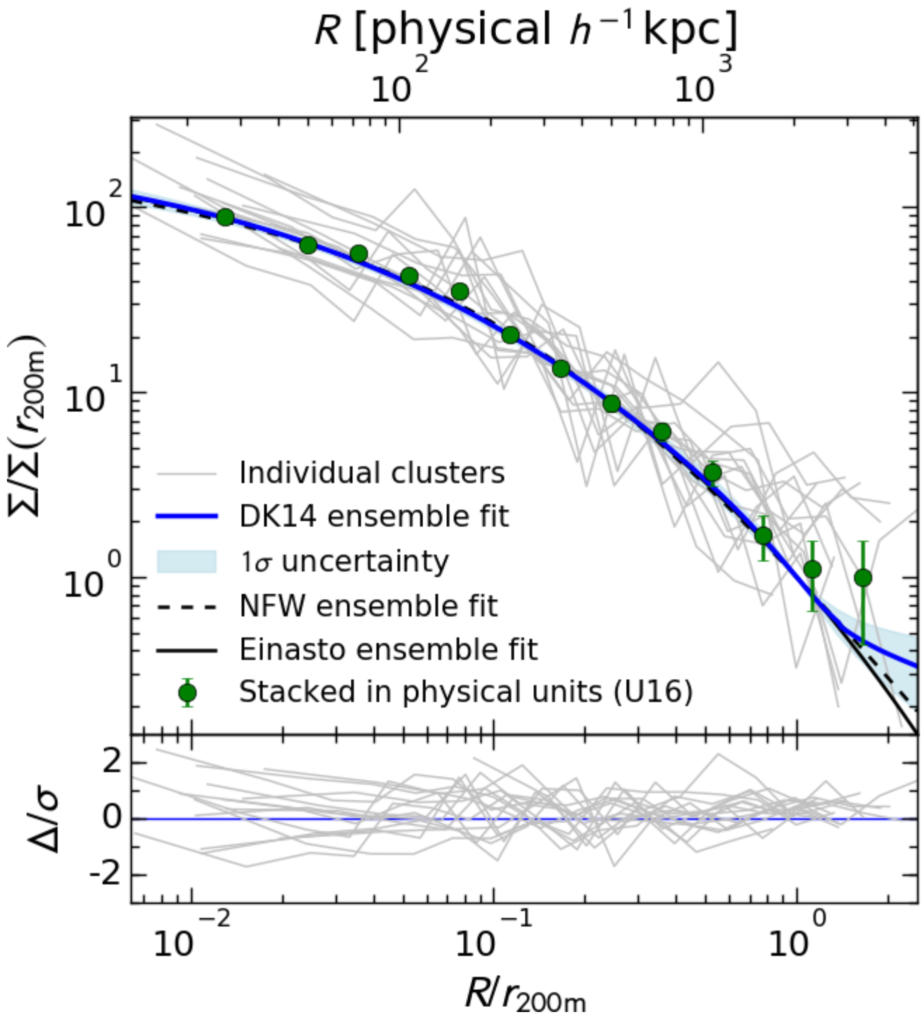

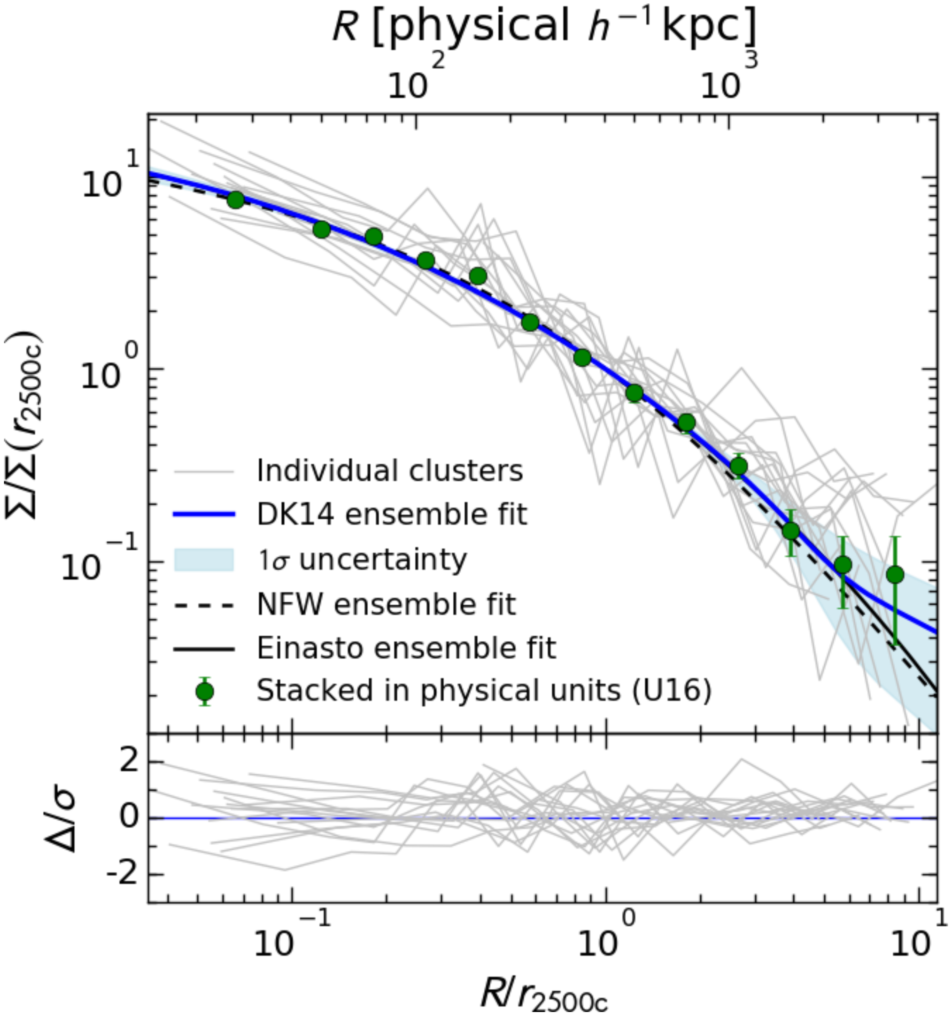

Results: CLASH logarithmic density gradient

$$r_\Delta = r_{200\mathrm{m}}$$

$$r_\Delta = r_{2500\mathrm{c}} \sim 0.2 r_{200\mathrm{m}}$$

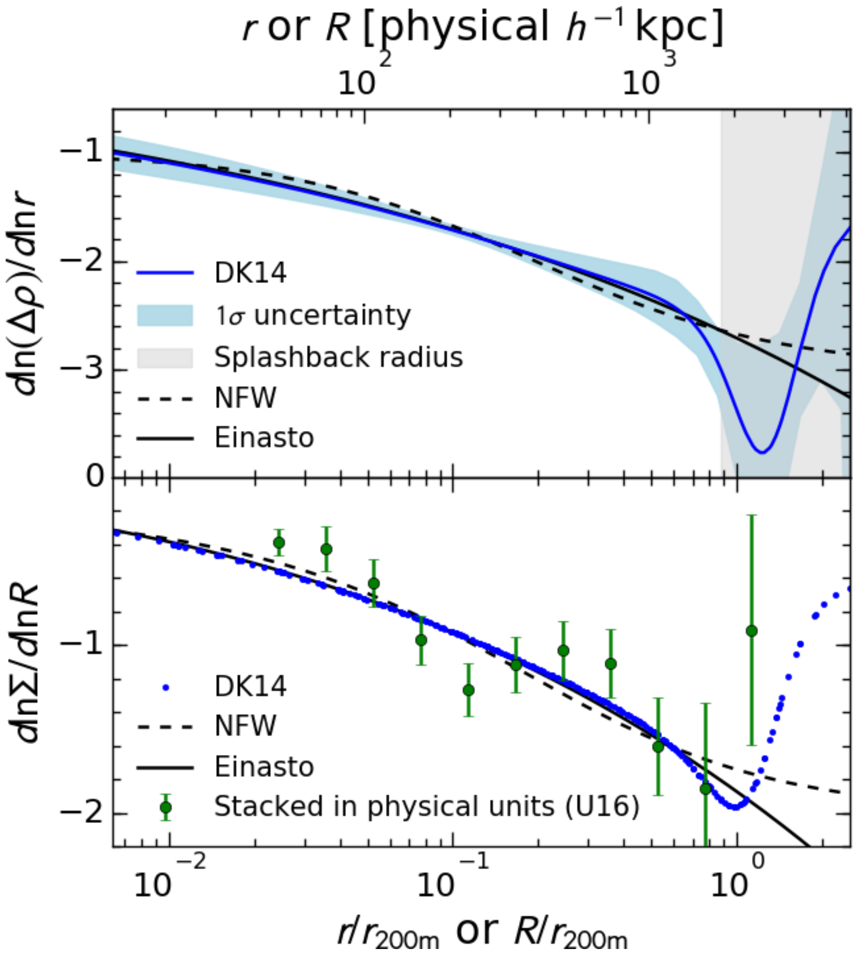

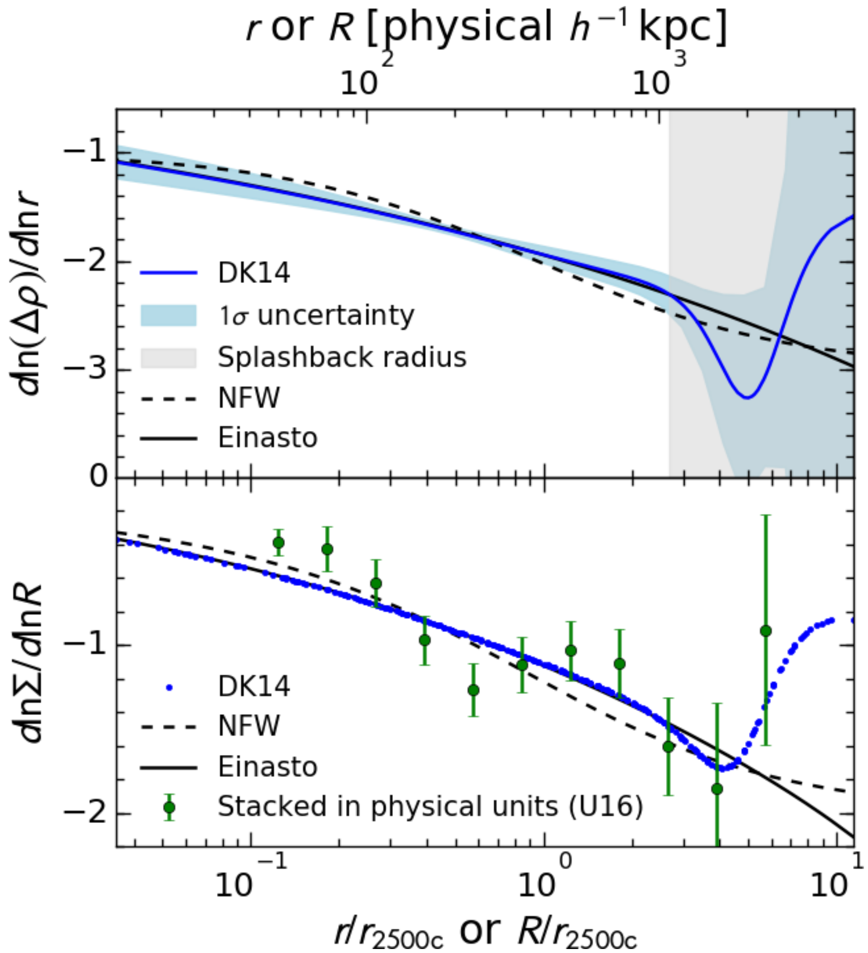

First lensing constraints on R_{sp}

$$R_{\mathrm{sp}}^{\mathrm{3D}} / r_{\mathrm{200m}} = 1.23^{+2.33}_{-0.34} \quad \Rightarrow \quad \Gamma := \frac{\Delta \ln M_{\mathrm{vir}}}{\Delta \ln a} < 4.0 \; (1\sigma)$$

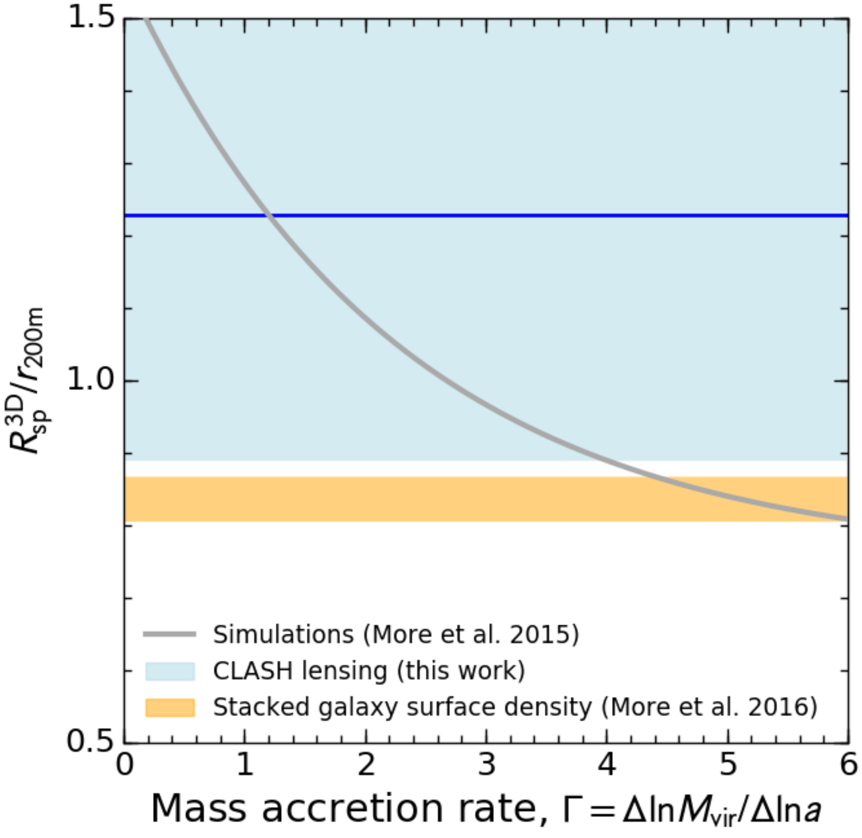

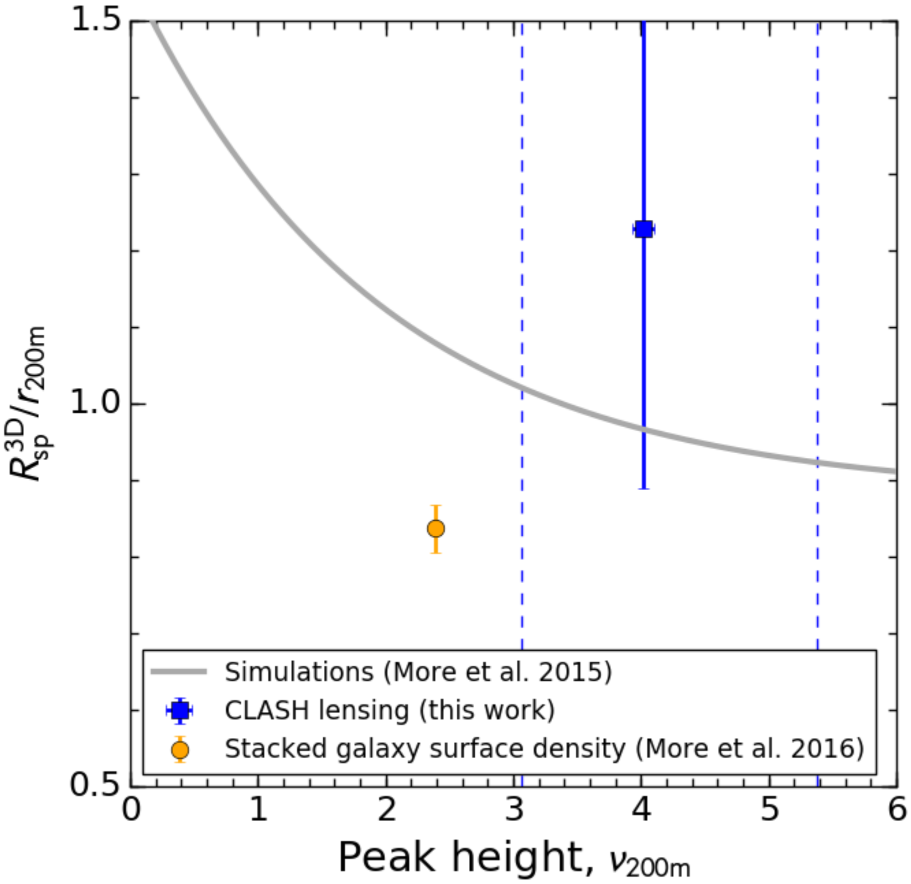

CLASH data consistent with a representative range of MAR

Next steps?

- Exploring low mass clusters/groups, higher-z systems (z>1) with HSC-SSP (1400 deg^2)
- Lensing "detection" of R_{sp} using improved statistics with HSC-SSP Large statistics of merging clusters with HSC-SSP.
- BCG-cluster-LSS connection: tidal effects, alignments, assembly histories of dark matter halos

Supplemental Slides

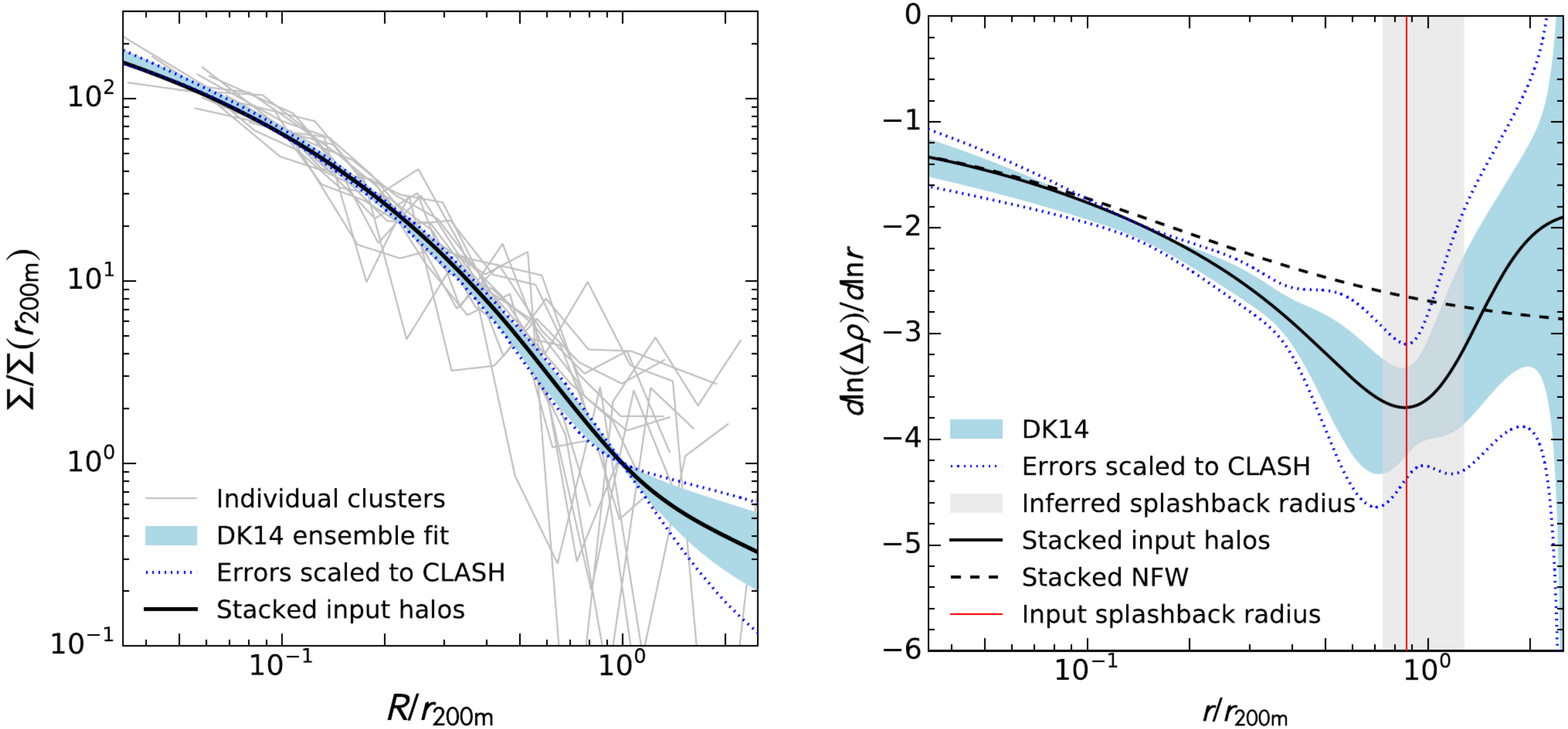

10^2
10^1
10^0
10^-1
Σ/Σ(r_200m)
10^-1
10^0
R/r_200m
Individual clusters
DK14 ensemble fit
Errors scaled to CLASH
Stacked input halos
0
−1
−2
−3
−4
−5
−6
dln(Δρ)/dlnr
10^-1
10^0
r/r_200m
DK14
Errors scaled to CLASH
Inferred splashback radius
Stacked input halos
Stacked NFW
Input splashback radius

Splashback radius, R_{sp}: Physical halo boundary

Outermost caustic of material reaching its first apocentric passage

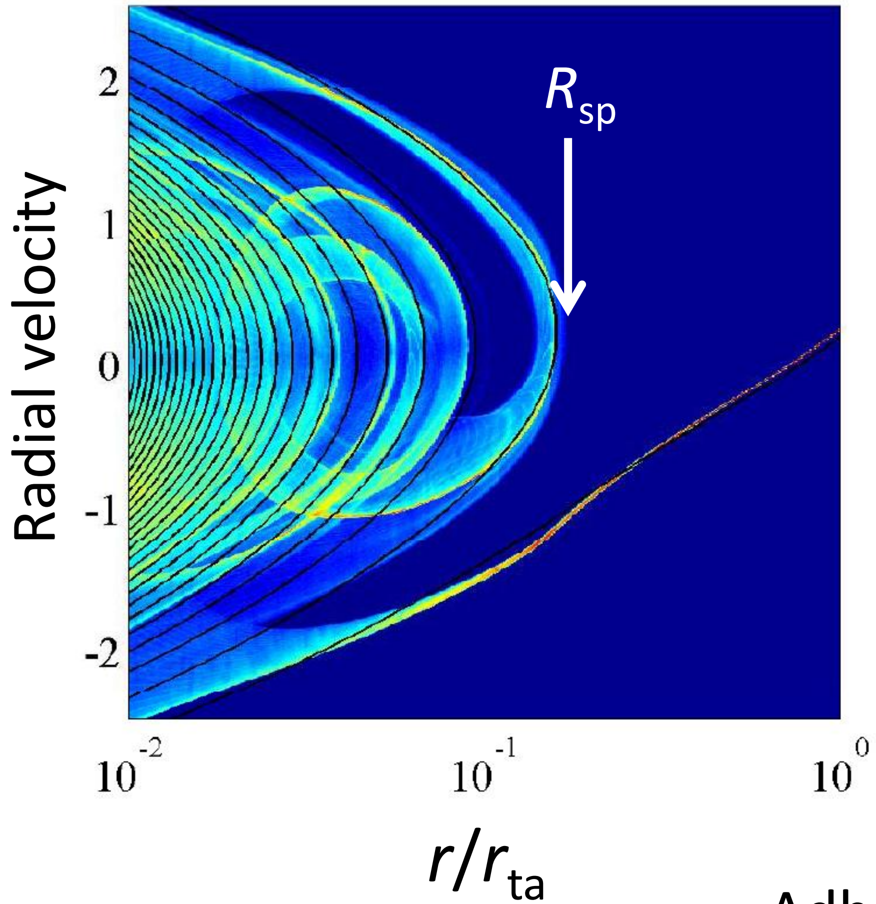

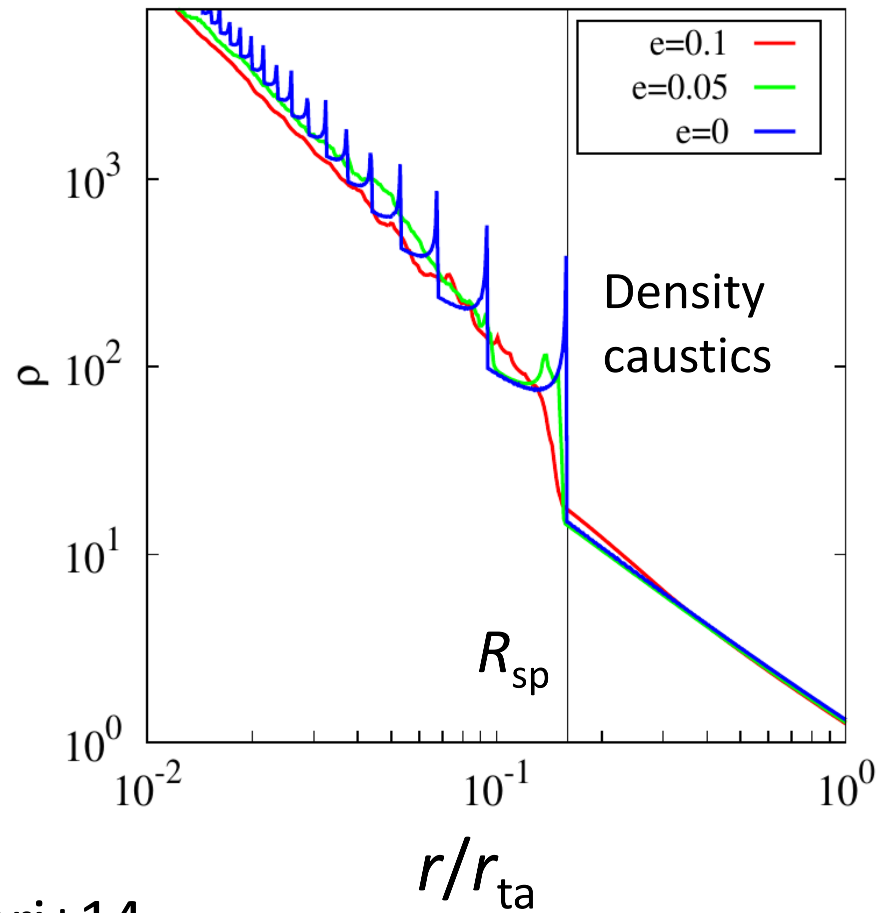

Adhikari+14

Splashback in CLASH lensing data?

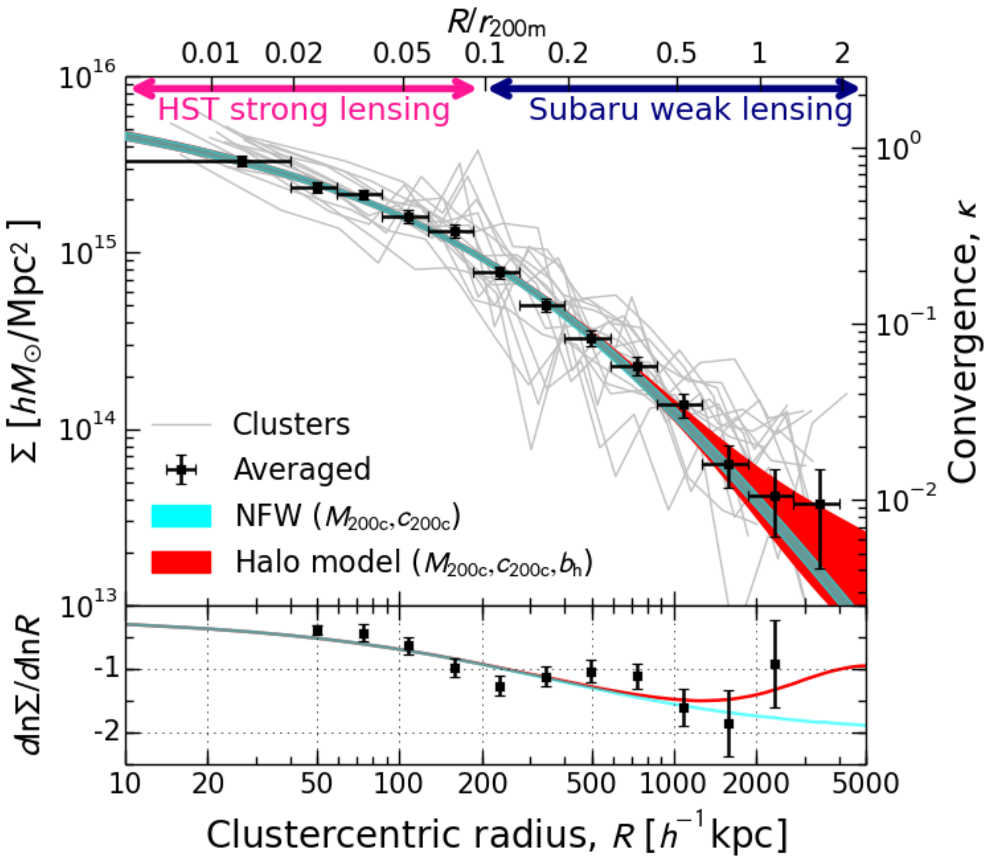

CLASH X-ray regular subsample prevalently composed of relaxed clusters (70%; Meneghetti+14)

$$\langle M_{200m} \rangle = (1.3 \pm 0.1) \times 10^{15} h^{-1} M_{sun}$$

$$\langle \nu_{200m} \rangle = 4.0 \pm 0.1$$

16 clusters with $\langle z \rangle \simeq 0.34$

Umetsu+16, *ApJ*, 821, 116

- CLASH spans a factor of ~5 (1.7) in mass (radius), so that sharp gradient feature is washed out when stacked in physical units.
- How to extract R_{sp} from coarsely binned ensemble profiles?

Parameter Constraints

$$r_\Delta = r_{200\mathrm{m}}$$

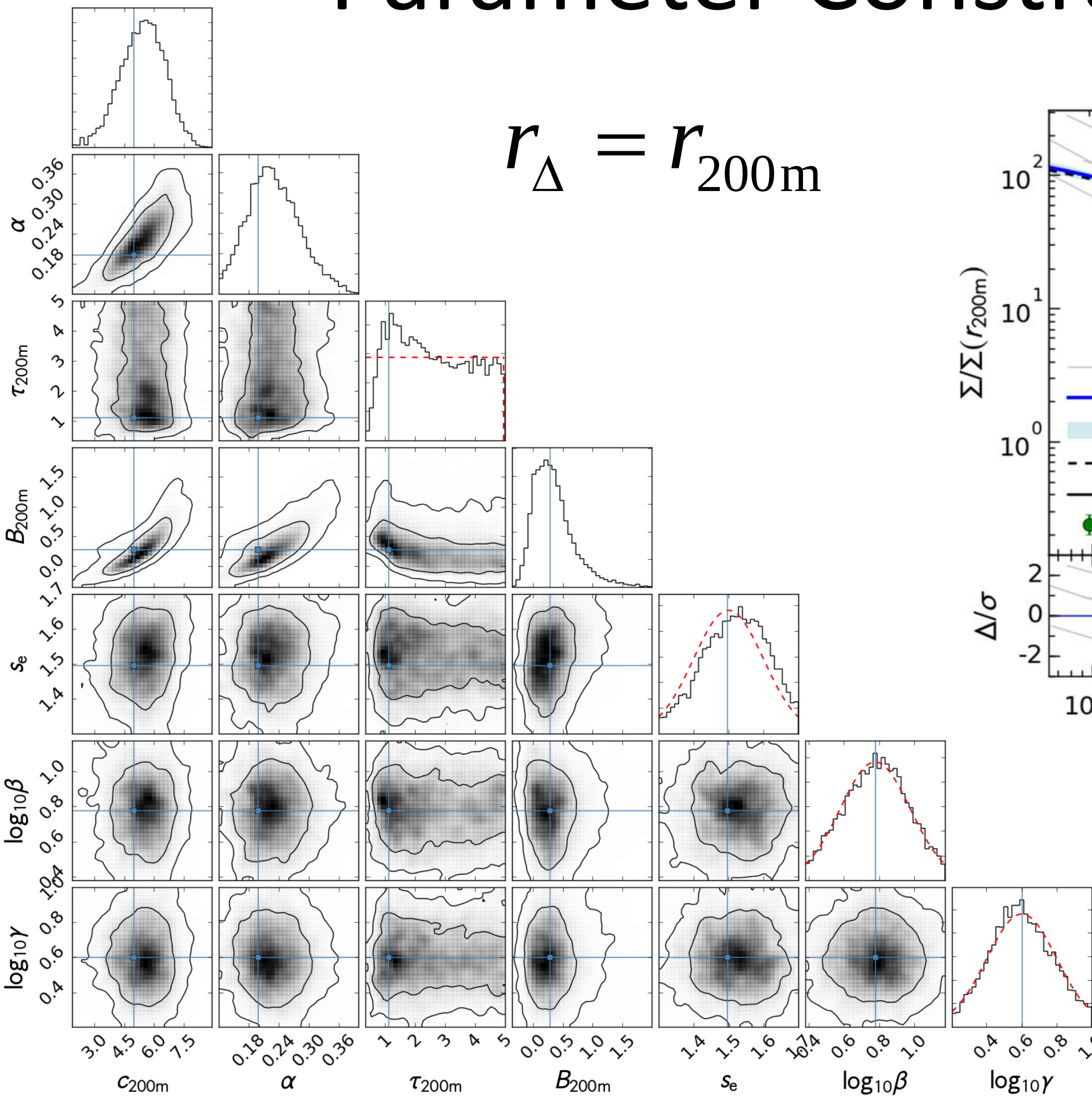

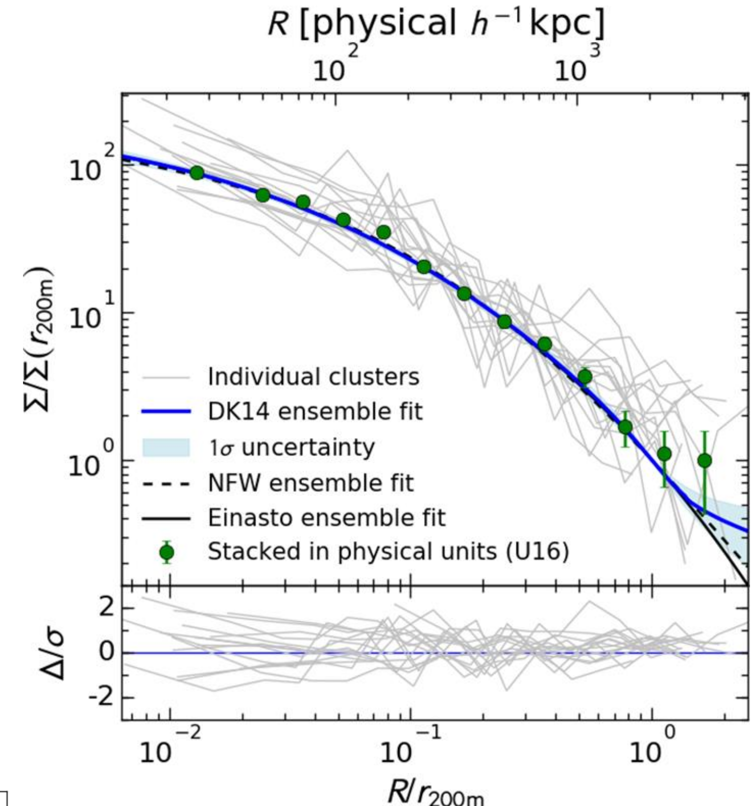

CLASH: Observational + Theory Efforts

Wide-field Subaru/Suprime-Cam imaging (0.4 - 0.9 μm) plays a unique role in complementing deep *HST* imaging of cluster cores (Umetsu+14, *ApJ*, 795, 163)

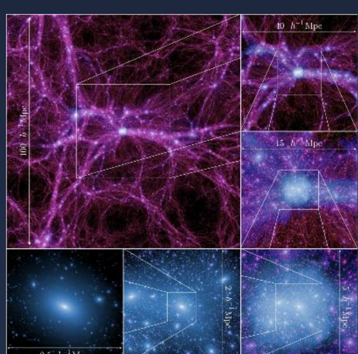

MUSIC-2 (hydro + *N*-body re-simulation) provides an accurate characterization of CLASH sample with testable predictions (Meneghetti+14, *ApJ*, 797, 34)

CLASH: Joint Analysis of Strong-lensing, Weak-lensing Shear and Magnification Data for 20 CLASH Galaxy Clusters

Umetsu, Gruen, Merten, Donahue, & Postman 2016, *ApJ*, 821, 116

See also other CLASH ensemble analysis papers:

- Umetsu et al. 2014, *ApJ*, 795, 163 (Weak lensing shear + magnification)
- Zitrin et al. 2015, *ApJ*, 801, 44 (Strong lensing)
- Merten et al. 2015, *ApJ*, 806, 4 (Strong lensing + weak shear)
- Donahue et al. 2014, *ApJ*, 794, 136 (X-ray *Chandra* & *XMM*)
- Meneghetti et al. 2014, *ApJ*, 797, 34 (theoretical predictions for CLASH)

Ensemble Calibration of Cluster Masses

CLUMI+: Multi-probe Lensing Analysis

Umetsu 2013, *ApJ*, 769, 13

Combining strong-lensing, weak-lensing shear and magnification

$$\{M_{2D,i}\}_{i=1}^{N_{SL}}, \{\langle g_{+,i}\rangle\}_{i=1}^{N_{WL}}, \{\langle n_{\mu,i}\rangle\}_{i=1}^{N_{WL}}.$$

$$P(\mathbf{\Sigma}|\mathrm{WL},\mathrm{SL}) \propto P(\mathrm{WL},\mathrm{SL}|\mathbf{\Sigma})P(\mathbf{\Sigma}) = P(\boldsymbol{n}_\mu|\mathbf{\Sigma})P(\boldsymbol{g}_+|\mathbf{\Sigma})P(\boldsymbol{M}_{2D}|\mathbf{\Sigma})P(\mathbf{\Sigma})$$

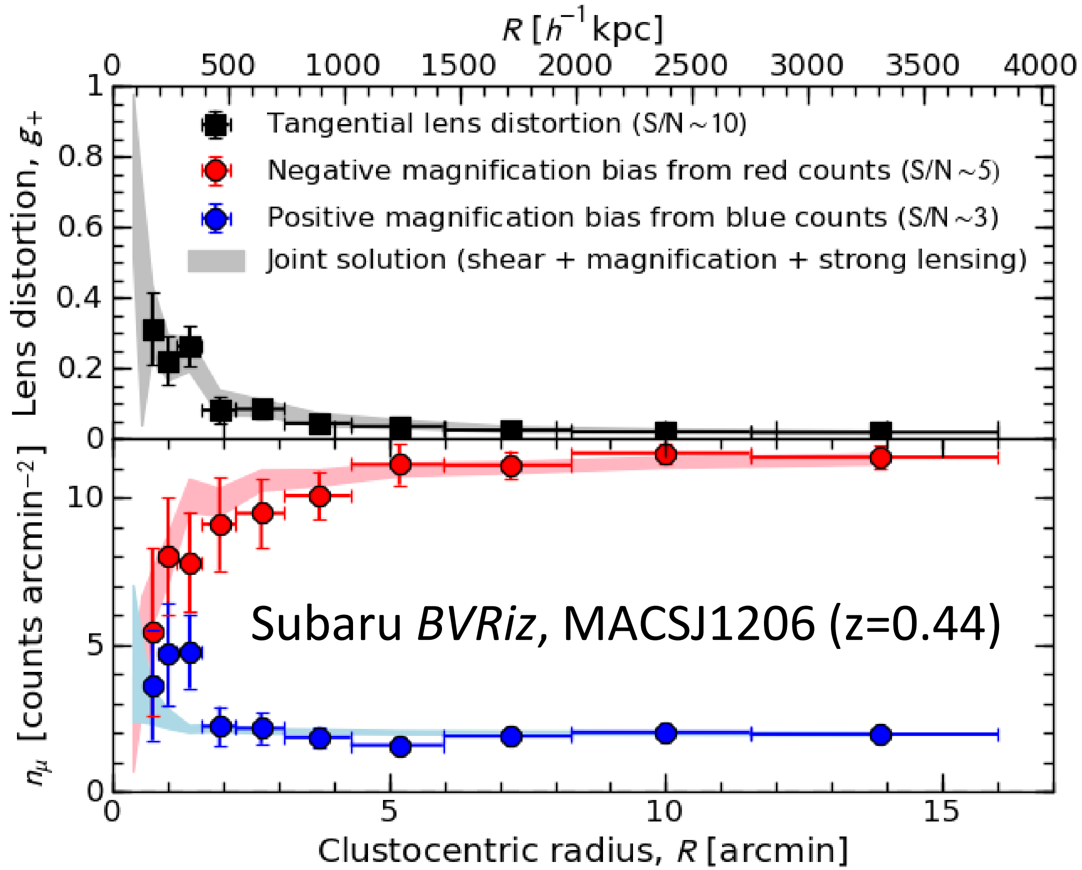

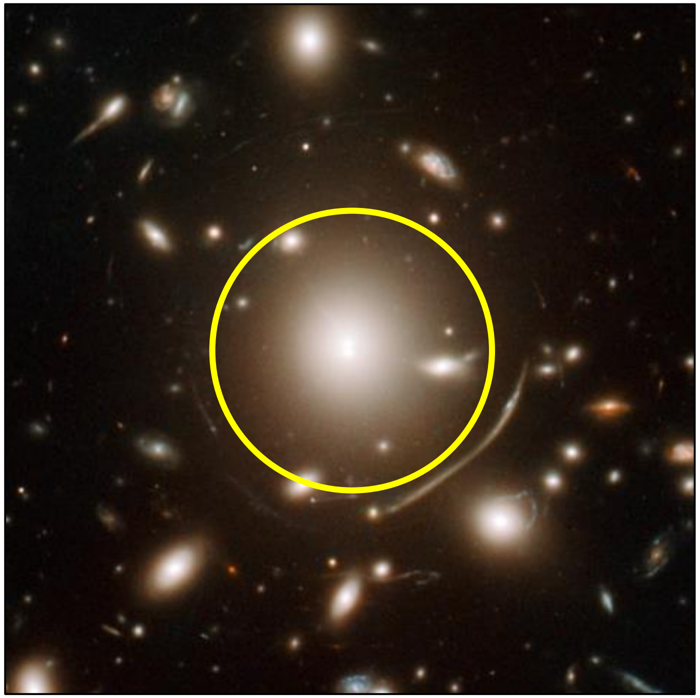

Results (3): Ensemble Mass Calibration

WtG [Subaru/S-Cam]
(Applegate+14)

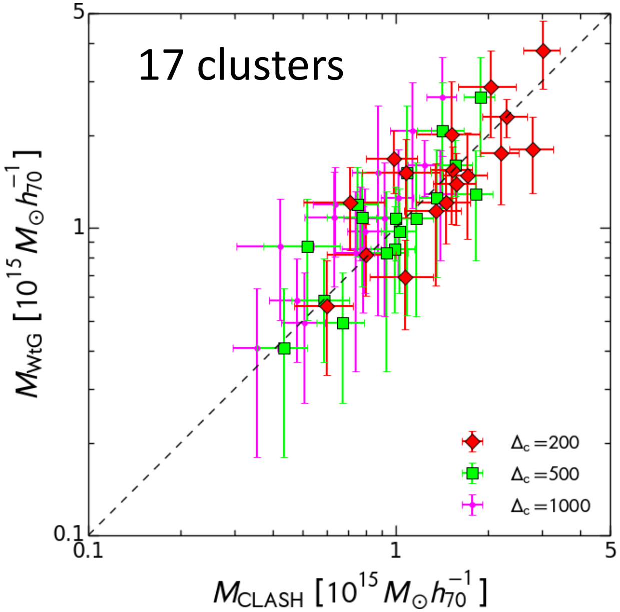

LoCuSS [Subaru/S-Cam]
(Okabe & Smith 16)

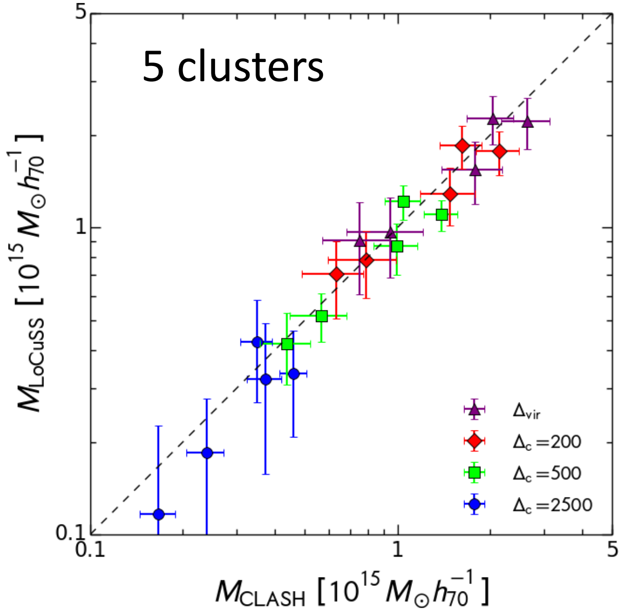

CCCP [CFHT]
(Hoekstra+15)

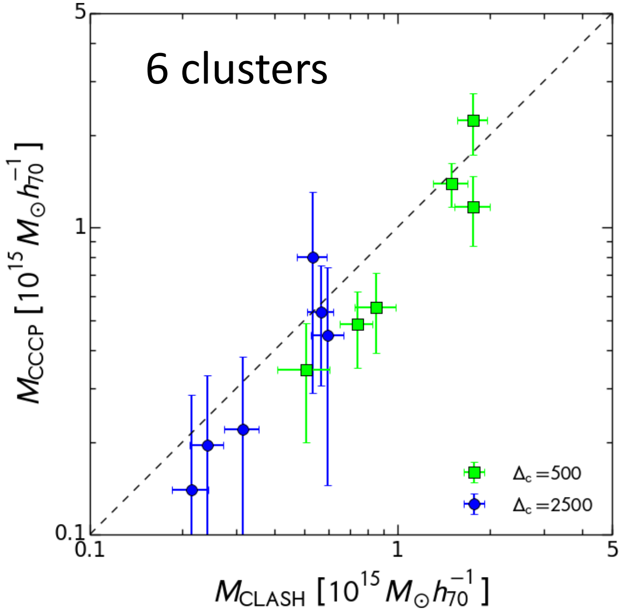

$$\langle M_{\rm WtG}/M_{\rm CLASH}\rangle = 1.03 \pm 0.09 \quad (\Delta = 200)$$
$$= 1.07 \pm 0.12 \quad (\Delta = 500)$$
$$= 1.07 \pm 0.12 \quad (\Delta = 1000)$$

$$\langle M_{\rm LoCuSS}/M_{\rm CLASH}\rangle = 1.00 \pm 0.15 \quad (\Delta = \Delta_{\rm vir})$$
$$= 0.98 \pm 0.13 \quad (\Delta = 200)$$
$$= 0.93 \pm 0.10 \quad (\Delta = 500)$$
$$= 0.84 \pm 0.22 \quad (\Delta = 2500)$$

$$\langle M_{\rm CCCP}/M_{\rm CLASH}\rangle = 0.84 \pm 0.10 \quad (\Delta = 500)$$
$$= 0.91 \pm 0.24 \quad (\Delta = 2500)$$

Umetsu+16, *ApJ*, 821, 116

Results (1): *Ensemble Mass Profile*

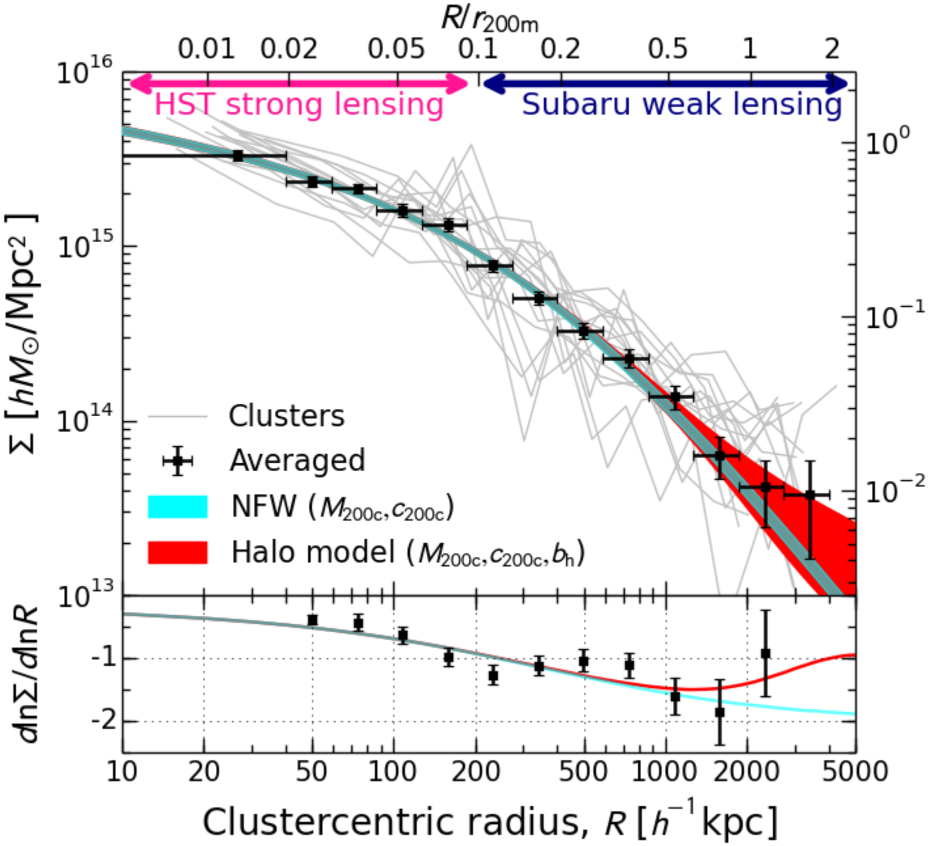

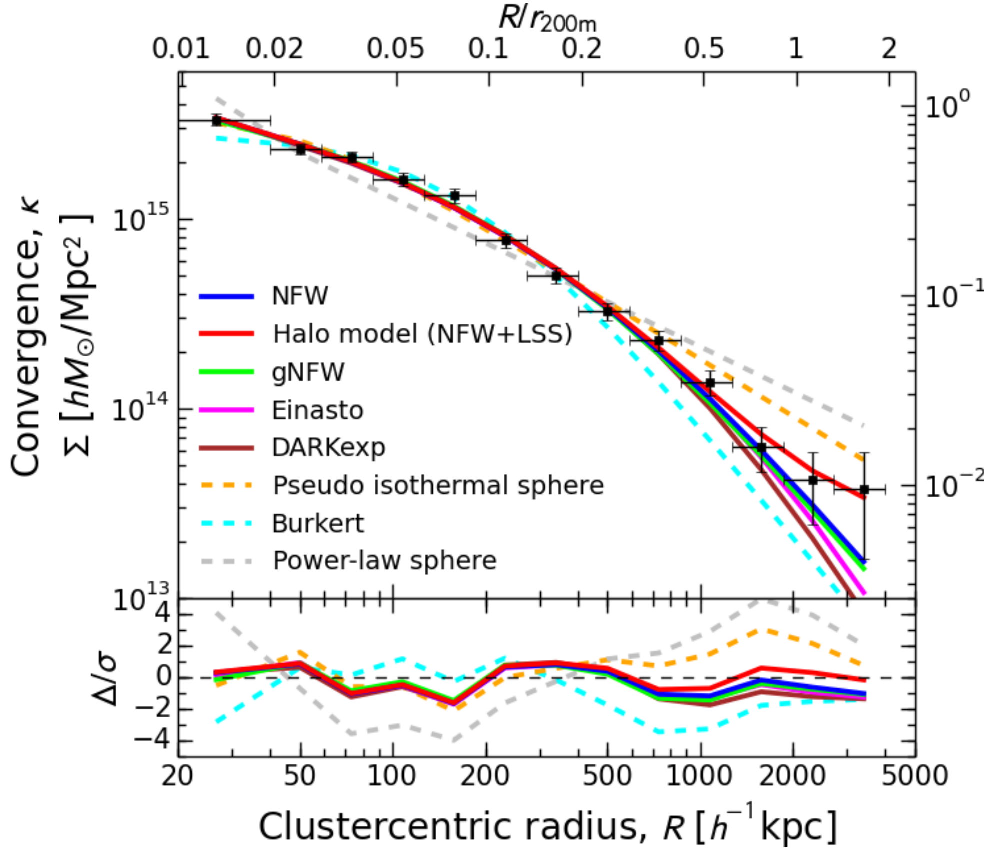

- 33σ detection of ensemble mass profile from $R \sim 0.01R_{vir}$ to $2R_{vir}$
- Consistent with cuspy, steepening density profiles (NFW, Einasto, DARKexp)
- Cored (Burkert, pseudo-isothermal) and power-law models are disfavored
- Cuspy models with truncation + ΛCDM 2-halo term (b_h~9.3) give improved fits

Results (2): Concentration—Mass Relation

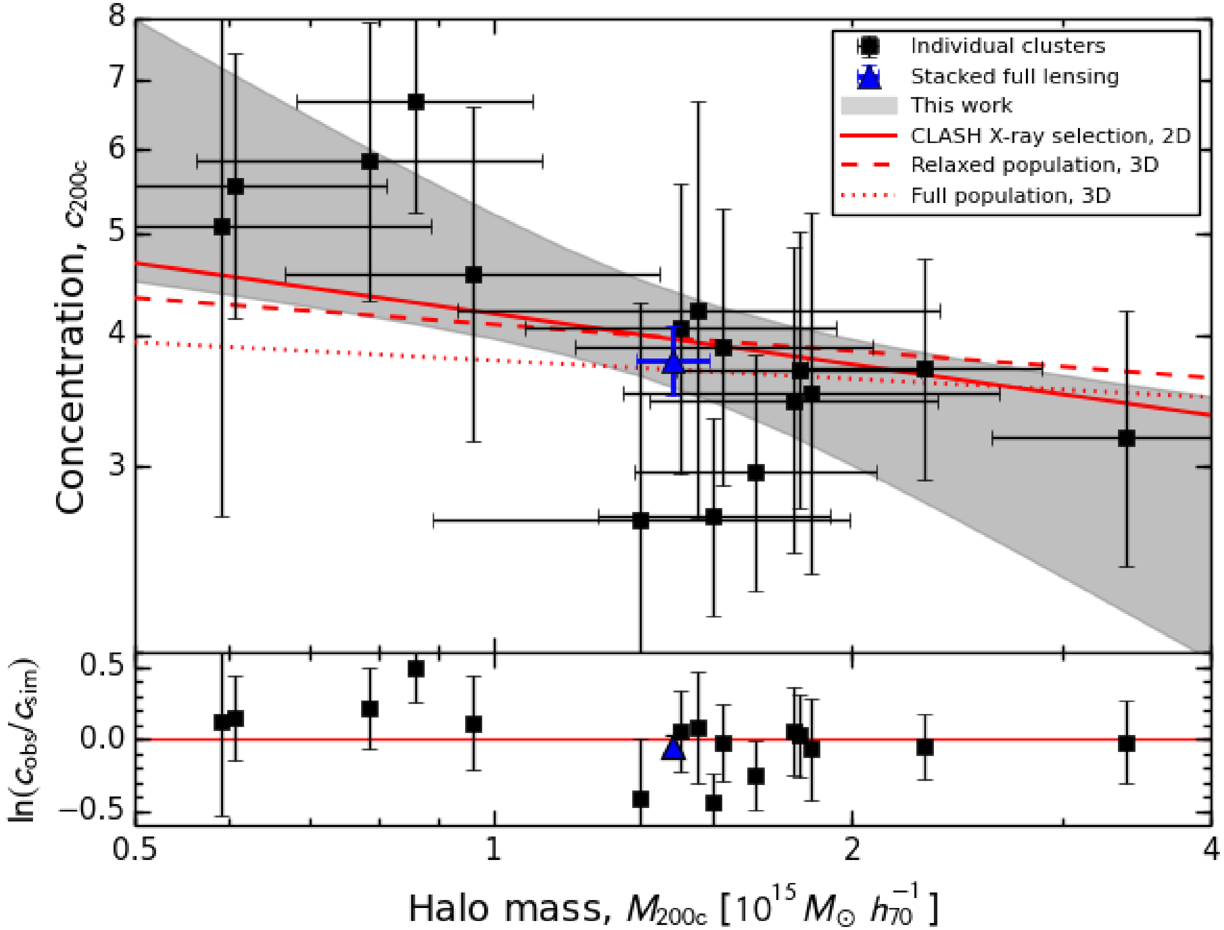

Predicted for CLASH (Meneghetti+14):

$\langle c_{200c} \rangle = 3.9,$

$3 \le c_{200c} \le 6,$

$\text{slope} = -0.16$

$\sigma(\ln c_{200c}) = 0.16$

Observed (this work):

$c_{200c}|_{z=0.34} = 3.95 \pm 0.35$

at $M_{200c} = 10^{15} M_{sun}/h,$

$\text{slope} = -0.44 \pm 0.19$

$\sigma(\ln c_{200c}) = 0.13 \pm 0.06$

Normalization, slope, & scatter are all consistent with ΛCDM (WMAP7 and later) within errors when the CLASH selection function based on X-ray morphological regularity and projection effects are taken into account.

Splashback in surface number density of SDSS cluster galaxies (S. More+16)

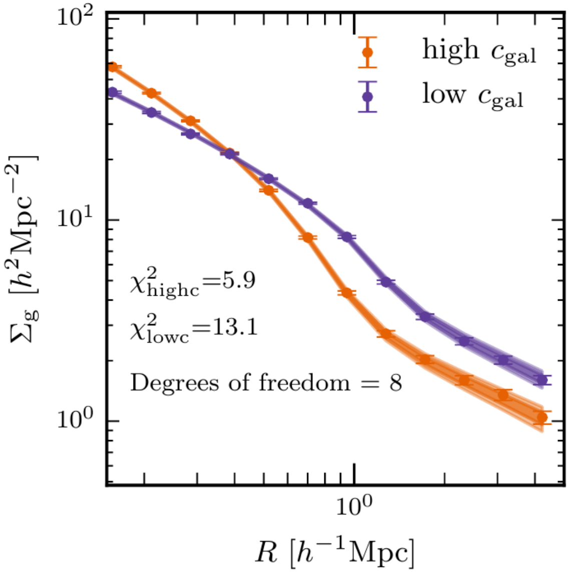

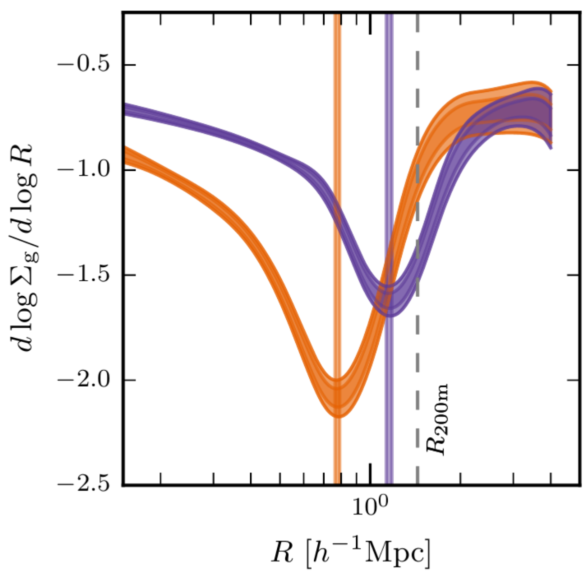

$$\langle M_{200m}\rangle \cong 0.19\times10^{15}\, h^{-1} M_{sun}$$

$$\langle \nu_{200m}\rangle \cong 2.4$$

$$\langle z\rangle \cong 0.24$$

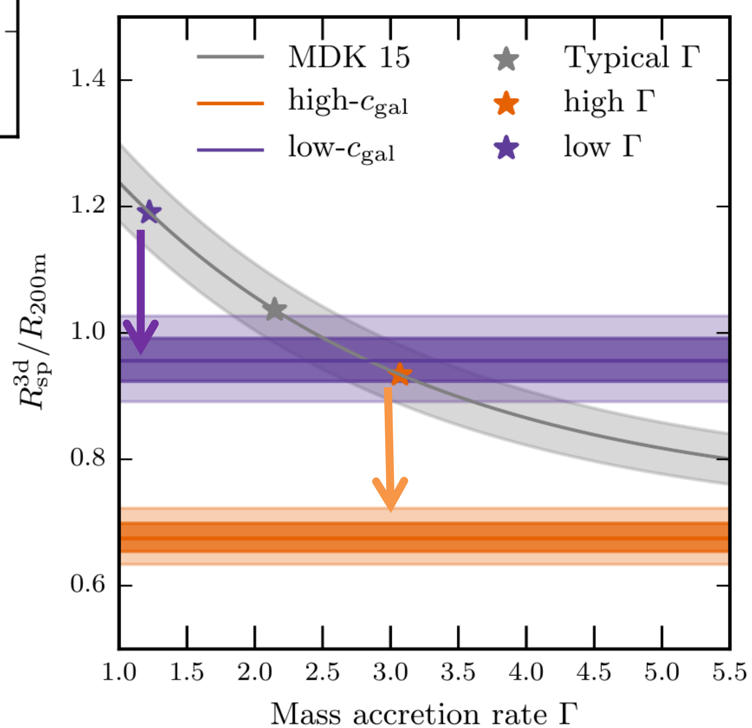

- Splashback feature clearly detected using "galaxies", instead of "mass", in both cluster subsamples.
- But the observed R_{sp}(gal)/R_{200m}(WL) values are *significantly smaller* than predicted!

Ensemble-averaged Error Budget

Diagonal elements (C_{ii}) averaged over all CLASH clusters

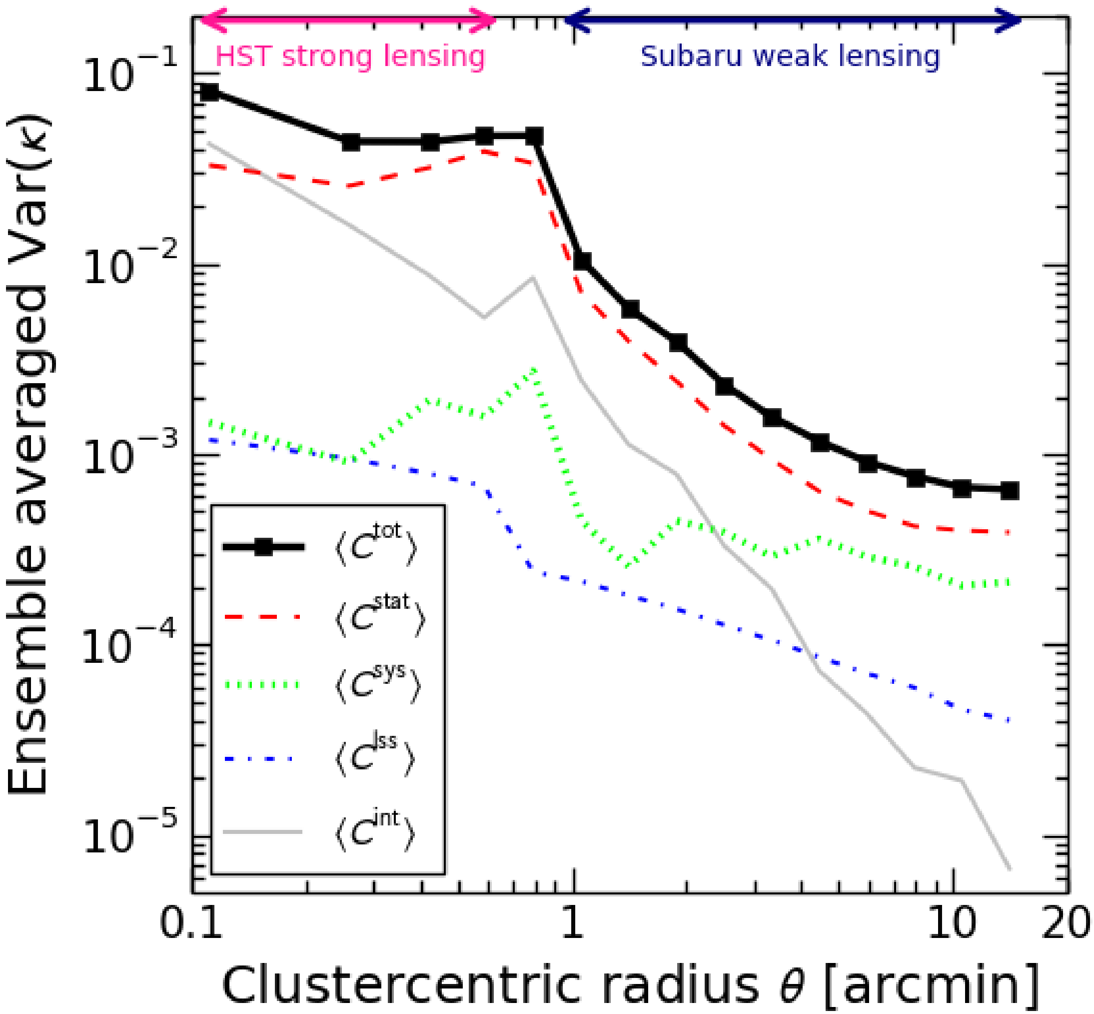

Residual mass-sheet uncertainty

$$(C_{\mathrm{sys}})_{ii} \sim \text{const.} \sim (0.02)^2$$

Intrinsic profile variations due to triaxiality, substructure, and *c*-*M* scatter (Gruen+15)

$$(C_{\mathrm{int}})_{ii} \approx (0.2)^2 \kappa_i^2$$

Planck13 CMB vs. Cluster Cosmology

b=0.2?? – 0.4??

- Planck: 3σ tension between SZ cluster counts and CMB cosmology
- assumes M_{Planck} / M_{true} = (1-b) = 0.8
- calibrated with XMM hydrostatic masses (Arnaud et al. 2010) + simulations

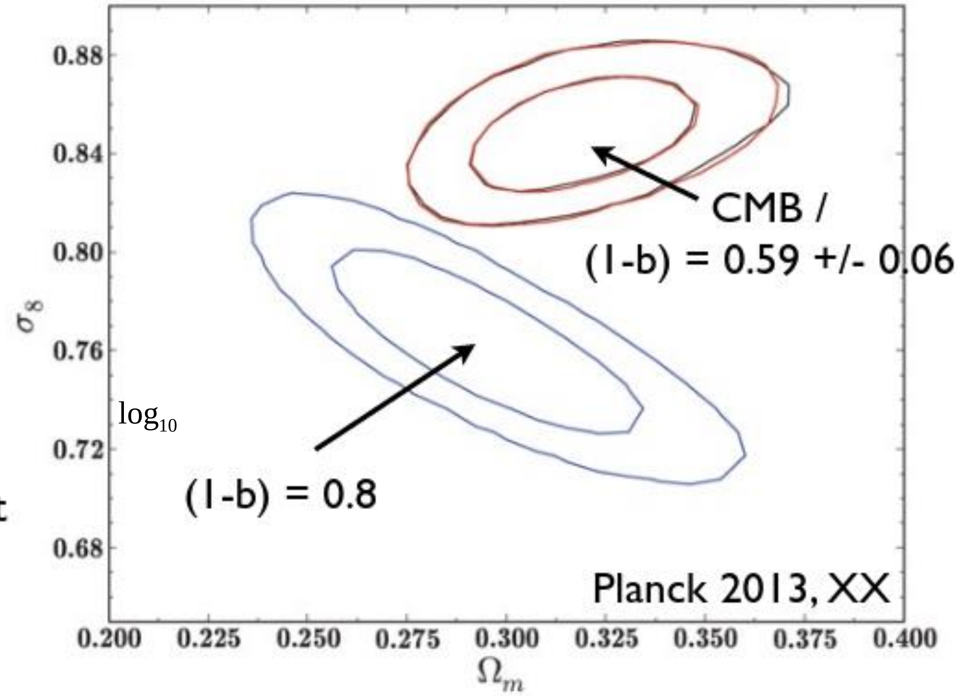

suggested explanations:

- mass bias underestimated (and no accounting for uncertainties)
- 2.9σ detection of neutrino masses: Σm_ν = (0.58 +/- 0.20) eV (Planck+WMAPpol+ACT+BAO: Σm_ν < 0.23 eV, 95% CL)

Slide taken from Anja von der Linden's presentation

Comparison with *Planck* Masses – Not so simple

Mass-dependent bias (20-45%) observed for *Planck*-SZE mass estimates

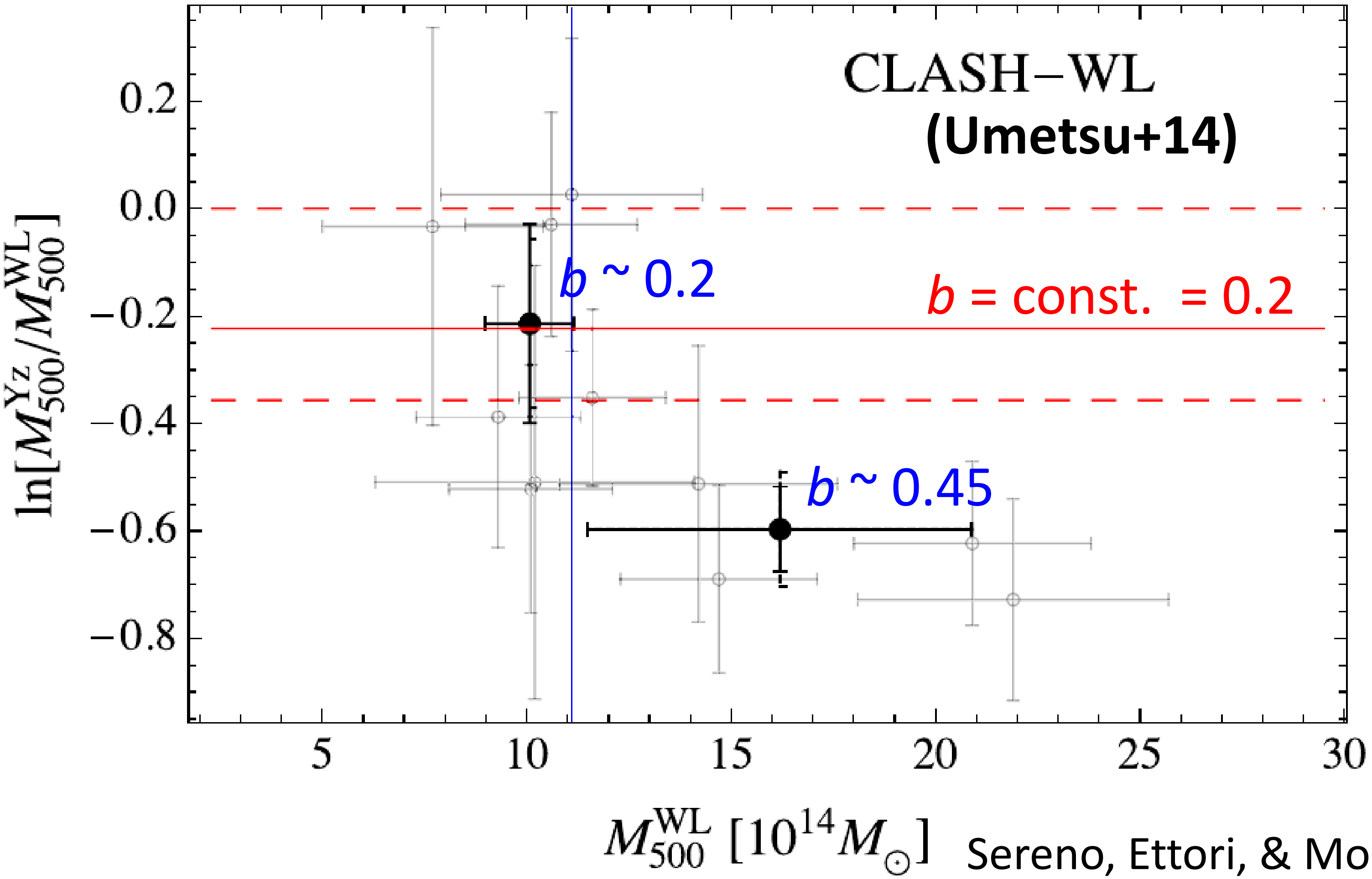

Sereno, Ettori, & Moscardini 15, CoMaLit II (arXiv:1407.7869)

CLASH Lensing: Internal Consistency

$M_{3D}(<r)$ for N=20 clusters de-projected assuming spherical NFW model

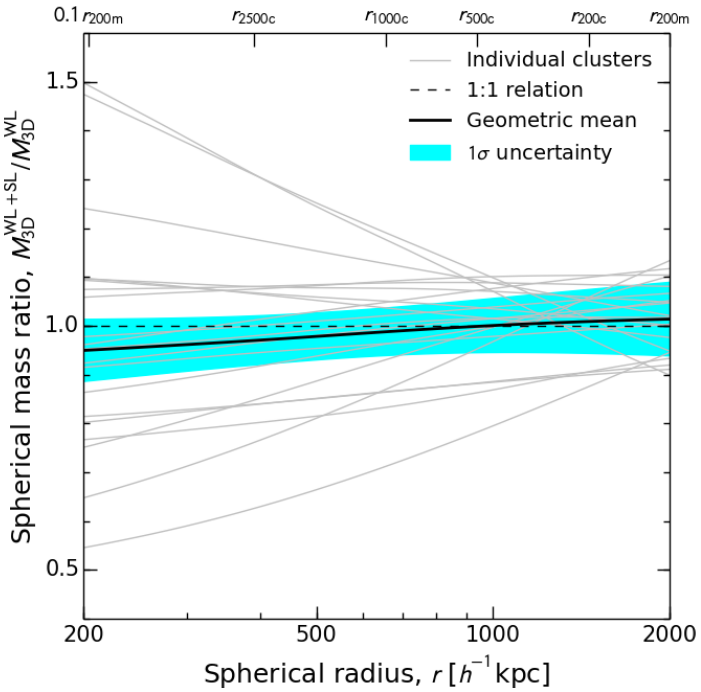

WL-only (U14) and WL+SL (U16) are consistent within 5% at *r* = [200, 2000] kpc/*h*

Umetsu+16, *ApJ*, 821, 116

CLASH ensemble mass calibration uncertainty

- Statistical uncertainty with *N*=20: 28%/sqrt(20) = 6.3%
- Systematic uncertainty: 5.6% [5% shear calibration, 2% dilution]
- Mass modeling bias (dev from NFW, orientation bias): 3%
- Total calibration uncertainty: 9%

Comparisons with Other WL Surveys

WtG [Subaru]
(Applegate+14)

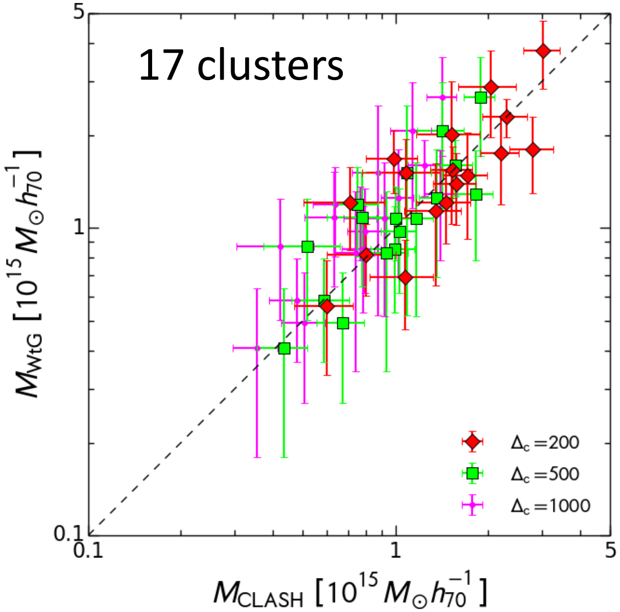

$$\langle M_{\rm WtG}/M_{\rm CLASH}\rangle = 1.03 \pm 0.09 \quad (\Delta = 200)$$
$$= 1.07 \pm 1.12 \quad (\Delta = 500)$$
$$= 1.07 \pm 1.12 \quad (\Delta = 1000)$$

LoCuSS [Subaru]
(Okabe & Smith 15)

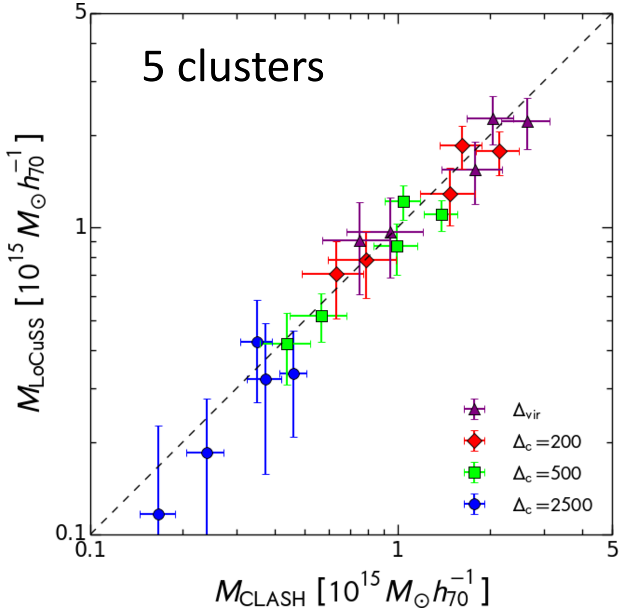

$$\langle M_{\rm LoCuSS}/M_{\rm CLASH}\rangle = 1.00 \pm 0.15 \quad (\Delta = \Delta_{\rm vir})$$
$$= 0.98 \pm 0.13 \quad (\Delta = 200)$$
$$= 0.93 \pm 0.10 \quad (\Delta = 500)$$
$$= 0.84 \pm 0.22 \quad (\Delta = 2500)$$

CCCP [CFHT]
(Hoekstra+15)

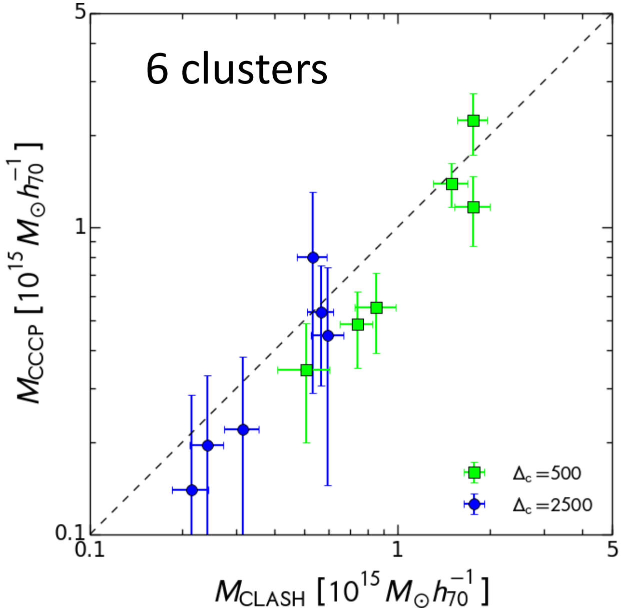

$$\langle M_{\rm CCCP}/M_{\rm CLASH}\rangle = 0.84 \pm 0.10 \quad (\Delta = 500)$$
$$= 0.91 \pm 0.24 \quad (\Delta = 2500)$$

Umetsu+16, *ApJ*, 821, 116

Comparison of Best-fit Models

Acceptable fits: *p* values (PTE) > 0.05

Table 4
Best-fit models for the stacked mass profile of the CLASH X-ray-selected subsample

Model	M_{200c} ($10^{14} M_\odot\, h_{70}^{-1}$)	c_{200c}	Shape/structural parameters	b_h	χ^2/dof	PTE[a]	Notes
NFW	$14.4^{+1.1}_{-1.0}$	$3.76^{+0.29}_{-0.27}$	$\gamma_c = 1$	—	11.3/11	0.419	No truncation
gNFW	$14.1^{+1.1}_{-1.1}$	$4.04^{+0.53}_{-0.52}$	$\gamma_c = 0.85^{+0.22}_{-0.31}$	—	10.9/10	0.366	No truncation
Einasto	$14.7^{+1.1}_{-1.1}$	$3.53^{+0.36}_{-0.39}$	$\alpha_E = 0.232^{+0.042}_{-0.038}$	—	11.7/10	0.306	No truncation
DARKexp–γ[b]	$14.5^{+1.2}_{-1.1}$	$3.53^{+0.42}_{-0.42}$	$\phi_0 = 3.90^{+0.41}_{-0.45}$	—	13.5/10	0.198	No truncation
Pseudo isothermal	—	—	$V_c = 1762^{+40}_{-39}$ km/s, $r_c = 69^{+7}_{-7}$ kpc	—	23.6/11	0.015	No truncation
Burkert	$11.6^{+0.8}_{-0.8}$	—	$r_{200c}/r_0 = 8.81^{+0.42}_{-0.41}$	—	29.9/11	0.002	No truncation
Power-law sphere	$12.5^{+0.8}_{-0.8}$	—	$\gamma_c = 1.78^{+0.02}_{-0.02}$	—	93.5/11	0.000	No truncation
Halo model[c]:							
NFW+LSS (i)	$14.1^{+1.0}_{-1.0}$	$3.79^{+0.30}_{-0.28}$	$\gamma_c = 1$	9.3	10.9/11	0.450	ΛCDM $b_h(M)$ scaling
NFW+LSS (ii)	$14.4^{+1.4}_{-1.3}$	$3.74^{+0.33}_{-0.30}$	$\gamma_c = 1$	$7.4^{+4.6}_{-4.7}$	10.8/10	0.377	b_h as a free parameter
Einasto+LSS (i)	$14.3^{+1.1}_{-1.1}$	$3.69^{+0.36}_{-0.42}$	$\alpha_E = 0.248^{+0.051}_{-0.047}$	9.3	10.7/10	0.385	ΛCDM $b_h(M)$ scaling
Einasto+LSS (ii)	$14.5^{+1.9}_{-1.6}$	$3.65^{+0.47}_{-0.61}$	$\alpha_E = 0.245^{+0.061}_{-0.053}$	$8.7^{+5.3}_{-5.6}$	10.6/9	0.301	b_h as a free parameter
DARKexp+LSS (i)	$14.2^{+1.2}_{-1.1}$	$3.64^{+0.44}_{-0.46}$	$\phi_0 = 3.89^{+0.51}_{-0.54}$	9.3	11.7/10	0.308	ΛCDM $b_h(M)$ scaling
DARKexp+LSS (ii)	$14.0^{+1.8}_{-1.6}$	$3.69^{+0.53}_{-0.57}$	$\phi_0 = 3.85^{+0.57}_{-0.61}$	$10.1^{+4.9}_{-5.1}$	11.6/9	0.235	b_h as a free parameter

[a] Probability to exceed the observed χ^2 value.
[b] We use Dehnen–Tremaine γ-models with the central cusp slope $\gamma_c = 3\log_{10}\phi_0 - 0.65$ $(1.7 \le \phi_0 \le 6)$ as an analytic fitting function for the DARKexp density profile.
[c] For halo model predictions, we decompose the total mass overdensity $\Delta\rho(r) = \rho(r) - \overline{\rho}_m$ as $\Delta\rho = f_t\rho_h + \rho_{2h}$ where $\rho_h(r)$ is the halo density profile, $\rho_{2h}(r) = \overline{\rho}_m b_h \xi^L_m(r)$ is the two-halo term, and $f_t(r) = (1 + r^2/r_t^2)^{-2}$ describes the steepening of the density profile in the transition regime around the truncation radius r_t, which is assumed to be $r_t = 3r_{200c}$.

Umetsu+16, arXiv:1507.04385

- Consistent with cuspy density profiles (NFW, Einasto, DARKexp)
- Cuspy models that include ΛCDM 2-halo term (b_h~9.3) give improved fits

Comparison with LCDM $c(M)$ models

Umetsu+16, arXiv:1507.04385

Table 5
Comparison of measured and predicted concentrations for the CLASH X-ray-selected subsample

Author	Sample	3D/2D	Function[a]	$c^{(\rm obs)}/c^{(\rm pred)}$ Average[c]	σ[d]	χ^2	PTE[b]
Theory:							
Duffy et al. (2008)	full	3D	c–M	1.331 ± 0.108	0.334	22.6	0.046
Duffy et al. (2008)	relaxed	3D	c–M	1.165 ± 0.094	0.290	13.6	0.399
Prada et al. (2012)	full	3D	c–ν	0.733 ± 0.065	0.244	24.6	0.026
Bhattacharya et al. (2013)	full	3D	c–ν	1.169 ± 0.095	0.292	14.1	0.369
Bhattacharya et al. (2013)	relaxed	3D	c–ν	1.131 ± 0.092	0.277	12.4	0.494
Dutton & Macciò (2014)	full	3D	c–M	1.061 ± 0.086	0.262	10.4	0.659
Meneghetti et al. (2014)	full	3D	c–M	1.061 ± 0.089	0.279	10.2	0.675
Meneghetti et al. (2014)	relaxed	3D	c–M	0.990 ± 0.083	0.249	9.2	0.760
Diemer & Kravtsov (2015)	full (median)	3D	c–ν	1.021 ± 0.083	0.330	14.4	0.349
Diemer & Kravtsov (2015)	full (mean)	3D	c–ν	1.060 ± 0.086	0.326	13.8	0.391
Meneghetti et al. (2014)	full	2D	c–M	1.087 ± 0.092	0.336	13.5	0.413
Meneghetti et al. (2014)	relaxed	2D	c–M	1.040 ± 0.086	0.283	10.8	0.628
Meneghetti et al. (2014)	CLASH	2D	c–M	0.988 ± 0.078	0.227	9.6	0.730
Observations:							
Merten et al. (2015)	CLASH	2D	c–M	1.133 ± 0.087	0.209	9.2	0.754

[a] c–M: power-law $c(M, z)$ relation; c–ν: halo concentration given as a function of peak height $\nu(M, z)$.
[b] Probability to exceed the measured χ^2 value assuming the standard χ^2 probability distribution function.
[c] Weighted geometric average of observed-to-predicted concentration ratios.
[d] Standard deviation of the distribution of observed-to-predicted concentration ratios.

WMAP5

High normalization

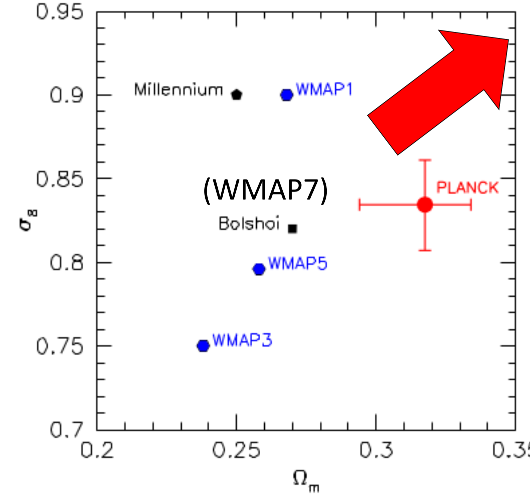

- Consistent with models that are calibrated for more recent cosmologies (WMAP7 and later)
- Better agreement is achieved when selection effects (overall degree of relaxation) are taken into account

Multi-probe Lensing Approach

Combining azimuthally-averaged strong and weak lensing observables

$$M_{2\mathrm{D}}(<R) = \int_{|\mathbf{R}'|<R} \Sigma(\mathbf{R}') d^2R'$$

$$\{M_{2\mathrm{D},i}\}_{i=1}^{N_{\mathrm{SL}}}, \{\langle g_{+,i}\rangle\}_{i=1}^{N_{\mathrm{WL}}}, \{\langle n_{\mu,i}\rangle\}_{i=1}^{N_{\mathrm{WL}}}.$$

$$P(\boldsymbol{\kappa} \mid \mathrm{WL,SL}) \propto P(\mathrm{WL,SL} \mid \boldsymbol{\kappa}) P(\boldsymbol{\kappa}) = P(\mathbf{g}_+ \mid \boldsymbol{\kappa}) P(\mathbf{n}_{\boldsymbol{\mu}} \mid \boldsymbol{\kappa}) P(\mathbf{M}_{\mathbf{2D}} \mid \boldsymbol{\kappa}) P(\boldsymbol{\kappa})$$

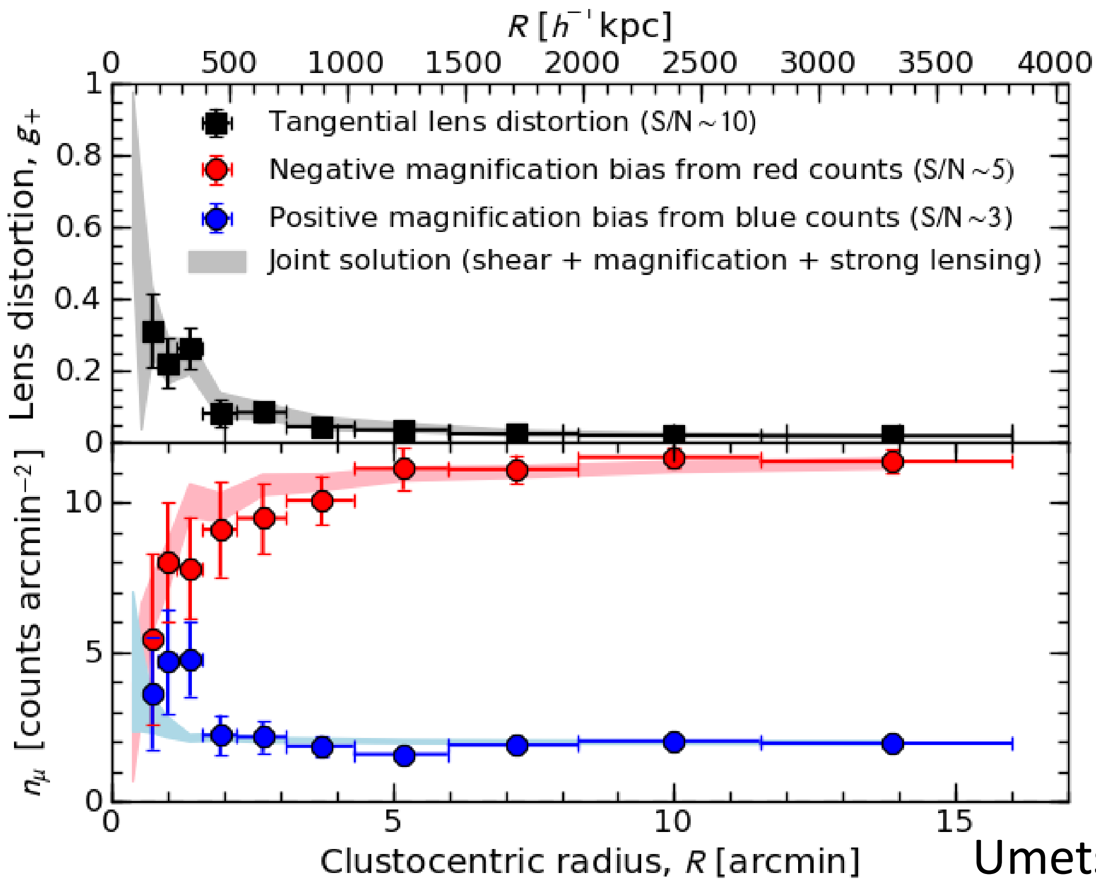

Umetsu 2013, *ApJ*, 769, 13

Multi-probe Lensing Approach

Combining azimuthally-averaged strong and weak lensing observables

$$M_{2D}(<R) = \int_{|\mathbf{R}'|<R} \Sigma(\mathbf{R}')\, d^2R'$$

$$\{M_{2D,i}\}_{i=1}^{N_{SL}}, \{\langle g_{+,i}\rangle\}_{i=1}^{N_{WL}}, \{\langle n_{\mu,i}\rangle\}_{i=1}^{N_{WL}}.$$

$$P(\boldsymbol{\kappa}\,|\,\mathrm{WL,SL}) \propto P(\mathrm{WL,SL}\,|\,\boldsymbol{\kappa})P(\boldsymbol{\kappa}) = P(\mathbf{g}_+\,|\,\boldsymbol{\kappa})P(\mathbf{n}_\mu\,|\,\boldsymbol{\kappa})P(\mathbf{M}_{2D}\,|\,\boldsymbol{\kappa})P(\boldsymbol{\kappa})$$

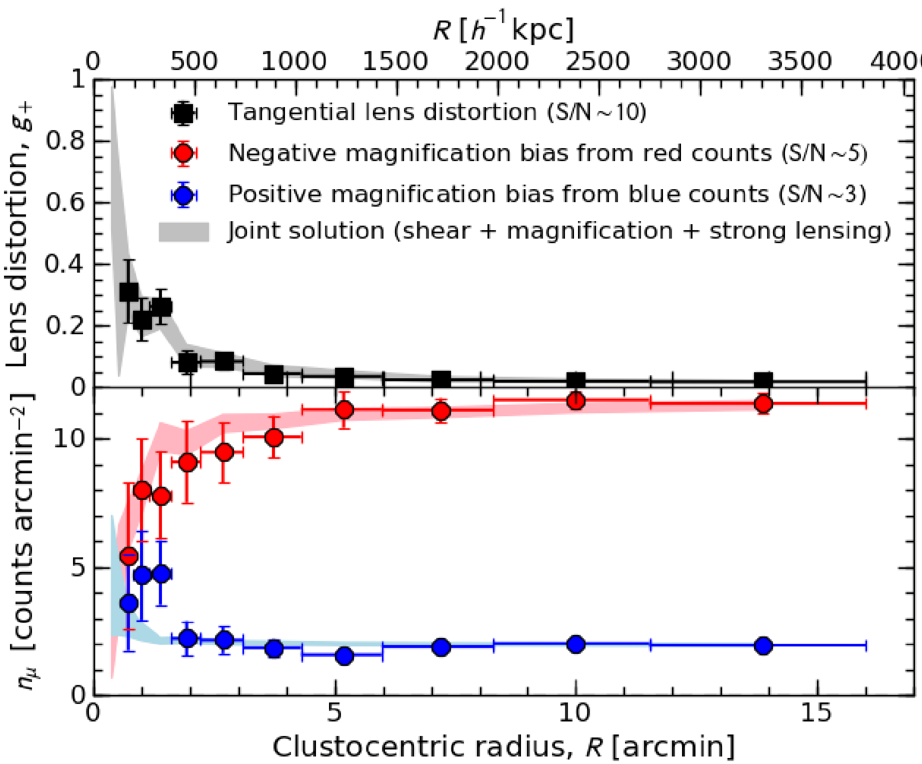

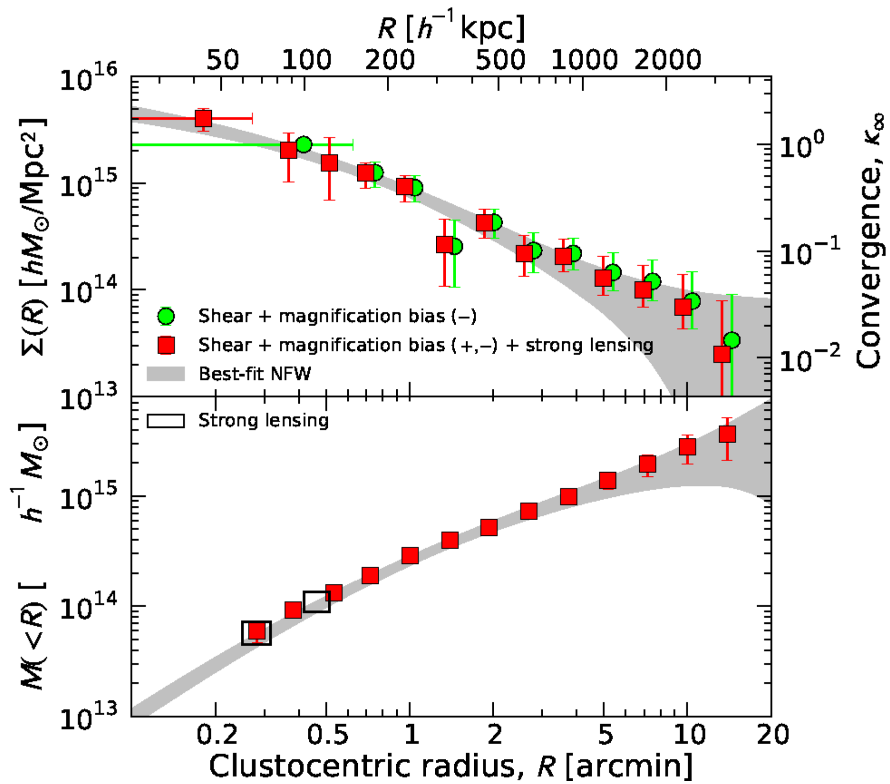

Umetsu 2013, *ApJ*, 769, 13

Shear strength as function of z (KSB+)

First detection of WL distance vs. redshift relation!!!

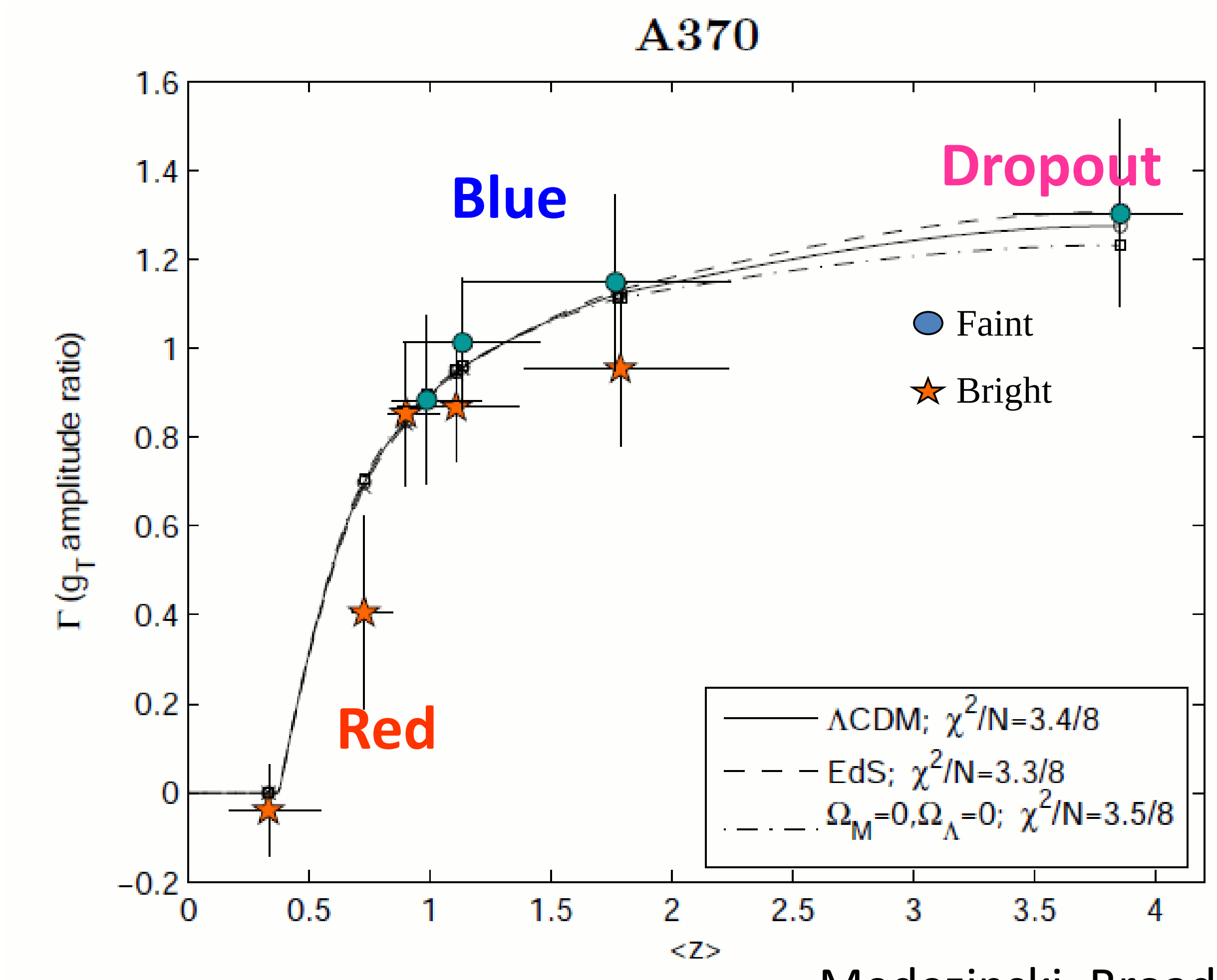

Medezinski, Broadhurst, Umetsu+11

Reionization Lensing Cluster Survey (RELICS)

Newly approved 190-orbit *HST* survey (7 ACS/WFC3 filters) of 41 high-mass clusters primarily selected from the *Planck* survey (P.I. Dan Coe; Oct 2015 – Apr 2017)

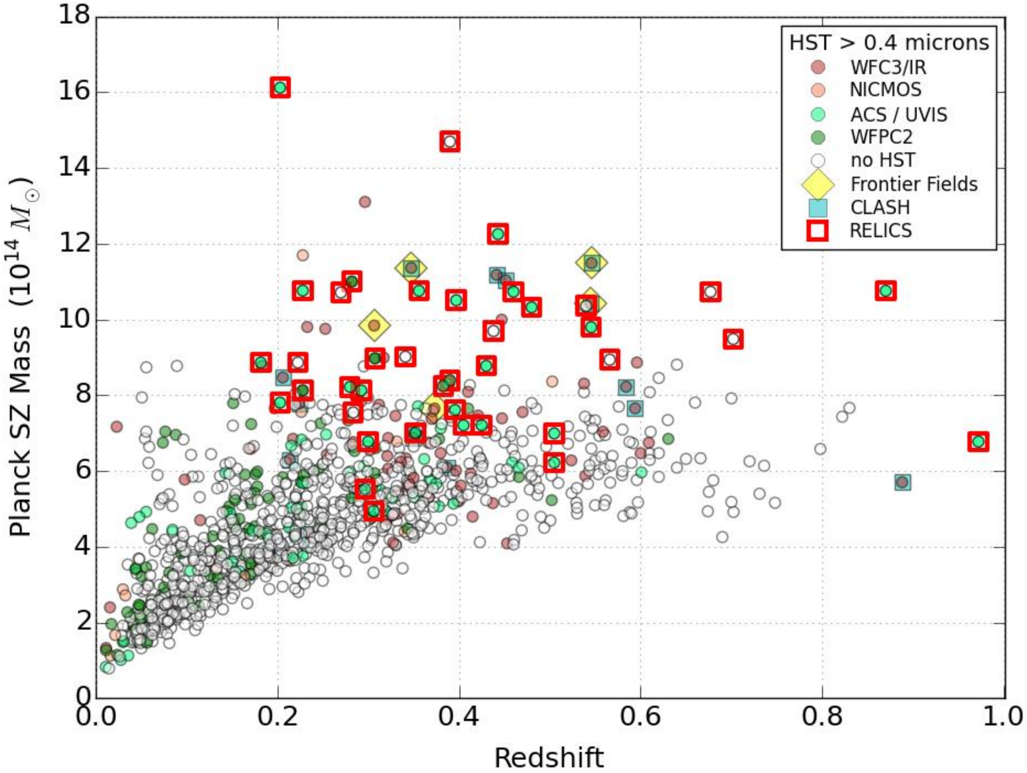

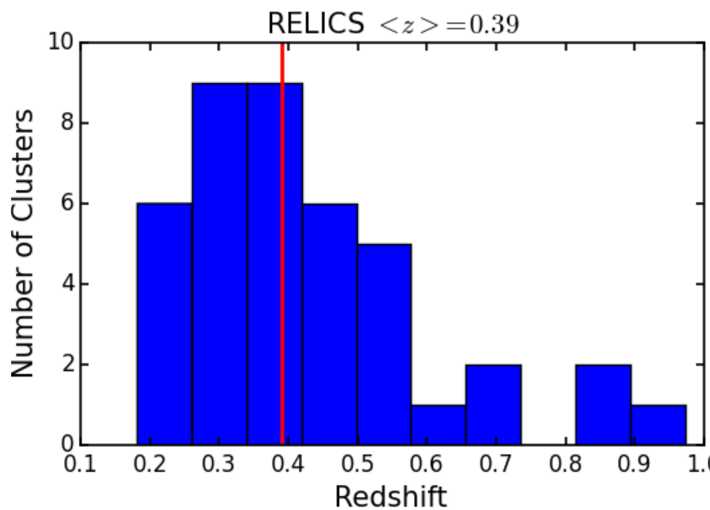

http://hstrelics.weebly.com

Intrinsic Scatter in $c(M)$: Mass Assembly Histories (MAH)

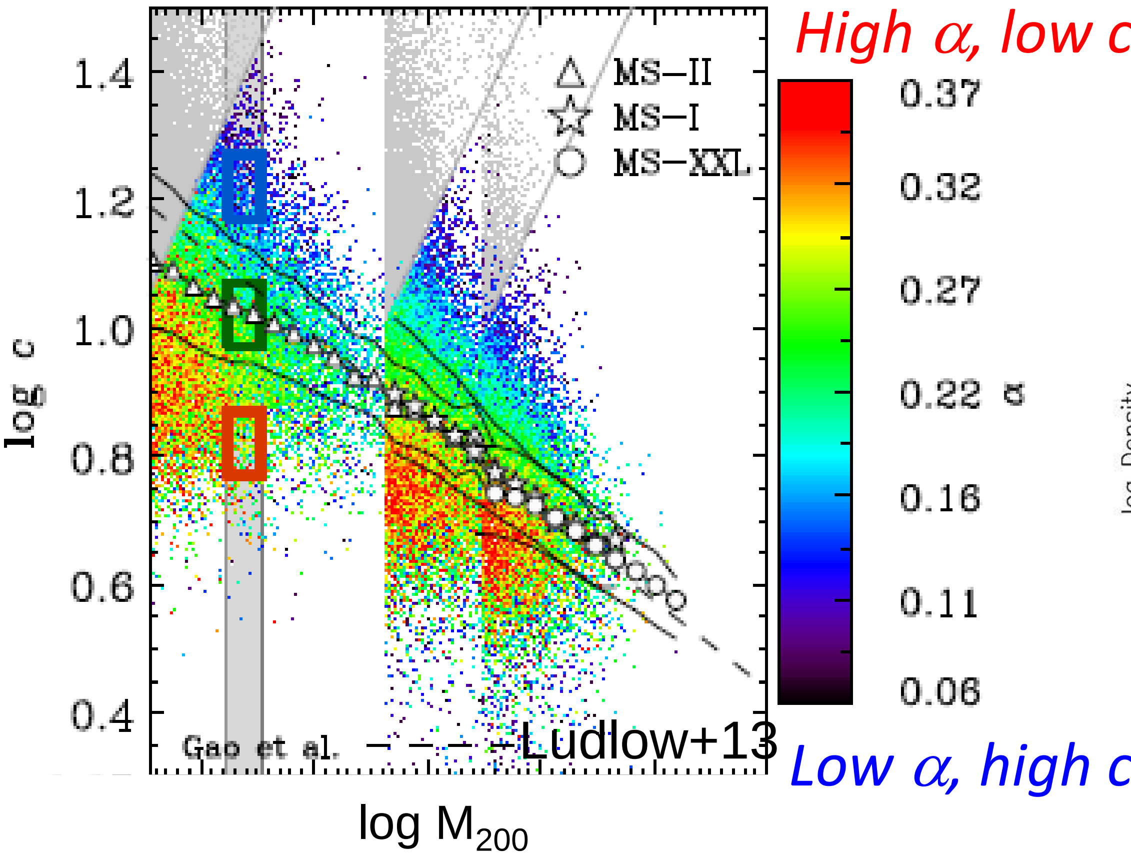

α: degree of curvature

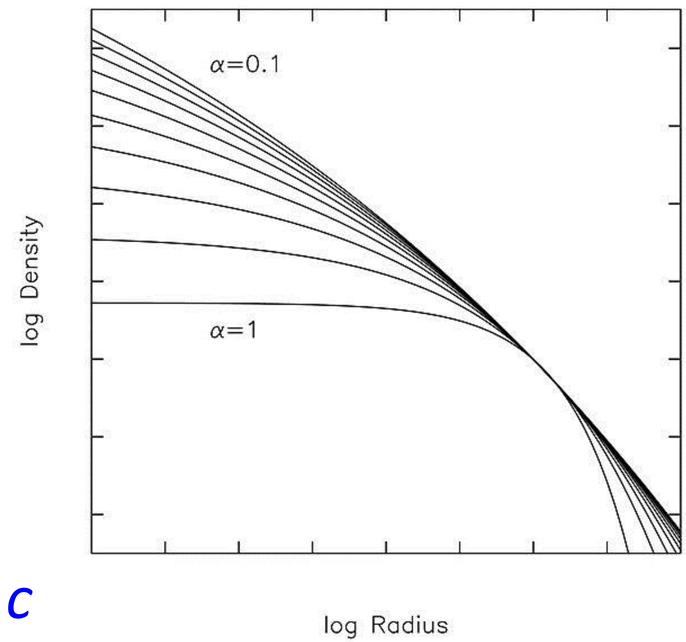

- Scatter is due to another DoF (α), related to MAH (Ludlow+13)
- Larger values of α correspond to halos that have been assembled more rapidly than the NFW curve
- Halos with average c_{200} have the NFW-equivalent α ~0.18

Key Predictions of nonlinear structure formation models

(3) Halo bias: surrounding large-scale structure

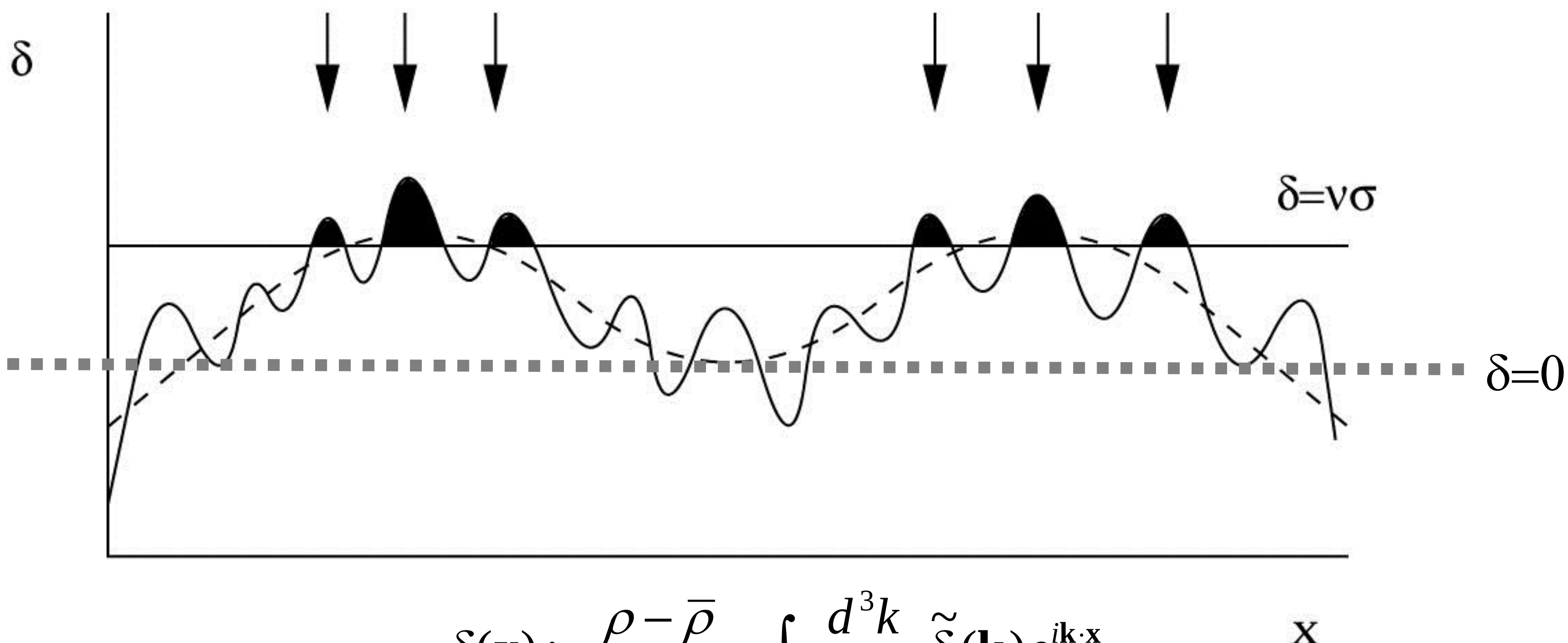

$$\delta(\mathbf{x}) := \frac{\rho - \bar{\rho}}{\bar{\rho}} = \int \frac{d^3k}{(2\pi)^3} \tilde{\delta}(\mathbf{k}) e^{i\mathbf{k}\cdot\mathbf{x}}$$

$$\left\langle \tilde{\delta}(\mathbf{k}) \tilde{\delta}(\mathbf{k}') \right\rangle = (2\pi)^3 \delta_D^3(\mathbf{k} + \mathbf{k}') P(k)$$

Shear doesn't see mass sheet

Averaged lensing profiles in/around LCDM halos (Oguri & Hamana 11)

Total

$$\kappa = \Sigma(R) / \Sigma_c$$

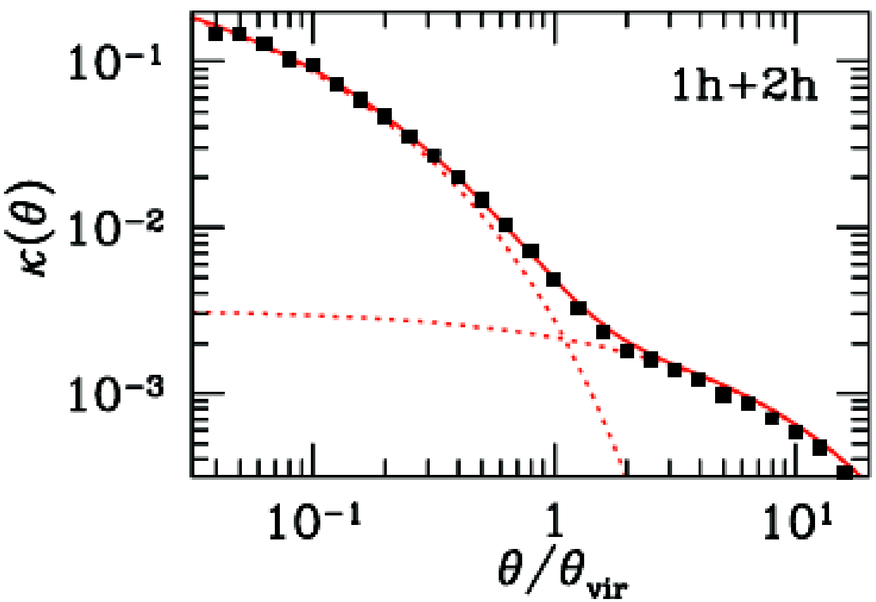

Modulated

$$\gamma_+ = \Delta\Sigma(R) / \Sigma_c$$

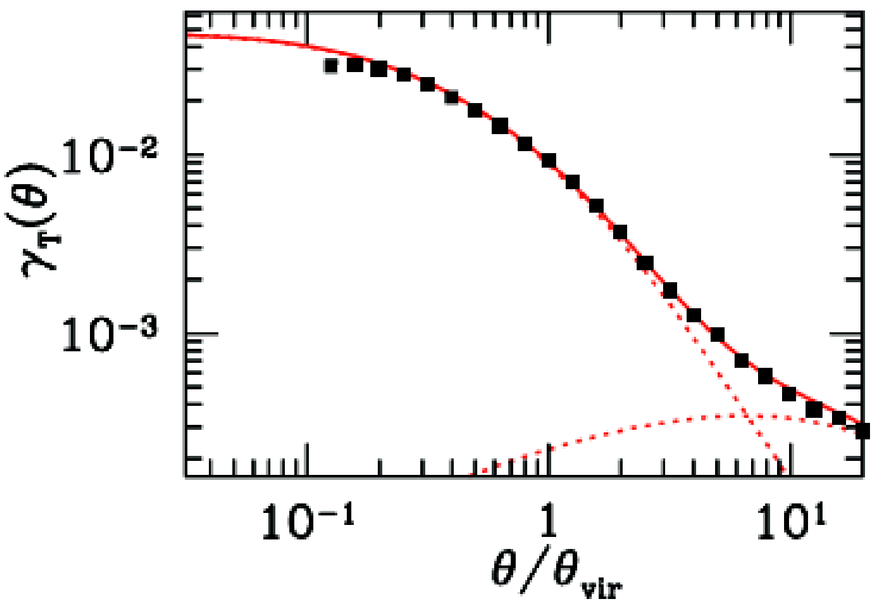

- **Tangential shear is a powerful probe of 1-halo term, or intra-halo structure.**
- **Shear alone cannot recover absolute mass, known as *mass-sheet degeneracy:***

γ remains unchanged by $\kappa \rightarrow \kappa + \mathrm{const.}$

Non-local substructure effect

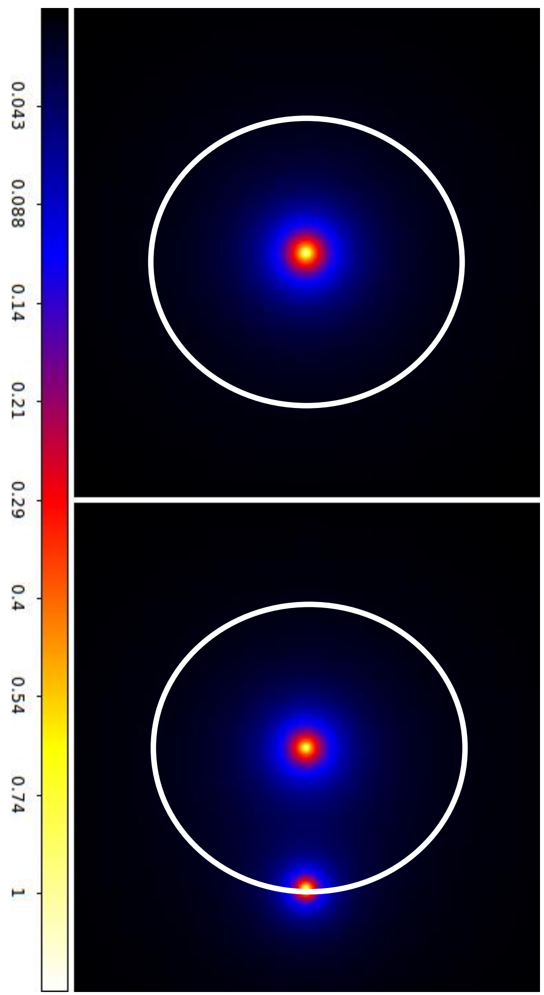

A substructure at $R \sim r_{\rm vir}$ of the main halo, modulating $\Delta\Sigma(R) = \Sigma(<R) - \Sigma(R)$

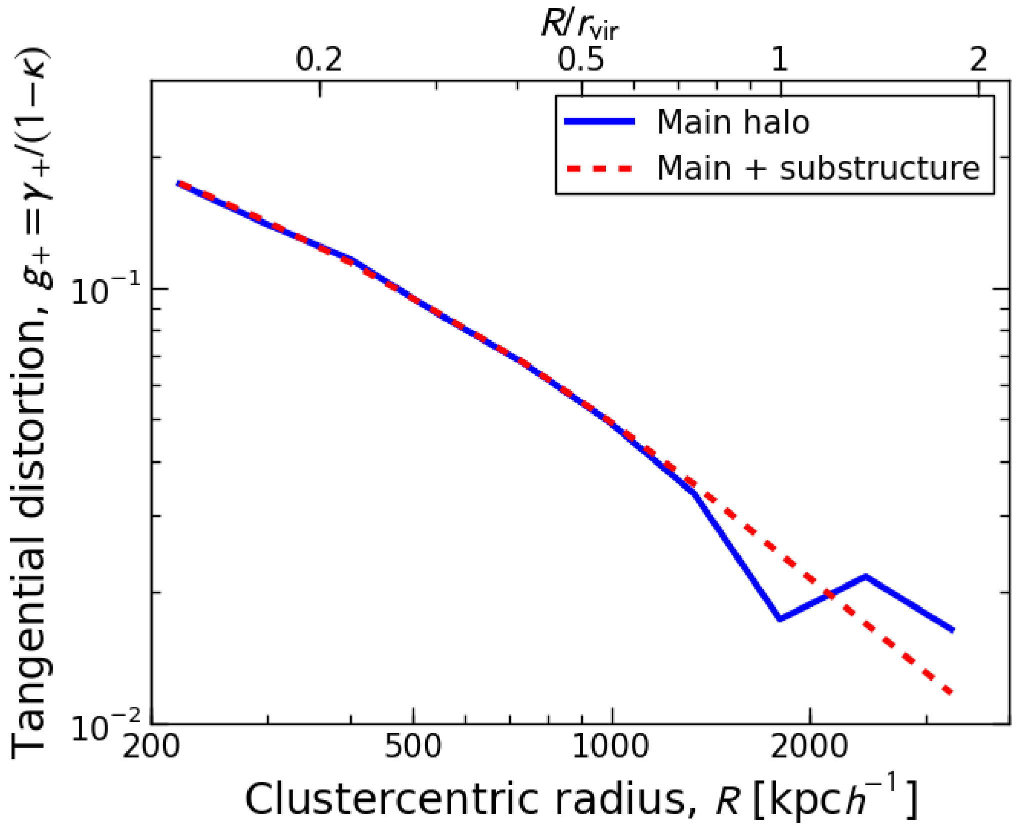

Known 5%-10% negative bias in mass estimates from tangential-shear fitting, inherent to rich substrucure in outskirts (Rasia+12)

Averaged Halo Density Profile $\Sigma(R)$

Stacking lensing signals of individual clusters by

$$\langle\langle \mathbf{\Sigma} \rangle\rangle = \left(\sum_n \mathcal{W}_n\right)^{-1} \left(\sum_n \mathcal{W}_n \mathbf{\Sigma}_n\right),$$

Summing over clusters (n=1, 2, ..)

with individual “sensitivity” matrix

$$(\mathcal{W}_n)_{ij} \equiv \Sigma^{-2}_{(\mathrm{c},\infty)n} \left(C_n^{-1}\right)_{ij},$$

defined with total covariance matrix

$$C = C^{\mathrm{stat}} + C^{\mathrm{sys}} + C^{\mathrm{lss}} + C^{\mathrm{int}},$$

With “trace-approximation”, averaging (stacking) is interpreted as

$$\langle\langle M_\Delta \rangle\rangle = \frac{\sum_n \mathrm{tr}(\mathcal{W}_n)\, M_{\Delta,n}}{\sum_n \mathrm{tr}(\mathcal{W}_n)}$$

Umetsu et al. 2014, *ApJ*, 795, 163

Concentration—Mass Scaling Relation

Consider a power-law scaling relation of the form:

$$c_{200c} = 10^{\alpha} \left(\frac{M_{200c}}{M_{piv}} \right)^{\beta} \left(\frac{1+z}{1+z_{piv}} \right)^{\gamma},$$

with pivot mass and redshift $M_{piv} = 10^{15} M_{sun} / h,\ z_{piv} = 0.34$

Define new independent (*X*) and dependent (*Y*) variables:

$$Y \equiv \log_{10} \left[\left(\frac{1+z}{1+z_{piv}} \right)^{-\gamma} c_{200c} \right],$$

$$X \equiv \log_{10} \left(M_{200c} / M_{piv} \right).$$

$$Y(X) = \alpha + \beta X$$

Redshift slope γ is fixed to the theoretical prediction for the CLASH sample, γ=-0.668 (Meneghetti+14)

Bayesian Regression Analysis

We take into account

- Covariance between observed *M* and *c*
- Intrinsic scatter in *c*
- Non-uniformity in mass probability distribution *P*(log*M*)

Conditional probability *P*(*y*|*x*) with (*x*,*y*) = observed (*X*,*Y*)

$$\ln \mathcal{P}(\boldsymbol{y}|\boldsymbol{x}) = -\frac{1}{2}\sum_n \left[\ln\left(2\pi\sigma_n^2\right) + \left(\frac{y_n - \langle y_n|x_n\rangle}{\sigma_n}\right)^2\right], \tag{35}$$

where $\langle y_n|x_n\rangle$ and $\sigma_n^2 \equiv \mathrm{Var}(y_n|x_n)$ are the conditional mean and variance of y_n given x_n, respectively:

$$\langle y_n|x_n\rangle = \alpha + \beta\mu + \frac{\beta\tau^2 + C_{xy,n}}{\tau^2 + C_{xx,n}}(x_n - \mu),$$

$$\sigma_n^2 = \beta^2\tau^2 + \sigma_{Y|X}^2 + C_{yy,n} - \frac{(\beta\tau^2 + C_{xy,n})^2}{\tau^2 + C_{xx,n}}, \tag{36}$$

where $\sigma_{Y|X}$ is the intrinsic scatter in the Y–X relation;

Marginalized Posterior Distributions

$$c_{200c} = 10^{\alpha} \left(\frac{M_{200c}}{M_{piv}}\right)^{\beta} \left(\frac{1+z}{1+z_{piv}}\right)^{\gamma}$$

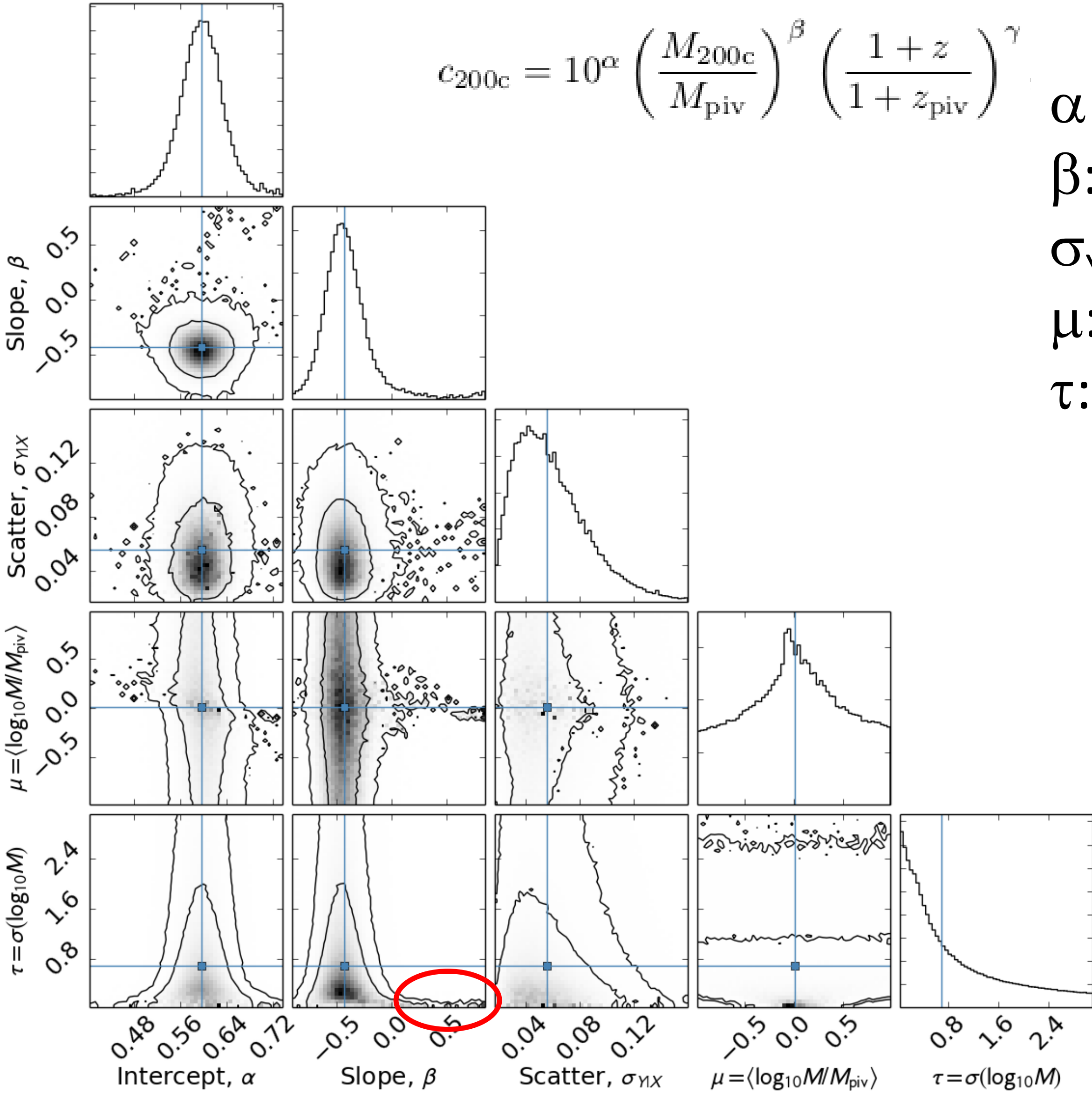

α: intercept

β: slope

$\sigma_{Y|X}$: scatter

μ: Gaussian mean of $P(\ln M)$

τ: Gaussian width of $P(\ln M)$

High β tail associated with small τ: i.e., localized $P(\ln M)$

Intrinsic Scatter in $c(M)$: Mass Assembly Histories

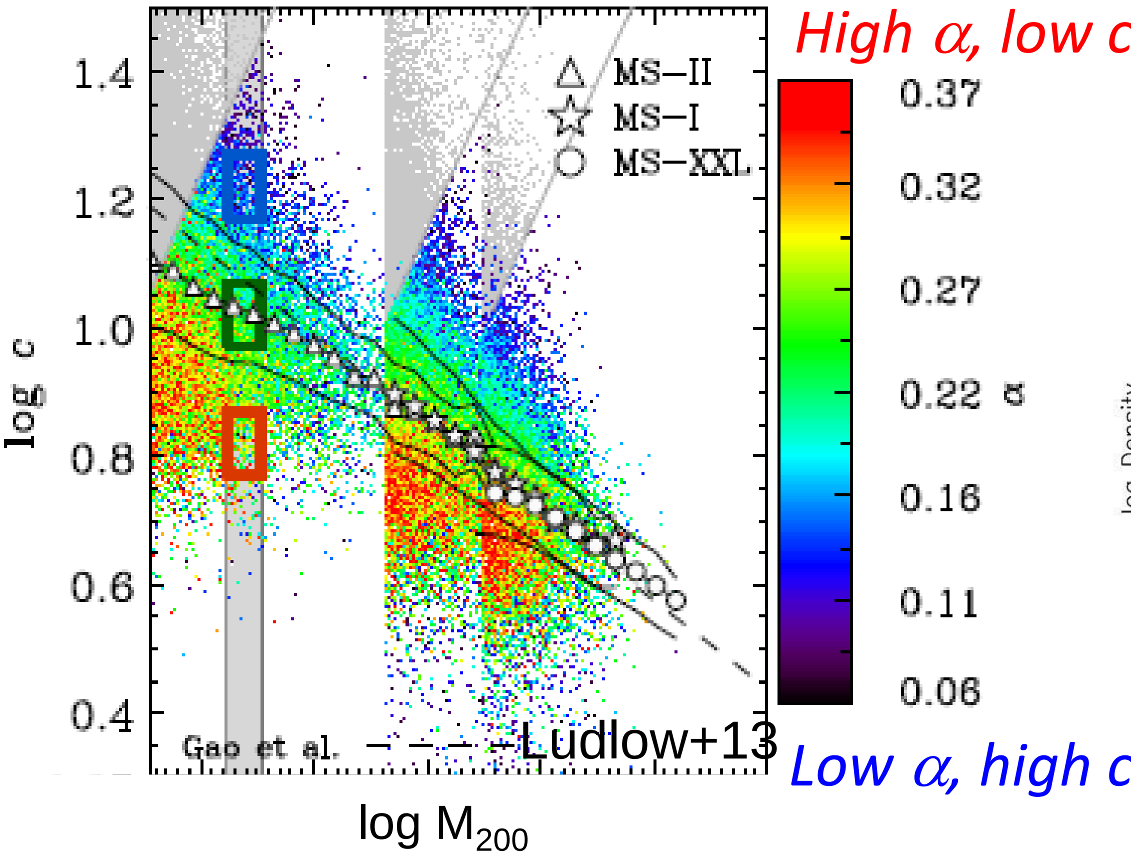

α: degree of curvature

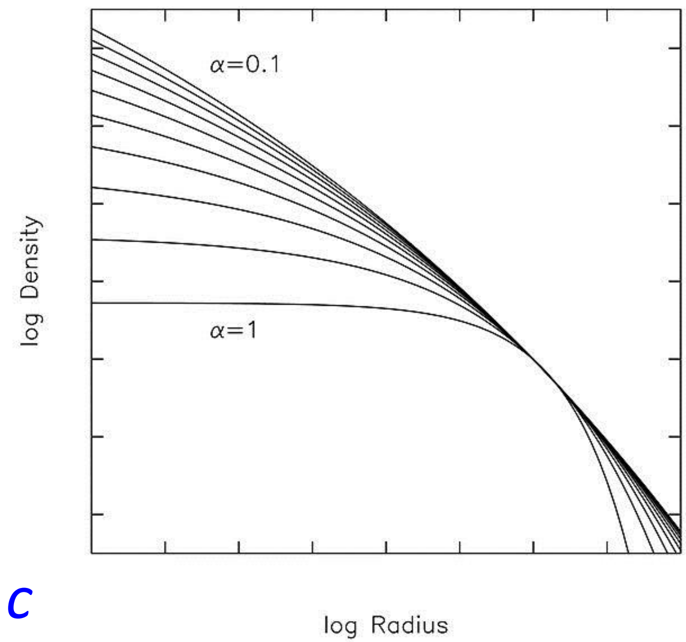

- Scatter is due to another dof (α), related to MAH (Ludlow+13)
- Larger values of α correspond to halos that have been assembled more rapidly than the NFW curve
- Halos with average c_{200c} have the NFW-equivalent α ~0.18

Cluster Counts as Cosmological Probe

$$\frac{dN(>M_{\rm lim},z)}{d\Omega dz} = \int_{M_{\rm lim}}^{\infty} dM \boxed{\frac{dV(z)}{d\Omega dz}} \boxed{\frac{d^2 n}{dV dM}(M,z)}$$

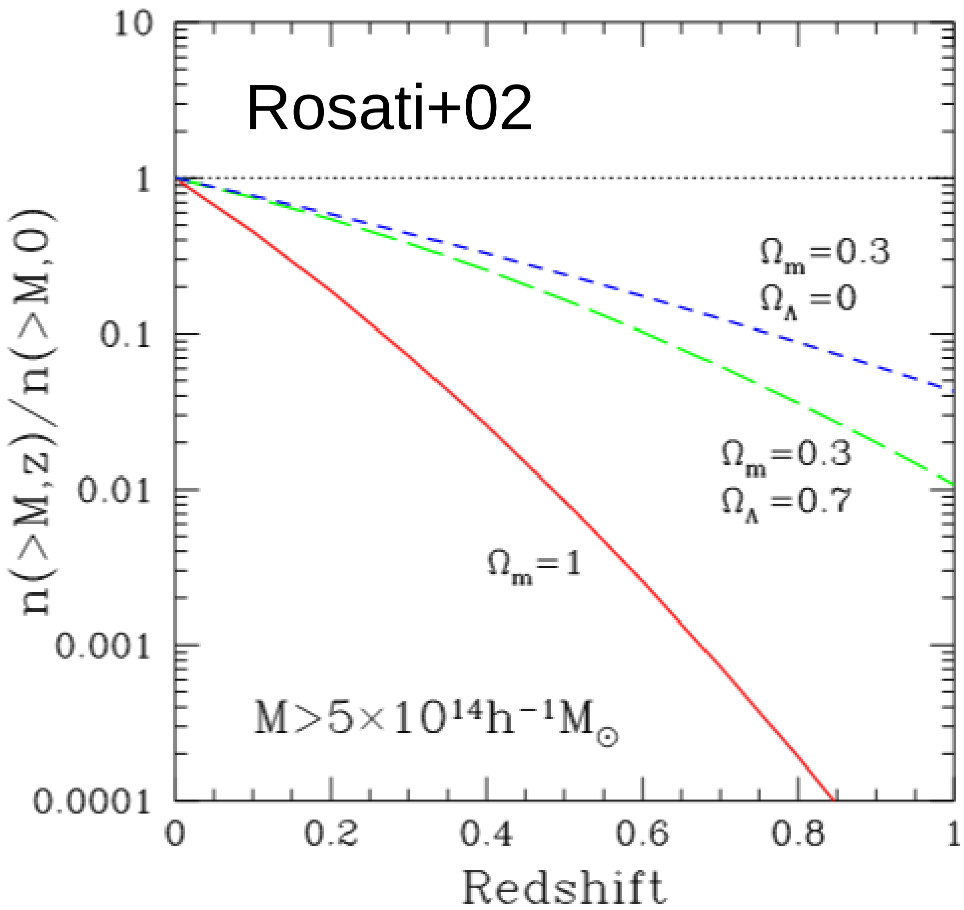

Comoving volume element

$$\frac{d^2V}{dz d\Omega} = \frac{c r^2[\chi(z)]}{H(z)}, \quad \chi(z) = \int_0^z \frac{dz'}{H(z')}$$

Halo mass function

$$\frac{d^2 n}{dV dM}(M,z) \propto \exp\left[-\frac{\nu^2}{2}\right]$$

$$\nu \equiv \frac{\delta_c(z)}{\sigma(M,z)} \approx \frac{1.69}{D_+(z)\sigma(M)} \sim 3 \text{ for clusters}$$

Cluster counts are exponentially sensitive to cosmology AND **cluster mass calibration**!!!

Weak shear fields around high-mass clusters

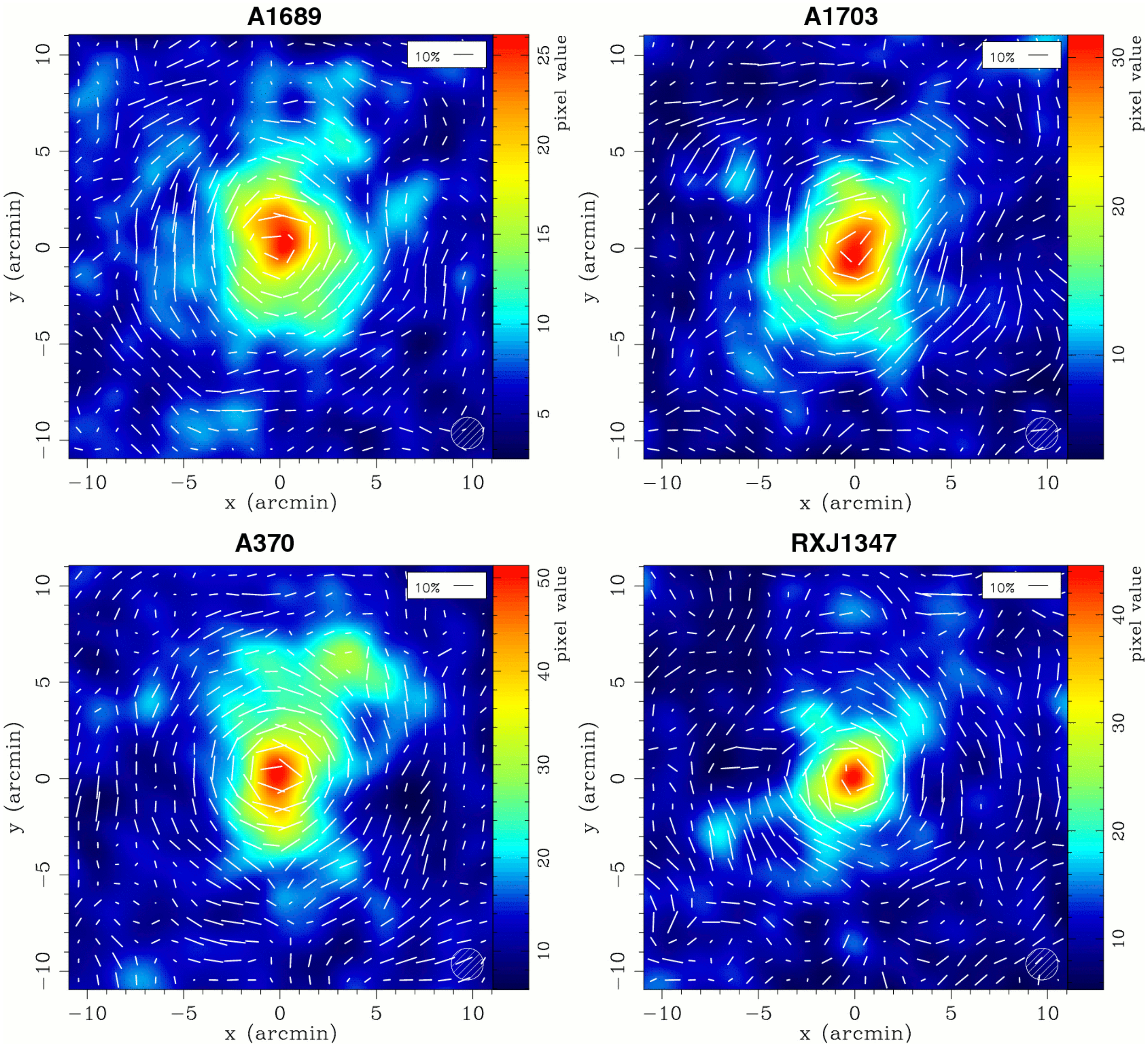

Map: **RS galaxies**
Whiskers: **shear**

Subaru/S-Cam archival data

Broadhurst, Umetsu, Medezinski+08, *ApJL*, 685, L9

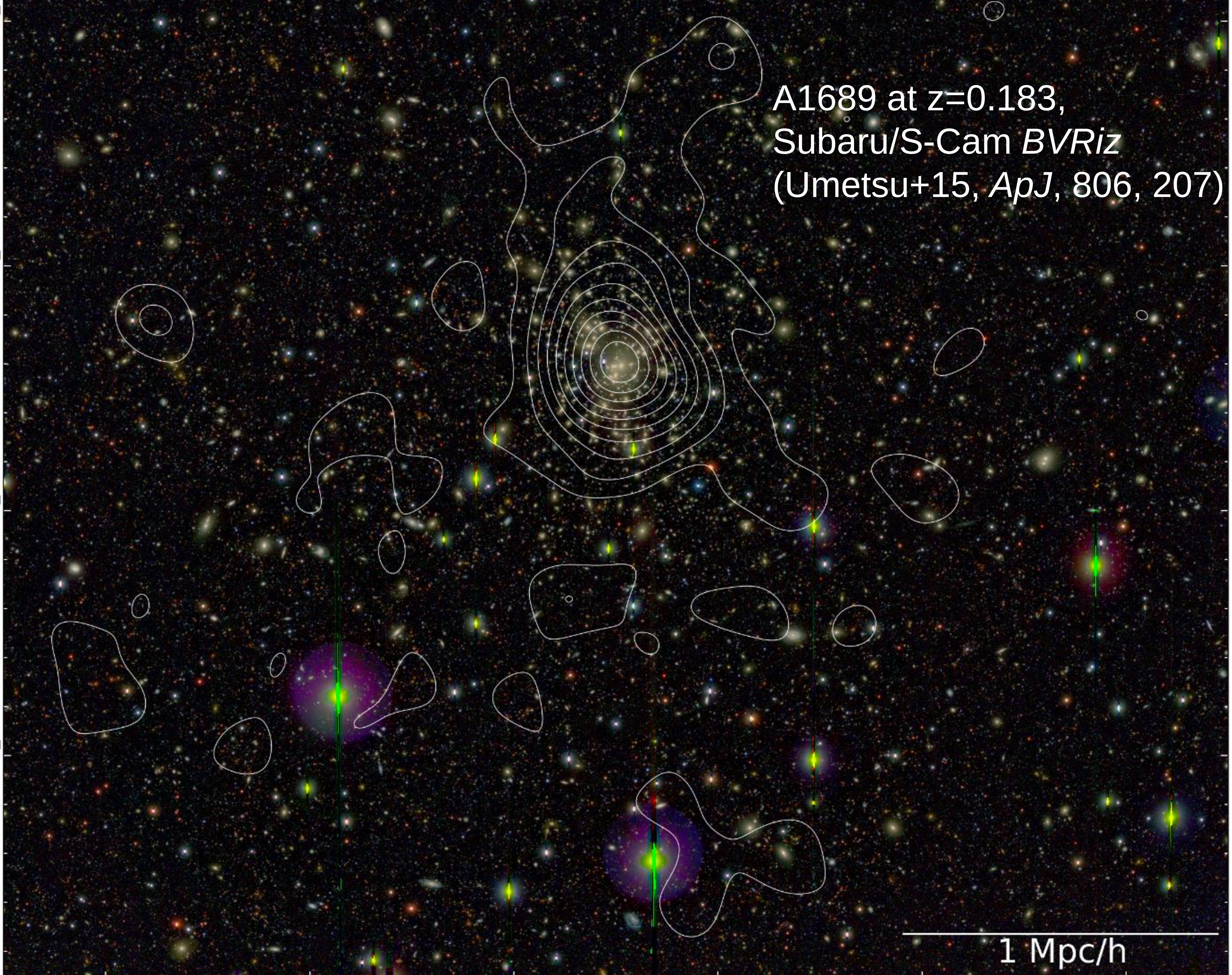
A1689 at z=0.183,
Subaru/S-Cam BVRiz
(Umetsu+15, ApJ, 806, 207)
1 Mpc/h

Splashback radius depends on halo mass accretion rate, $\Gamma := \Delta(\ln M_{\mathrm{vir}})/\Delta(\ln a)$ (contd.)

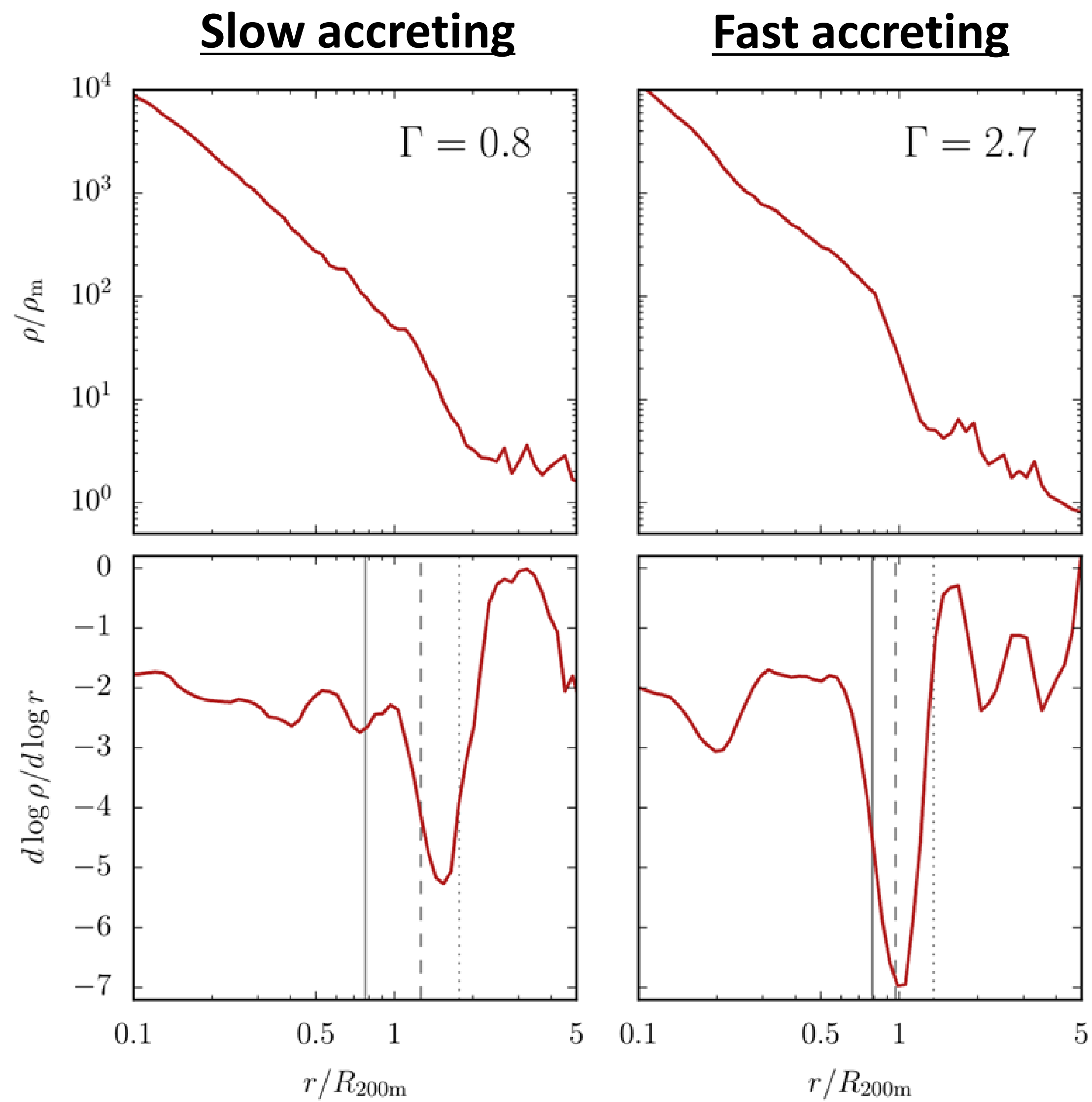

N-body simulations in LCDM

More, Diemer, & Kravtsov 15

(1) Quasi-universal DM density profiles

Spherically-averaged density profiles $\rho_h(r)$ of collisionless DM halos from numerical simulations $\rho_h(r) \sim \rho_s f(r/r_s;\alpha)$

Cuspy, outwardly-steepening density profiles

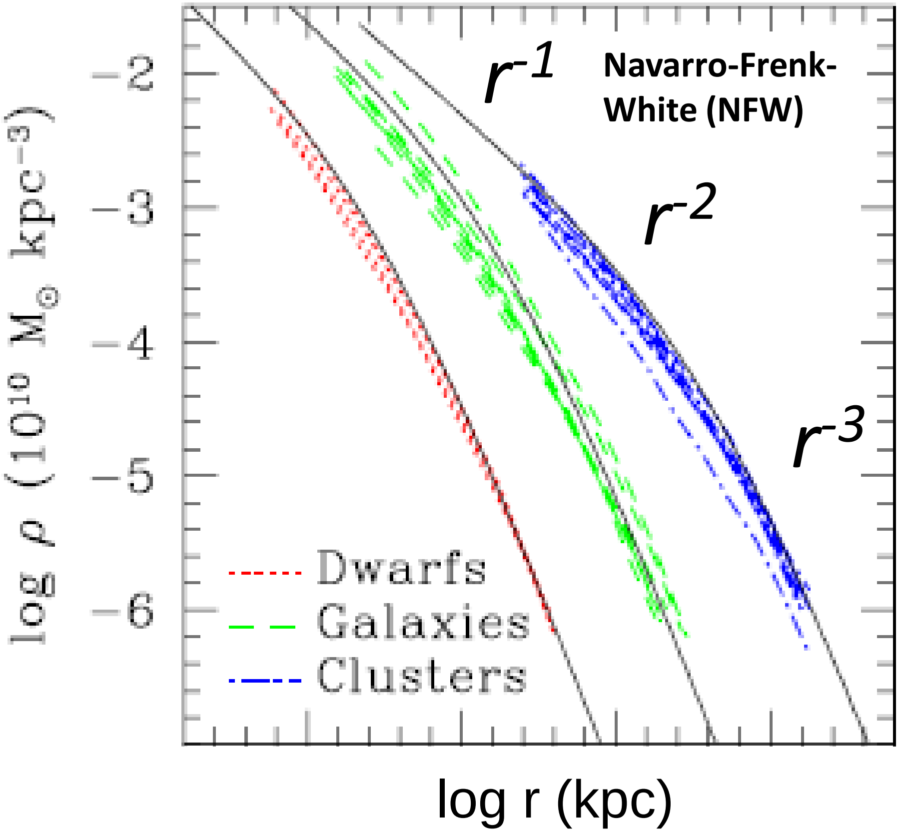

Theoretical models:

- **DARKexp** (Hjorth & Williams 10): Statistical mechanical arguments to describe the distribution of particle energies in finite, self-gravitating, collisionless systems with isotropic orbits.
- Pontzen & Governato 13: Maximum-entropy arguments to derive the phase-space distribution for an end product of violent relaxation
- Adhikari, Dalal, & Chamberlain 14: outskirt steepening (splashback radius) associated with first apocentric passage after accretion

CLASH X-ray-selected subsample optimized for mass-profile analysis

- **High-mass clusters with smooth X-ray morphology**
  - $T_x > 5$keV ($6e14 M_{sun} < M_{200c} < 30e14 M_{sun}$)
  - Small BCG -X-ray offset, $\sigma_{off} \sim 10$kpc/h
  - Smooth, regular X-ray morphology
- **CLASH theoretical predictions** (Meneghetti+14, *ApJ*, 797, 34)
  - Composite relaxed (70%) and unrelaxed (30%) clusters
  - Mean $<c_{200c}>=3.9$, $c_{200c}=[3, 6]$
  - Small scatter in c_{200c} : $\sigma(\ln c_{200c}) = 0.16$
  - Largely free of orientation bias (~2% in $<M_{3D}>$)
  - 90% of CLASH clusters to have strong-lensing features

Tangential shear signal

Source selection in Subaru color-color (*BRz'*) space

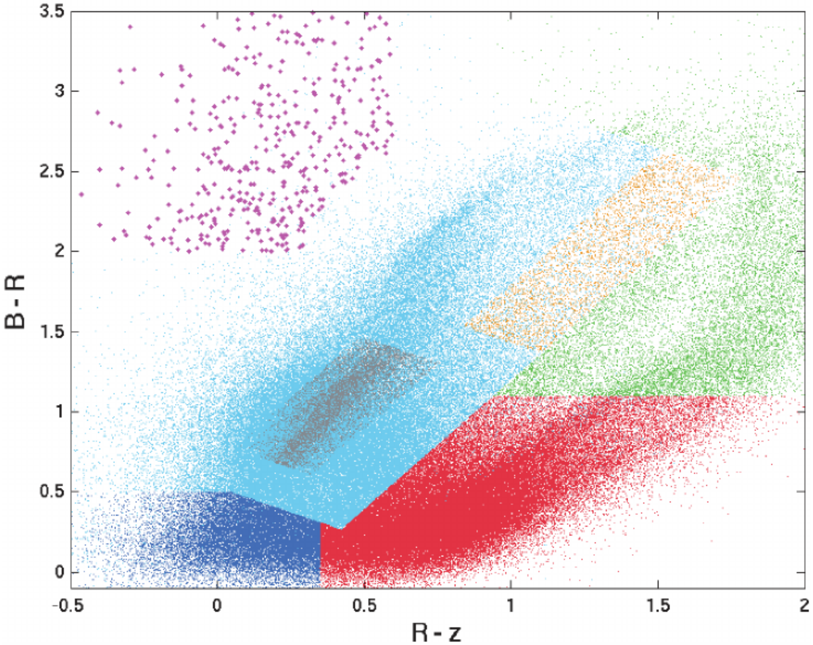

Subaru WL signal (Abell 370) $\gamma_+ \propto \frac{D_{\mathrm{LS}}}{D_{\mathrm{S}}}$

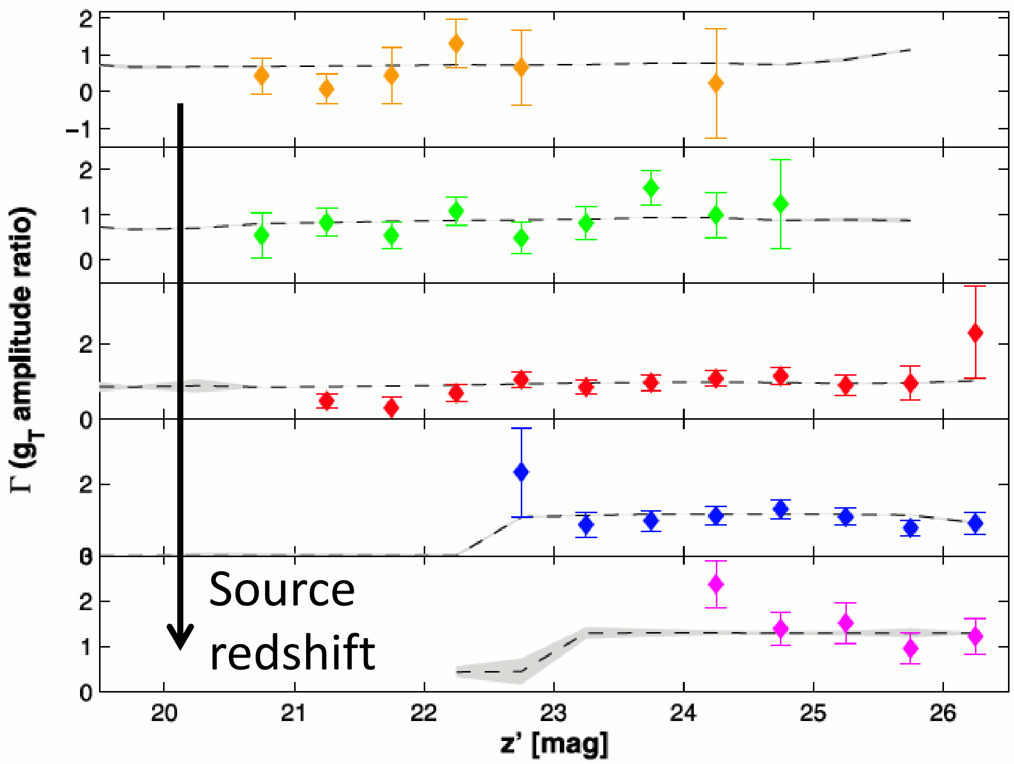

KSB+ shape pipeline of Umetsu+10 used

Medezinski, Broadhurst, Umetsu et al. 2011, *MNRAS*, 414, 1840

Key predictions of structure formation models

(1) **DM halo density profile**
(2) **Halo concentration—mass relation**
(3) **Halo bias**

(1) Quasi-universal DM density profiles

N-body simulations of collisionless DM produce cuspy, outwardly steepening density profiles of halos in equilibrium.

Navarro-Frenk-White 96, 97 (NFW)

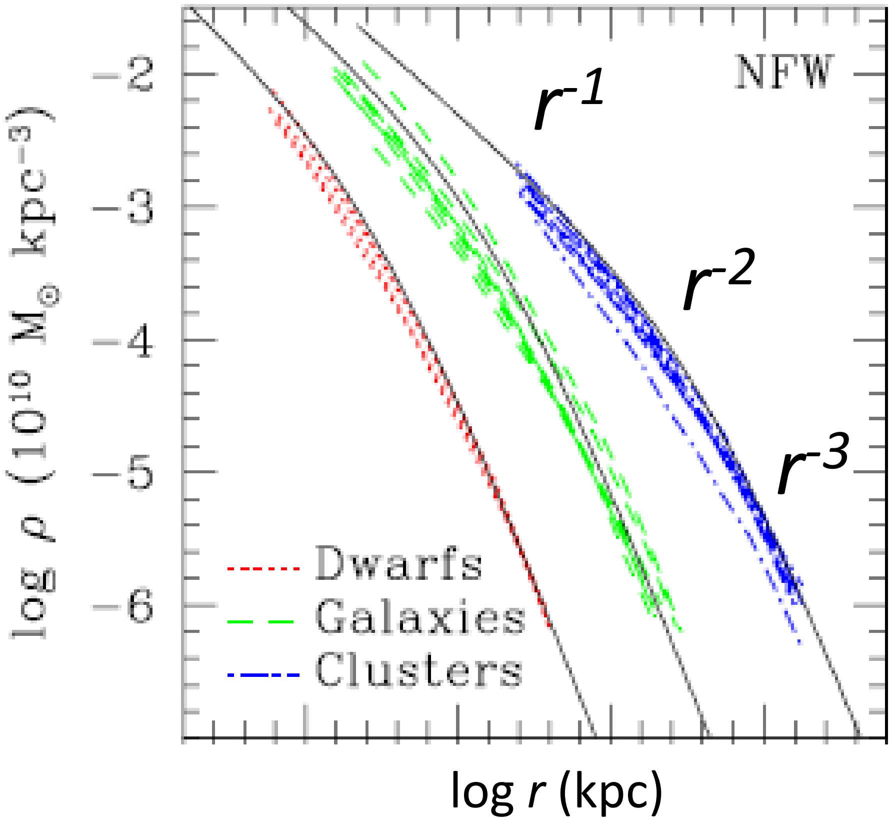

Universal? (e.g., NFW profile)

$$\langle \rho_{\rm h} \rangle({\rm r}) \sim \rho_s f(r/r_s)$$

Non-universal? (e.g., Einasto profile) – diversity due to additional "degree of freedom"

$$\langle \rho_{\rm h} \rangle({\rm r}) \sim \rho_s f(r/r_s;\alpha)$$

- Velocity anisotropy (Lapi+Cavaliere 09)
- Central potential depth (Hjorth+Williams 10)
- Mass accretion history (Ludlow+13)
- $<\alpha_{\rm Einasto}>=0.155+0.0095\,\nu^2(M)$ (Gao+08)

Key predictions of structure formation models

(1) DM halo density profiles

(2) Halo concentration—mass relation

(3) Halo bias

(2) Halo concentration, c_Δ

$$c_{200c} \equiv \frac{R_{200c}}{r_s} = \frac{\text{(Outer scale radius)}}{\text{(Inner scale radius)}}$$

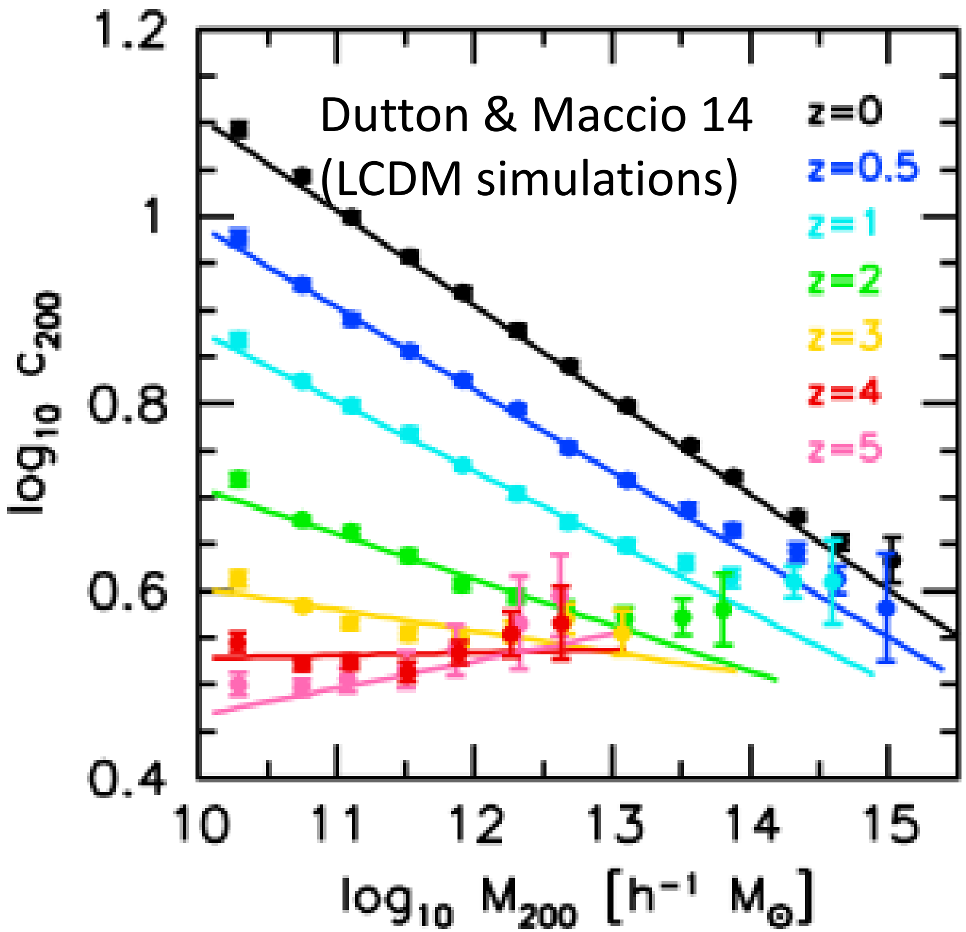

In hierarchical structure formation, <*c*> is predicted to correlate with *M:*

DM halos that are more massive collapse later on average, when the mean background density of the universe is correspondingly lower.

Sizable intrinsic scatter (at fixed *M*) ~30%-40%, reflecting diversity of mass accretion history & formation epoch.

Concentration is sensitive to cosmology

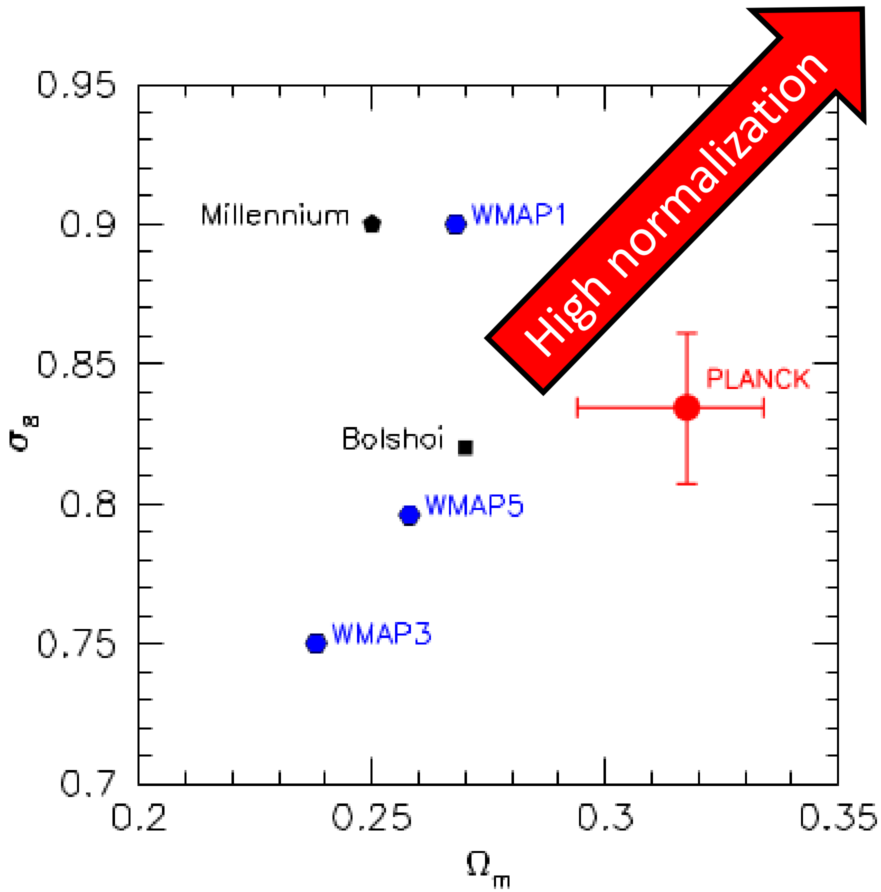

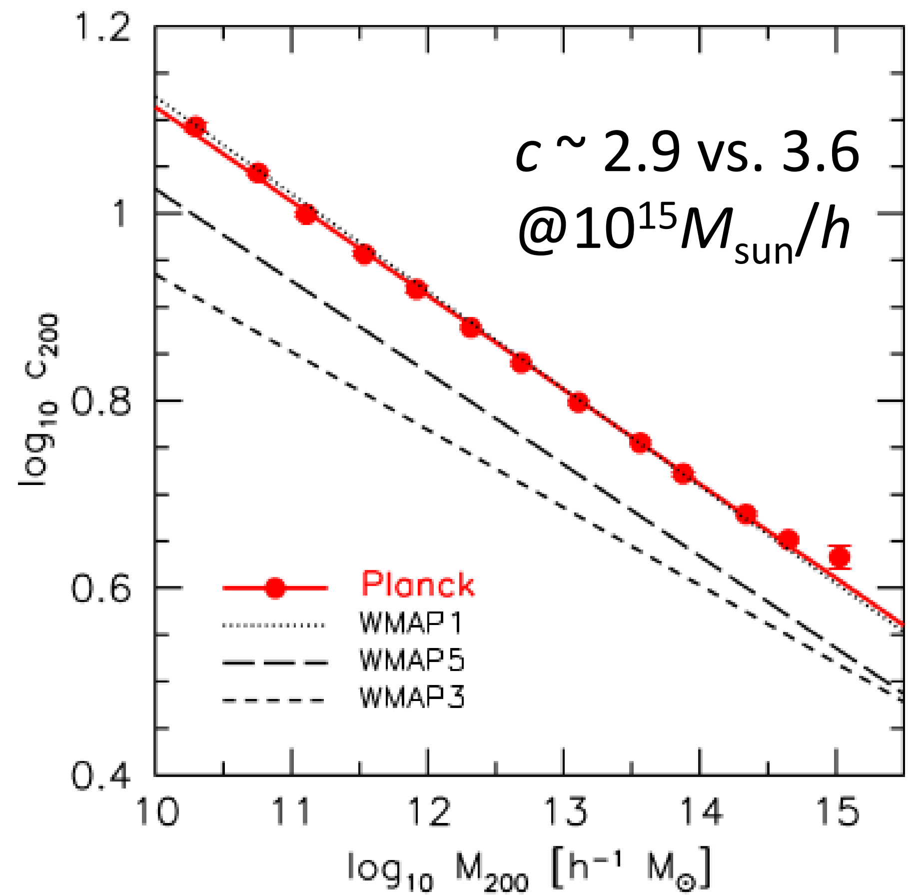

Dutton & Maccio 14

Key predictions of structure formation models

(1) DM halo density profiles

(2) Halo concentration—mass relation

(3) Halo bias

(3) Halo bias factor, b_h

Clustering of matter around halos with *M*: $\xi_\mathrm{hm}(r\,|\,M) = \dfrac{\langle\rho_\mathrm{h}\rangle(r\,|\,M)}{\rho_m} + b_\mathrm{h}(M)\xi_\mathrm{mm}(r)$

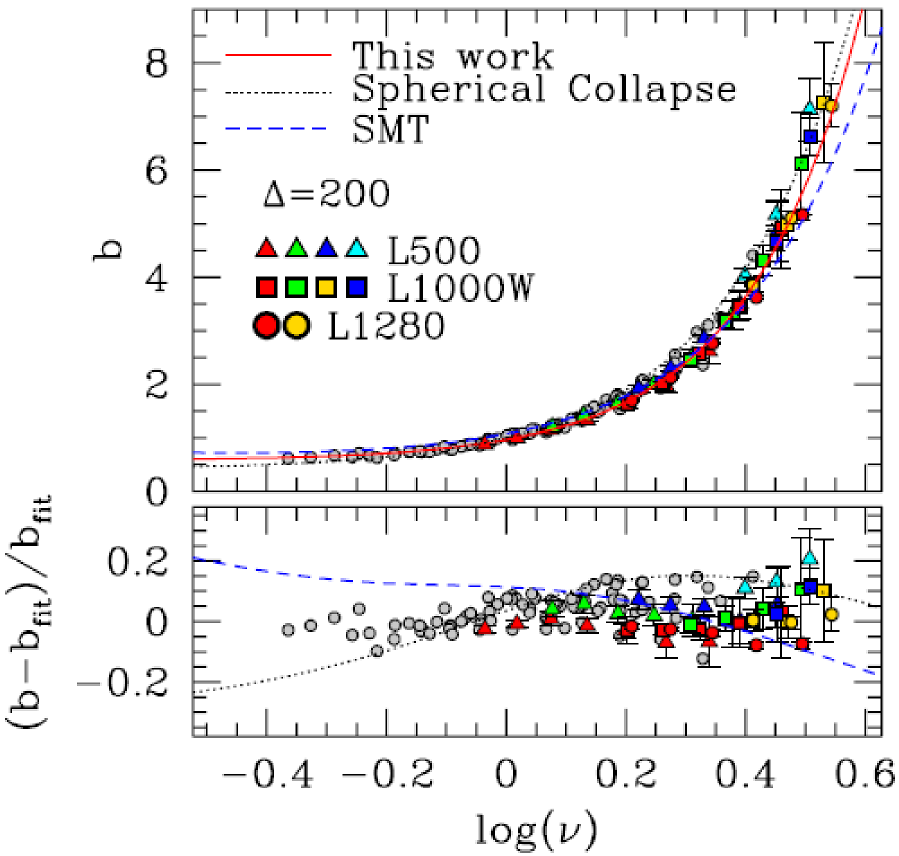

Tinker+10 LCDM simulations

Correlated matter distribution (2h term)

Matter correlation function:

$$\xi_\mathrm{mm}(\mathbf{r}) = \mathrm{FT}\left[P_\mathrm{L}(\mathbf{k})\right] \propto \sigma_8^2$$

Linear halo bias:

$$b_\mathrm{h}(\nu) \approx 1 + \frac{\nu^2 - 1}{\delta_c}$$

$$\nu \equiv \frac{\delta_c}{\sigma(M,z)} \sim 3-4 \text{ for clusters}$$

Clusters of Galaxies

Optical/NIR(cluster member galaxies and lensed background galaxies)

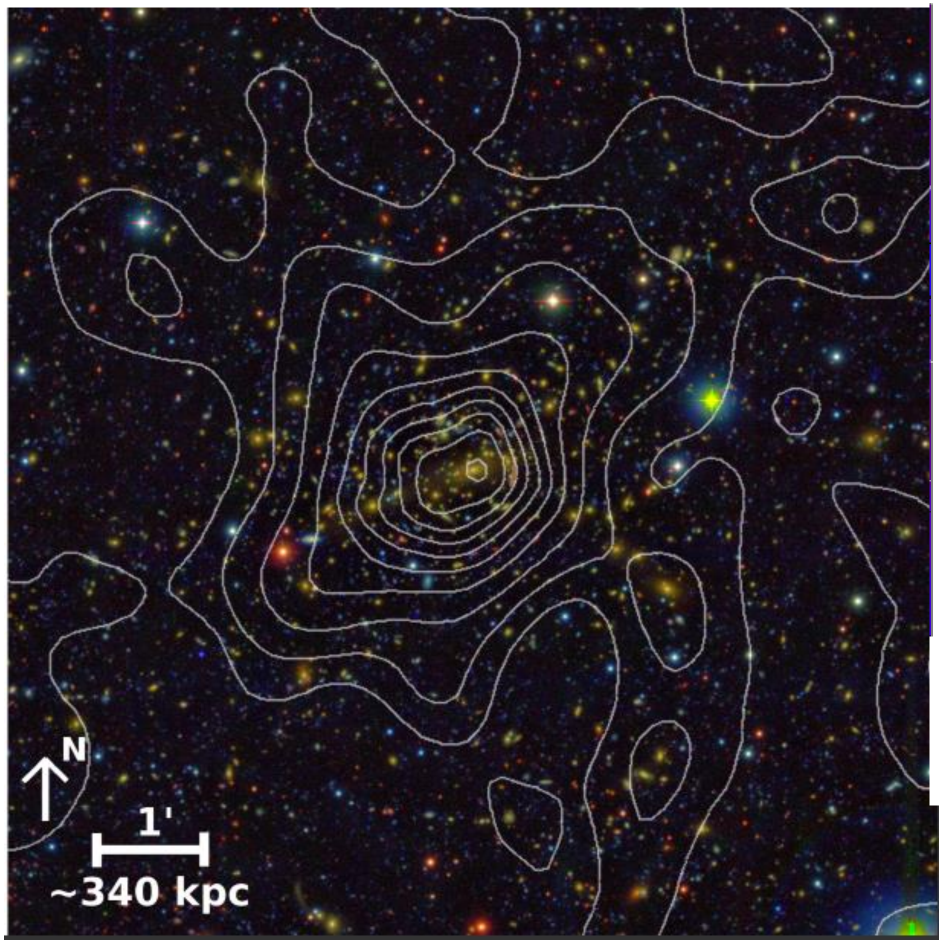

Radio/mm (intracluster plasma)

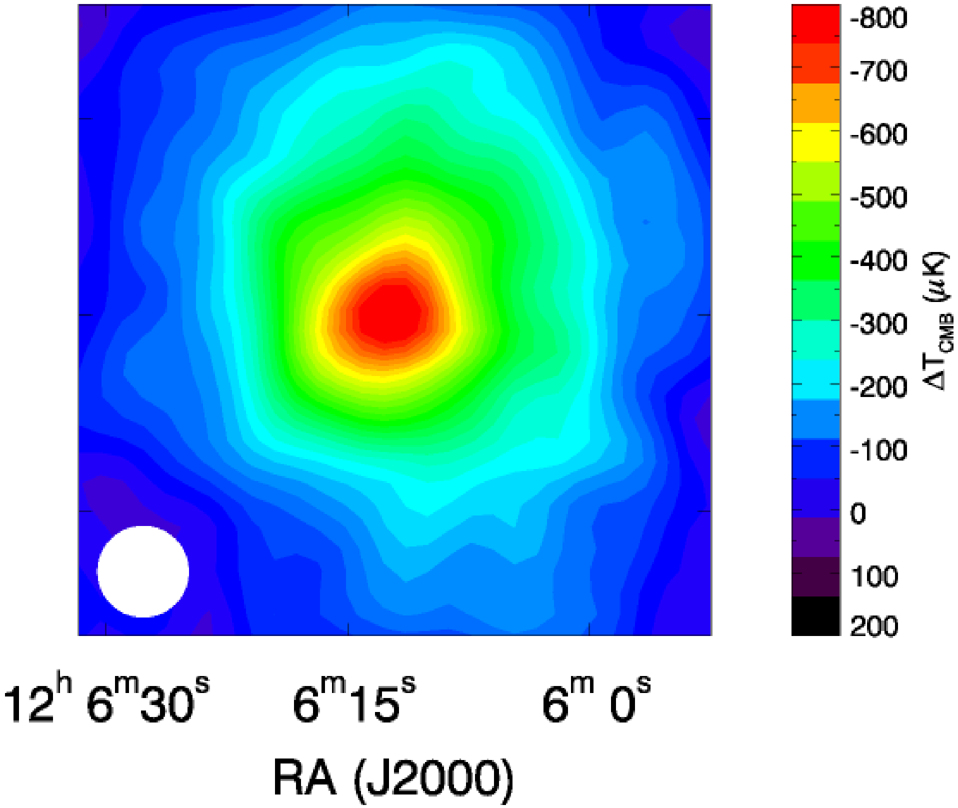

MACS1206 cluster at *z*=0.44
(Umetsu+12, *ApJ*, 755, 56)

2. Approach

Cluster Gravitational Lensing

Cluster cosmology: Key ingredients

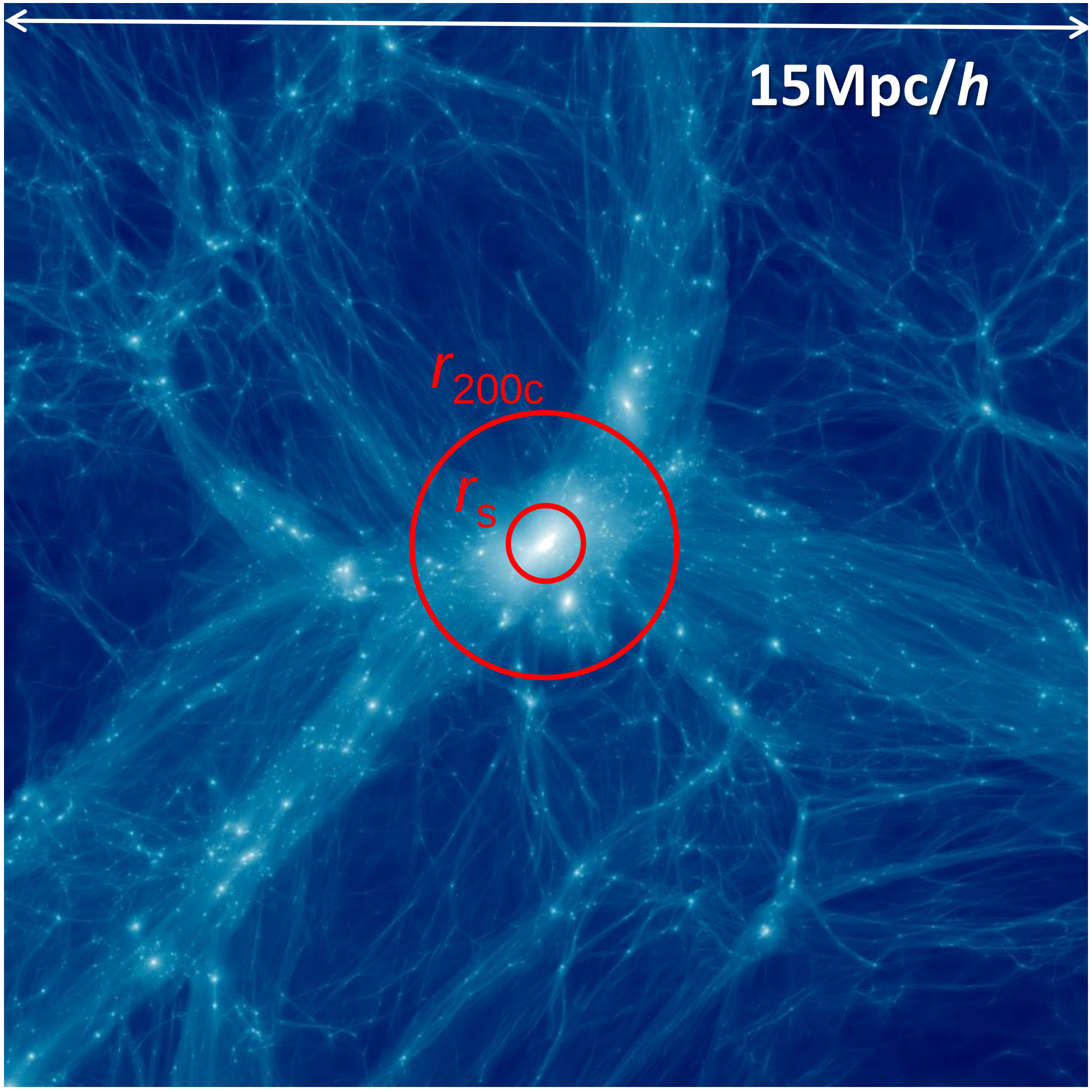

Intra-halo structure

Density profile shape, $\rho(r)$

Halo mass, $M_\Delta = M(<r_\Delta)$

Concentration, $c_\Delta = r_\Delta / r_s$

Splashback radius, R_{sp}

Halo shape

Surrounding LSS

Halo bias b_h

DM clustering strength, σ_8

Assembly bias

Approach: Gravitational Lensing

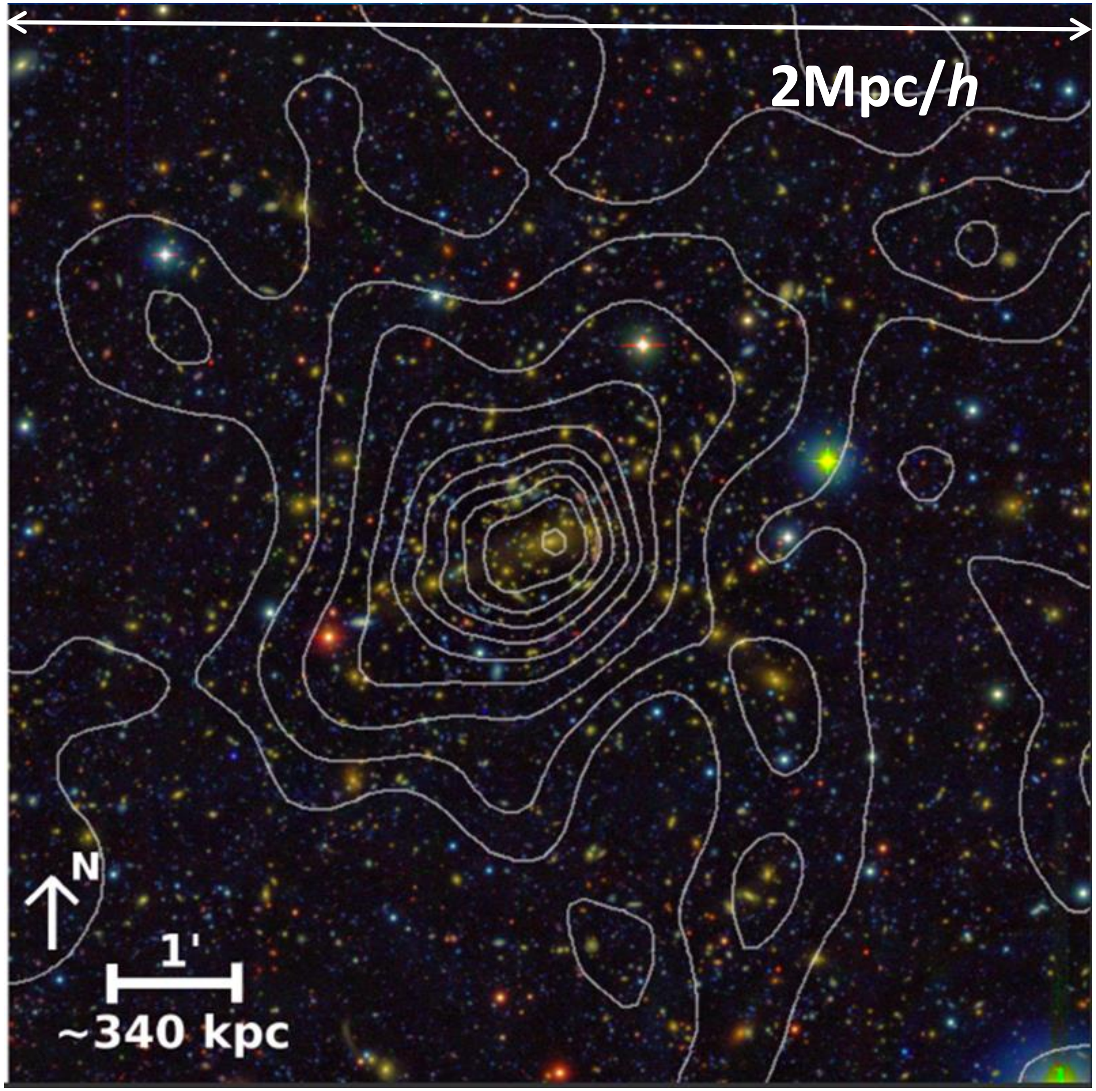

Intra-halo structure

Density profile shape, $\rho(r)$
Halo mass, $M_\Delta = M(<r_\Delta)$
Concentration, $c_\Delta = r_\Delta / r_s$
Splashback radius, R_{sp}

Halo shape

Surrounding LSS

Halo bias b_h
DM clustering strength, σ_8
Assembly bias

(Umetsu+12, *ApJ*, 755, 56)

Multiple Imaging (Strong Lensing)

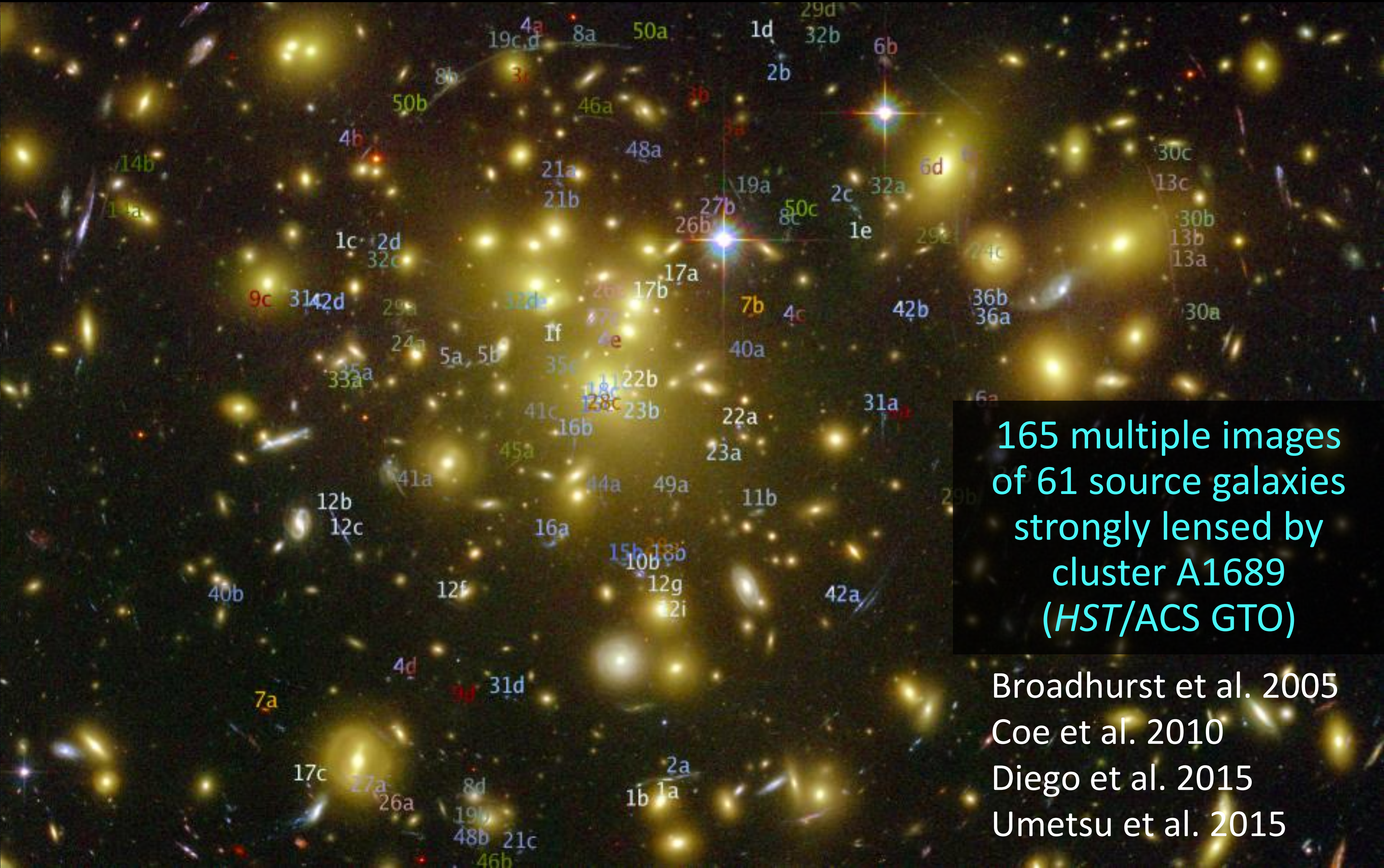

165 multiple images of 61 source galaxies strongly lensed by cluster A1689 (*HST*/ACS GTO)

Broadhurst et al. 2005
Coe et al. 2010
Diego et al. 2015
Umetsu et al. 2015

Gravitational Shear

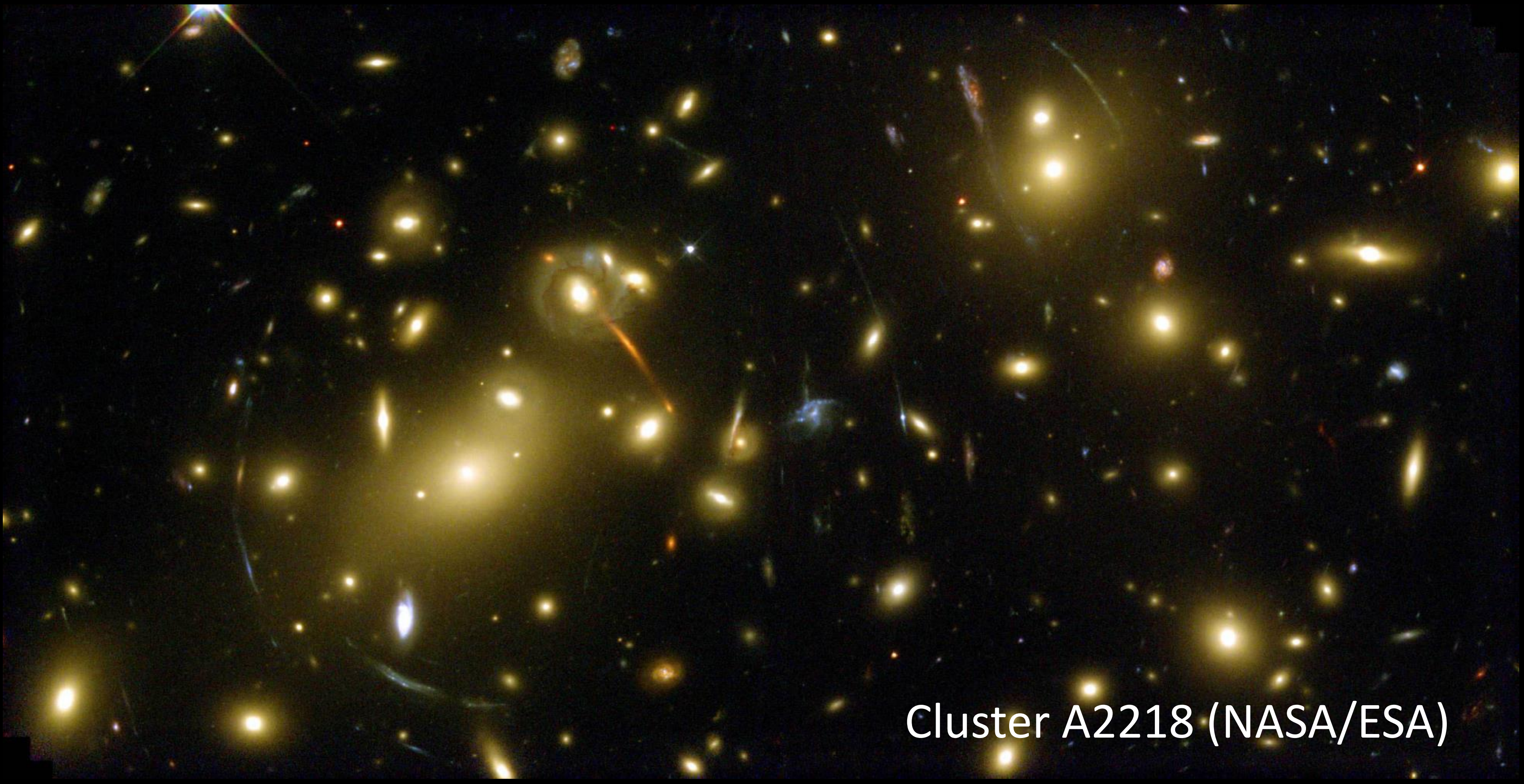

Cluster A2218 (NASA/ESA)

Gravitational Magnification

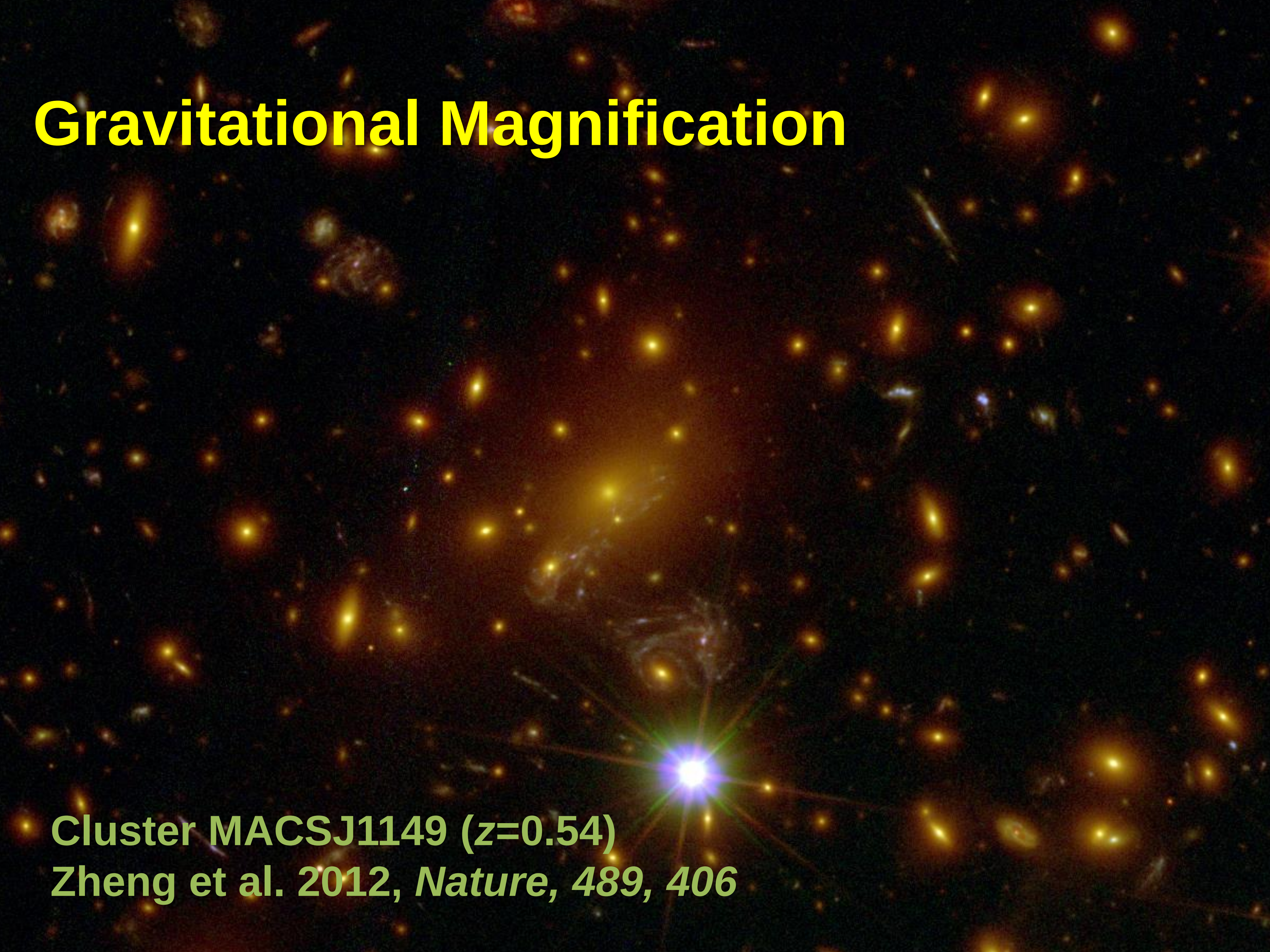

Cluster MACSJ1149 (*z*=0.54)
Zheng et al. 2012, *Nature, 489, 406*

Weak lensing: shear & magnification

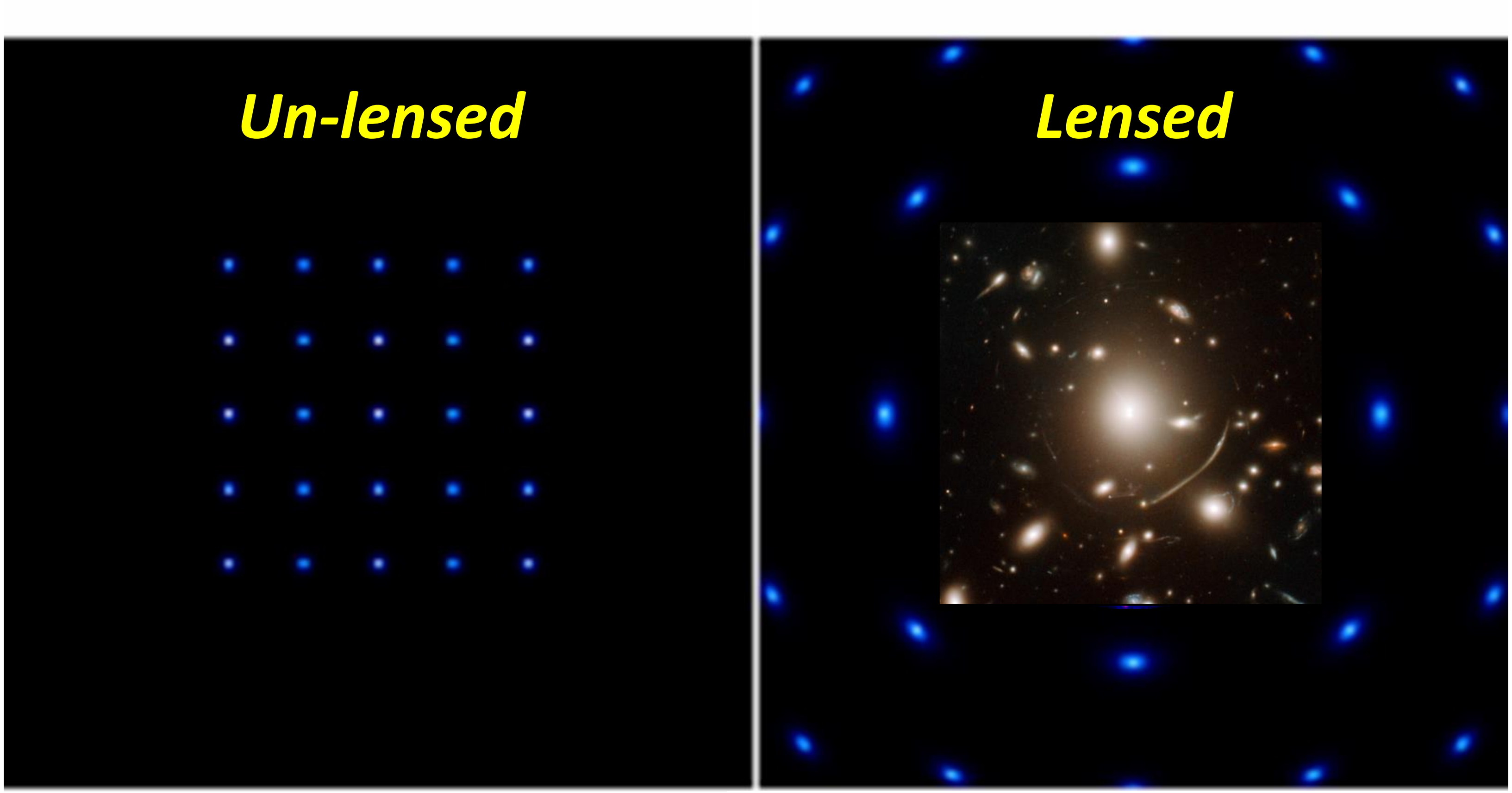

- **Shear** (Kaiser 92)
  - ✓ Shape distortion: $\delta e \sim \gamma$
- **Magnification** (Broadhurst+95)
  - ✓ Flux amplification: μF
  - ✓ Area distortion: $\mu \Delta \Omega$

Sensitive to "modulated" matter density

$$\Sigma_c \gamma_+ = \Delta\Sigma(R) \equiv \Sigma(<R) - \Sigma(R)$$

Sensitive to "total" matter density

$$\mu \approx 1 + 2\kappa; \quad \Sigma_c \kappa = \Sigma(R) = \int (\rho - \bar{\rho}_m) dl$$

Shear vs. Magnification

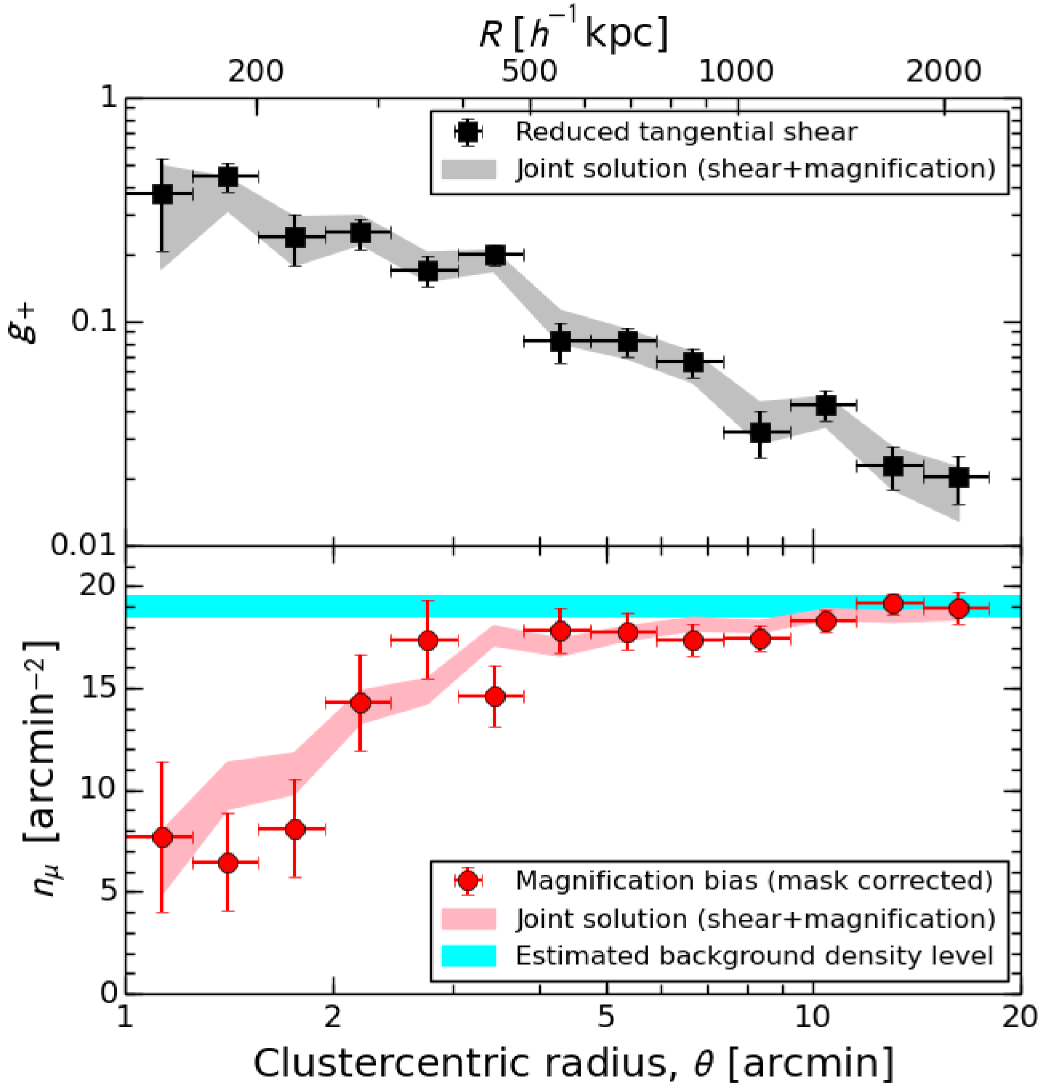

Reduced tangential shear

$$g_+ \approx \gamma_+ = \Delta\Sigma / \Sigma_c$$

Number count depletion due to magnification

$$n(<m_{\mathrm{lim}}) = \bar{n}(<m_{\mathrm{lim}})\,\mu^{-1+2.5s}$$

$$\text{with } s = \left[d\log_{10}\bar{n}(<m)/dm\right]_{m=m_{\mathrm{lim}}} < 0.4$$

Subaru *BVRiz* data, A1689
(Umetsu+15, *ApJ*, 806, 207)

Cluster Lensing Mass Inversion (CLUMI) code

Umetsu+11a, *ApJ*, 729, 127

$$P(\boldsymbol{\Sigma}|\mathrm{WL}) \propto P(\mathrm{WL}|\boldsymbol{\Sigma})P(\boldsymbol{\Sigma}) = P(\boldsymbol{n}_\mu|\boldsymbol{\Sigma})P(\boldsymbol{g}_+|\boldsymbol{\Sigma})P(\boldsymbol{\Sigma})$$

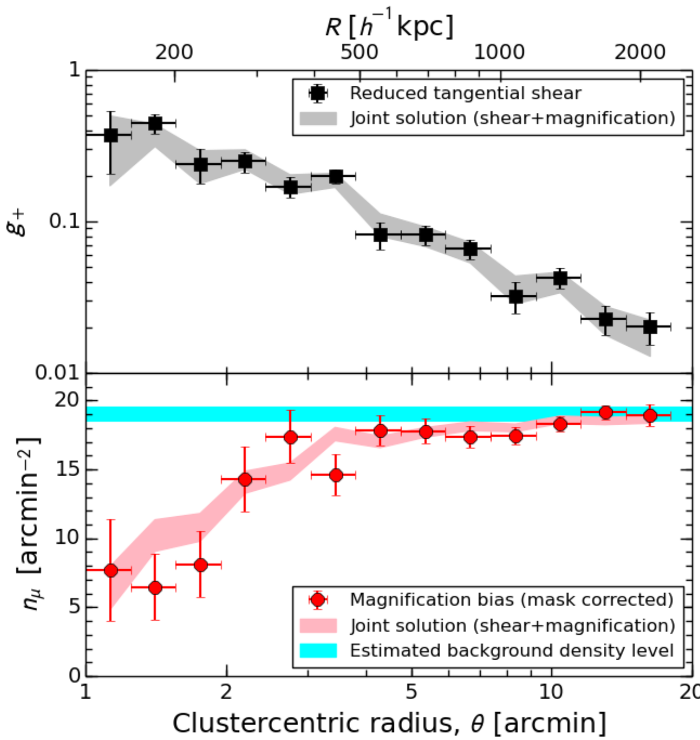

Joint reconstruction

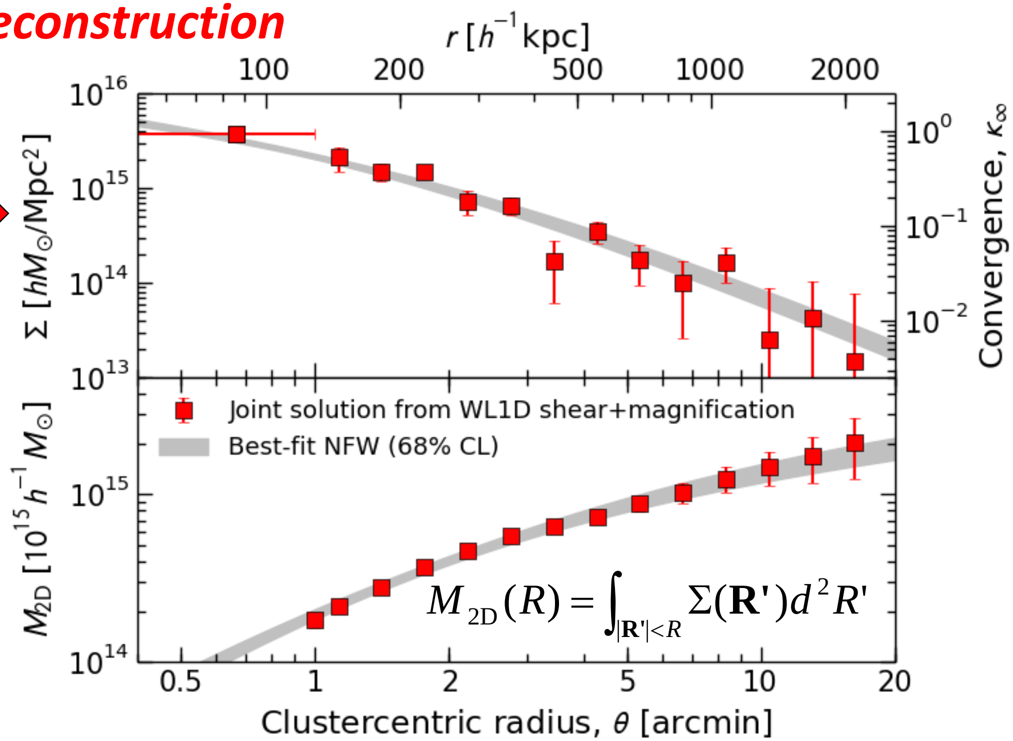

- Mass-sheet degeneracy broken
- Total statistical precision improved by ~20-30%
- Calibration uncertainties marginalized over: $c = \{\langle W\rangle_s, f_{W,s}, \langle W\rangle_\mu, \overline{n}_\mu, s_{\rm eff}\}$.